NMR studies of radical polymerization processes

by
Bert Klumperman
Professor in Polymer Science
South African Research Chair in
Advanced Macromolecular Architectures

Dissertation presented for the degree of Doctor of Science in the Faculty of Science at Stellenbosch University

Promoter: Prof Peter E Mallon
Faculty of Science
Department of Chemistry and Polymer Science

August 2012

DECLARATION

By submitting this dissertation electronically, I declare that the entirety of the work contained therein is my own, original work, that I am the senior author (and principal investigator) of the publications of which it is composed, that reproduction and publication thereof by Stellenbosch University will not infringe any third party rights and that I have not previously in its entirety or in part submitted it for obtaining any qualification.

Date: 21 September 2012

Table of content

Summary

Examples of the use of NMR spectroscopy in the study of radical polymerization processes have been described. The studies presented have made a significant contribution to the understanding of the fundamental mechanistic processes in these polymerization systems. It is pointed out that NMR in conventional radical polymerization is of limited use due to the concurrent occurrence of all elementary reactions (initiation, propagation and termination). Conversely, for living radical polymerization, NMR has great value. In that case, the elementary reactions are somewhat more restricted to specific times of the polymerization process. This allows for example the detailed study of the early stages of chain growth in Reversible Addition-Fragmentation Chain Transfer (RAFT) mediated polymerization.

Two different studies are described. The first is related to the early stages of RAFT-mediated polymerization. A process for which we coined the name *initialization* was studied via *in situ* ^{1}H NMR spectroscopy. It is shown that in many cases, there is a selective reaction that converts the original RAFT agent into its single monomer adduct. A few different examples and their mechanistic interpretation are discussed. It is also shown that NMR spectroscopy can be a valuable tool for the assessment of a RAFT agent in conjunction with a specific monomer and polymerization conditions.

In the second study, ^{15}N NMR, ^{31}P NMR and ^{1}H NMR are used for two different types of experiments. The first is a conventional radical copolymerization in which the growing chains are trapped by a ^{15}N labeled nitroxide to yield a stable product. In the second experiment, a similar copolymerization is conducted under nitroxide-mediated conditions. The nitroxide of choice contains phosphorous, which enables the quantification of the terminal monomer in the dormant chains. Each of the experiments individually provides interesting information on conventional radical copolymerization and nitroxide-mediated copolymerization, respectively. Combination of the experimental data reveals an interesting discrepancy in the ratio of terminal monomer units in active chains and dormant chains. Although not unexpected, this result is interesting and useful from a mechanistic as well as a synthetic point of view.

In terms of future perspectives, it is expected that the advanced analytical techniques as described here will remain crucial in polymer science. Present developments in radical polymerization, such as investigations into monomer sequence control, rely on accurate knowledge of kinetic and mechanistic details of elementary reactions. It is expected that such detailed studies will be a main challenge for the next decade of polymer research.

Opsomming

Voorbeelde van die gebruik van KMR-spektroskopie in die studie van radikaalpolimerisasies word beskryf. Hierdie studies het ’n beduidende bydrae gelewer tot die verstaan van die fundamentele meganistiese prosesse in hierdie polimerisasiesisteme. Dit het daarop gewys dat KMR beperkte gebruike het in konvensionele radikaalpolimerisasies as gevolg van die gelyktydige voorkoms van alle basiese reaksies (afsetting, voortsetting en beëindiging). Aan die anderkant het KMR groot waarde vir lewende radikaalpolimerisasie. In hierdie geval is die elementêre reaksies ietwat meer beperk tot spesifieke tye van die polimerisasieproses. Gedetailleerde studies kan byvoorbeeld van die vroeë stadiums van die kettinggroei in Omkeerbare Addisie-Fragmentasie-KettingOordrag (OAFO)-bemiddelde polimerisasie gedoen word.

Twee verskillende studies is beskryf. Die eerste het betrekking op die vroeë stadiums van die OAFO-bemiddelde polimerisasie. 'n Proses wat “inisialisering” genoem is, is bestudeer deur middel van *in situ* ^{1}H KMR-spektroskopie. Dit is bewys dat daar in baie gevalle 'n selektiewe reaksie is wat die oorspronklike OAFO-agent in sy enkelmonomeeradduk verander voor polimerisasie. 'n Paar ander voorbeelde en hul meganistiese interpretasie is bespreek. Dit is ook bewys dat KMR-spektroskopie 'n waardevolle hulpmiddel kan wees vir die assessering van 'n OAFO-agent in samewerking met 'n spesifieke monomeer en polimerisasie toestande.

In die tweede studie is ^{15}N KMR, ^{31}P KMR en ^{1}H KMR gebruik vir twee verskillende tipes van die eksperiment. Die eerste is 'n konvensionele radikaalkopolimerisasie waarin die groeiende kettings vasgevang word deur 'n ^{15}N-gemerkte nitroksied om 'n stabiele produk te lewer. In die tweede eksperiment is 'n soortgelyke kopolimerisasie gedoen onder nitroksied-bemiddelde toestande. Die gekose nitroksied bevat fosfor wat die kwantifisering van die terminale monomeer in die dormante kettings moontlik maak. Elkeen van die individuele eksperimente lewer interessante inligting oor konvensionele radikale kopolimerisasie en nitroksied-bemiddelde kopolimerisasie, onderskeidelik. ’n Kombinasie van die eksperimentele data toon 'n interessante verskil aan in die verhouding van die terminale monomeereenhede in die aktiewe en sluimerende kettings. Alhoewel dit nie onverwags is nie, is die resultate interessant en van waarde vanuit 'n meganistiese- sowel as 'n sintetiese oogpunt.

In terme van toekomstige perspektiewe word daar verwag dat gevorderde analitiese tegnieke soos hier beskryf, belangrik sal bly in polimeerwetenskap. Huidige ontwikkelinge in radikaalpolimerisasie, soos ondersoeke na die beheer van monomeervolgorde, maak staat op akkurate kennis van kinetiese en meganistiese besonderhede van die basiese reaksies. Daar word verwag dat sulke gedetailleerde studies ’n uitdaging sal bied vir die volgende dekade van polimeernavorsing.

CHAPTER 1

Chapter 1 provides an introduction into the field of NMR studies of radical polymerization kinetics. The difficulties of such studies in the case of conventional radical polymerization will be highlighted. The development of living radical polymerization (LRP) techniques led to a strong gain in power of the NMR techniques for studying reaction kinetics.

An outline of the subsequent chapters will be given, and it will be shown how the chapters can be grouped around a few different applications. The subsequent chapters themselves comprise previously published work over the period 2003 to 2012.

NMR studies of radical polymerization processes

Introduction

Conventional radical polymerization (RP) is a typical example of a chain growth polymerization process. The formation of a complete polymer chain is the result of a kinetic chain reaction. The growth of a single chain starts by the creation of a radical, typically from the decomposition of a thermal initiator. After the formal initiation step (addition of the first monomer unit to the initiator-derived primary radical) a large number of propagation steps take place that cause the chain to grow. When the growing polymeric radical encounters another radical species (low or high molar mass), termination takes place to yield a dead chain. This whole process usually takes no longer than around one second. Elementary reactions such as the propagation step may even take less than a millisecond. As a consequence, it is hard to study detailed processes in RP. From the early days of RP in the 1940s, the great majority of experimental studies relied on monomer conversion *versus* time data. Such data would then mathematically be described by typical equations that contain the rate constants of initiator decomposition, of propagation and of termination. Monomer conversion in such experiments would usually be obtained via traditional techniques such as gravimetry, gas chromatography (GC) or high-performance liquid chromatography (HPLC). These techniques are restricted to a fairly low sampling rate, which in most cases was quite sufficient to perform parameter estimation and curve fitting exercises to the relevant rate equations. *In situ* analysis techniques such as infrared spectroscopy, near-infrared spectroscopy, Raman spectroscopy and nuclear magnetic resonance (NMR) spectroscopy were occasionally used. However, the benefit of the higher time resolution was quite limited due to the nature of RP, *i.e.* continuous initiation of new chains, growth of active chains and termination of active chains.

All of this changed drastically with the advent of living radical polymerization (LRP) processes from the 1980s onwards. The growth of individual polymer chains is spread out over the duration of an LRP experiment. The polymer chains possess a narrow chain length distribution. As a consequence, spectroscopic techniques can be used to monitor processes that occur at a specific stage of the chain growth. Since it is widely accepted that the elementary reactions of RP are identical to most of those in LRP, detailed studies of LRP can be very beneficial to the understanding of RP processes in general.

An interesting example in this respect is the specificity of addition of an initiator-derived primary radical to one of the two monomers in a copolymerization. As indicated above, the growth of a full polymer chain takes in the order of a second. Moreover, new chains are continuously formed. As a consequence, it is very hard to single out the characteristic signals of the α-chain end in an attempt to measure the ratio of the two first monomer additions. A very elegant study in this respect is shown by work from the group of D.A. Tirrell.[1-3] As one of the techniques, ^{13}C labeled initiators were used that allowed the specific detection of the end-groups. However elegant, it is obvious that the techniques used in the study by Tirrell are laborious and difficult to implement for a wide variety of primary radicals.

In this thesis we show a few different examples where the combination of LRP and (mainly) *in situ* NMR spectroscopy provides a very powerful tool to elucidate mechanistic and kinetic features of radical polymerization processes.

Thesis outline

In this thesis, a number of different studies will be displayed. The individual studies have been conducted over the span of the past decade. Chapter 2 and Chapter 3 belong together. In Chapter 2, the synthesis of ^{15}N labeled nitroxides and alkoxyamines is described. The ^{15}N NMR chemical shifts of the low molar mass alkoxyamine model compounds can be used in the interpretation of data from Chapter 3. In Chapter 3, styrene – acrylate copolymerization experiments are carried out in a conventional radical polymerization fashion. The growing chains are irreversibly trapped by a nitroxide after a certain average chain length has been reached. The presence of the ^{15}N label in the nitroxide allows for the determination of the terminal monomer unit in the trapped chain. This ultimately leads to an efficient method of model discrimination between copolymerization models.

Chapters 4 to 6 also belong together. These chapter deal with an investigation of the initial stages of Reversible Addition Fragmentation Chain Transfer (RAFT) mediated polymerization. Especially in the case of dithiobenzoate-mediated polymerization, there had been a number of reports on inhibition and retardation phenomena. In Chapters 4 and 5, the RAFT-mediated polymerization of styrene with two different dithiobenzoates is investigated. *In situ* ^{1}H NMR experiments are conducted to follow the concentration profiles of the relevant species. These include the original RAFT agent (dithiobenzoate), and the RAFT agent with one or two monomer units inserted in the C–S bond. Based on the experimental data from Chapters 4 and 5, a mechanistic interpretation is presented in Chapter 6. Chapter 6 is part of a scientific debate that took place for several years around mechanistic aspects of RAFT-mediated polymerization.

Where Chapter 4-6 deal with a well-behaved monomer (styrene), Chapter 7 shows that a very similar methodology can be used for poorly stabilized monomers such as *N*-vinylpyrrolidone (NVP). It is know that for the RAFT-mediated polymerization of monomers like NVP, xanthates or dithiocarbamates should be used as RAFT agent. In Chapter 7, the role of the leaving group is studied in greater detail. It is shown that the *initialization* process that was introduced in Chapters 4 and 5 takes place efficiently for some leaving groups and not at all for others.

In Chapters 8 and 9, we return to styrene – acrylate copolymerization. In this case, a nitroxide-mediated polymerization (NMP) is utilized with a frequently used nitroxide (SG1, or DEPN) as the mediating agent. The presence of phosphorous in the nitroxide allows for ^{31}P NMR as a tool to follow the terminal monomer unit in the dormant polymer chain. In Chapter 8, an adequate model for the nitroxide-mediated copolymerization is developed that strongly relies on the rate constants of activation and deactivation of the NMP equilibriums for styrene-terminal chains as well as for acrylate-terminal chains. In Chapter 9, the

data from Chapter 3 and 8 are brought together. Although not completely unexpected, it remains remarkable that the ratio of chain-end monomer units is vastly different for active chains (radicals) and dormant chains (alkoxyamines) in a nitroxide-mediated copolymerization of styrene and acrylates.

Chapter 10 is an epilogue in which the impact of the work described in this thesis will be assessed. Further, this Chapter will provide an outlook on remaining questions and research topics for the next decade in this field of research.

References

1. Jones, S. A.; Prementine, G. S.; Tirrell, D. A. *J. Am. Chem. Soc.* **1985**, *107*, 5275-5276.
2. Cywar, D.A.; Tirrell, D.A. *Macromolecules* **1986**, *19*, 2908-2911.
3. Prementine, G.S.; Tirrell, D.A. *Macromolecules* **1987**, *20*, 3034-3038.

CHAPTER 2

Chapters 2 and 3 are related to ^{15}N NMR studies of conventional radical polymerization. In this chapter, the synthesis of a ^{15}N-labeled nitroxide and its alkoxyamine is described. The use of ^{15}N-labeled compounds is necessary due to the low natural abundance of ^{15}N, which would make it impossible to detect end groups of polymer chains.

Low molar mass model alkoxyamines will be used in this chapter to investigate the effect of the nature of the trapped transient radical on the chemical shift in ^{15}N NMR.

Reprinted with permission from *J. Org. Chem.* **2003**, *68*, 7322-7328.

JOC Article

^{15}N NMR Spectroscopy of Labeled Alkoxyamines. ^{15}N-Labeled Model Compounds for Nitroxide-Trapping Studies in Free-Radical (Co)polymerization

Peter Kelemen,[†] Johan Lugtenburg,[‡] and Bert Klumperman*,[†]

Laboratory of Polymer Chemistry, Eindhoven University of Technology, P.O. Box 513, 5600 MB Eindhoven, The Netherlands, and Leiden Institute of Chemistry, Gorlaeus Laboratories, Leiden University, P.O. Box 9502, 2300 RA Leiden, The Netherlands

L.Klumperman@tue.nl

Received May 19, 2003

Eight ^{15}N-labeled derivatives of 1-ethoxy-2,2,6,6-tetramethylpiperidine were synthesized in order to investigate the effects of their structural units on ^{15}N NMR spectra. A single peak is found for each alkoxyamine. The chemical shift depends extensively on the nature of the α carbon atom of the alkoxy group. The remote functional group attached to position 4 of the piperidine ring has a smaller but still significant effect. The results of the ^{15}N NMR measurements are supported by the detection of the N−H and N−C spin−spin coupling from the ^{1}H and ^{13}C NMR. The investigated alkoxyamines are model compounds for the radical-trapping products of styryl, methyl methacryloyl, α-methylstyryl, and methyl acryloyl radicals by ^{15}N-labeled nitroxides. The potential of ^{15}N NMR spectroscopy to analyze such products is discussed. In addition, it is shown that the ^{13}C chemical shifts of the α carbon atom of the alkoxy group fall in an empty part of the ^{13}C NMR spectrum, which allows the identification of trapped (macro)radicals via natural abundance ^{13}C NMR.

Introduction

The present work describes the preparation and NMR spectroscopy of substituted hydroxylamines (alkoxyamines) having the general formula depicted in Scheme 1.

The investigated compounds participate in many important free-radical reactions. They are known as initiators in the nitroxide-mediated controlled radical polymerization[1] and as products of radical trapping.[2] Radical trapping is used in the investigation of complex radical reactions. It is based on the conversion of a reactive carbon-centered (macro)radical into an alkoxyamine stable at ambient conditions (Scheme 2).

Radical trapping is followed by the analysis of the trapping products. Determination of the substituents R_1 and R_2 is of particular importance. These substituents characterize the structure of the reactive center of the original (macro)radical. Since they are located in the vicinity of the nitrogen atom of the trapping product, they may also affect the chemical shifts of the ^{15}N nuclei of the alkoxyamine. ^{15}N NMR spectroscopy can therefore be utilized for analysis of the trapping products. However, the ^{15}N NMR of substituted hydroxylamines has not been studied to date.[3] ^{15}N-labeled alkoxyamines of the general structure shown in Scheme 1 are synthesized for the first time in our work and their characterization by NMR produced original results. The compounds studied were chosen as low molecular weight models resembling the terminal unit structure of the macromolecular trapping products. The alkoxyamines resemble trapping products of terminal units formed by methyl methacrylate (**I** and **II**), methyl acrylate (**III** and **IV**), α-methyl styrene (**V** and **VI**), and styrene (**VII** and **VIII**). The effects of the various

SCHEME 1. Substituted Alkoxyamines Studied by ^{15}N NMR Spectroscopy in This Work

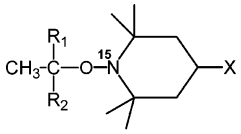

		X = -OH	X = -OSO$_2$-C$_6$H$_4$-CH$_3$
R_1 = -COOCH$_3$	R_2 = -CH$_3$	**I**	**II**
	R_2 = -H	**III**	**IV**
R_1 = -C$_6$H$_5$	R_2 = -CH$_3$	**V**	**VI**
	R_2 = -H	**VII**	**VIII**

SCHEME 2. Formation of a Macromolecular Alkoxyamine by Trapping of a Macroradical with 2,2,6,6-Tetramethylpiperidin-1-oxyl Derivatives

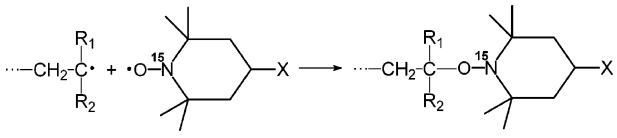

* Corresponding author.
[†] Eindhoven University of Technology.
[‡] Leiden University.

(1) Solomon, D. H.; Rizzardo, E. US 4,581,429.
(2) Moad, G.; Shipp, D. A.; Smith, T. A.; Solomon, D. H. *J. Phys. Chem. A* **1999**, *103*, 6580.
(3) Berger, S.; Braun, S.; Kalinowski, H. O. *NMR Spectroscopy of the Non-Metallic Elements*; John Wiley & Sons, Ltd.: Chichester, 1997; p 15.

10.1021/jo034667q CCC: $25.00
Published on Web 08/19/2003

SCHEME 3. Preparation Scheme of 4-Hydroxy-2,2,6,6-tetramethylpiperidin-1-oxyl- ^{15}N

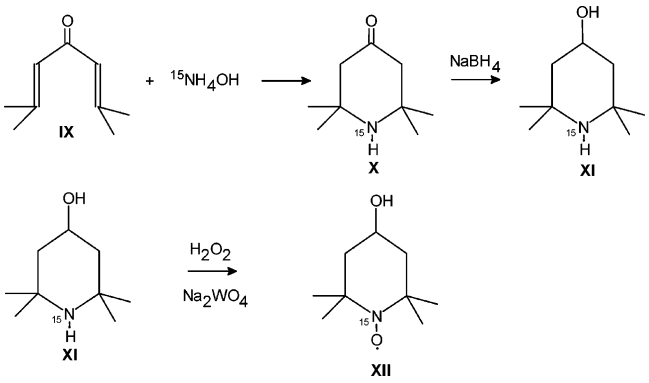

substituents on the ^{15}N NMR shifts are subsequently compared, and the ability of ^{15}N NMR spectroscopy to identify the structure of trapping products is tested in this way.

Discussion

Synthesis of the ^{15}N-Labeled Model Compounds. Stable free-radical 4-hydroxy-2,2,6,6-tetramethylpiperidin-1-oxyl-*^{15}N* **(XII)** is used as a precursor for the synthesis of the alkoxyamines. The radical is prepared in three synthetic steps depicted in Scheme 3. The first step, synthesis of the 2,2,6,6-tetramethyl-4-piperidinone-*^{15}N* **(X),** is performed according to Yost et al.[4] Reduction of **X** by sodium borohydride according to Lutz et al.[5] is applied to obtain 2,2,6,6-tetramethyl-4-piperidinol-*^{15}N* **(XI)**. The selective oxidation of this cyclic amine using the procedure described by Rosantsev[6] provides the desired radical **XII**. The application of this scheme allowed the preparation of 12.1 mmol of **XII** from 22.1 mmol of ammonium-*^{15}N* hydroxide. The most expensive reactant (ammonium-*^{15}N* hydroxide) was utilized with efficiency higher than 50%.

Various methods for the conversion of **XII** into the desired alkoxyamines **I**−**VIII** were tested using the unlabeled analogues of **XII** and **XIII**. The preferred procedures of the alkoxyamines' syntheses are based on the coupling of the nitroxyl radical with an alkyl radical of suitable structure formed in situ. The details of the preparation are determined by the particular way of alkyl radical formation. Three alternatives are applied in this work as shown in Scheme 4: (1) the decomposition of a suitable azo compound, (2) the reaction of an alkylbromide with a Cu^{I} complex, (3) peroxide decomposition and subsequent hydrogen abstraction from a suitable hydrocarbon.

(1) Alkoxyamine **I** is prepared by heating of **XII** with dimethyl 2,2′-azobisisobutyrate. The reaction temperature and time are crucial parameters for the efficiency of the synthesis. Heating of equivalent amounts of the reactants at 85 °C for 16 h failed due to the low stability of **I** under these conditions. The reaction temperature was

SCHEME 4. Three Alternative Methods for the Generation of Carbon-Centered Radicals Employed in the Synthesis of Alkoxyamines

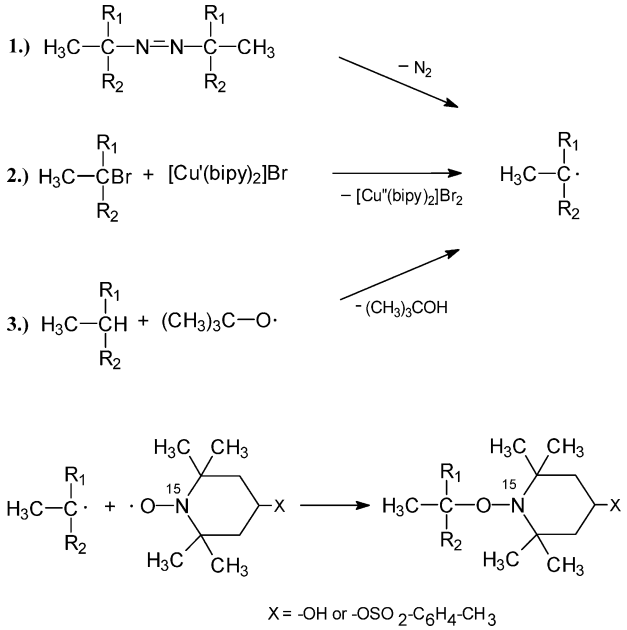

decreased to 65 °C, and a large excess of the azo compound was applied. The reaction is then completed in 4 h and **I** is isolated with sufficient yield. Application of this method for the preparation of other alkoxyamines is restricted by the limited availability of suitable azo compounds.

(2) The method utilizing alkyl bromides in the alkoxyamine preparation has been developed by Matyjaszewski and co-workers. The availability of a large variety of bromo-substituted compounds enhances its versatility, which has been demonstrated by the synthesis of various alkoxyamines from 2,2,6,6-tetramethylpiperidin-1-oxyl.[7] This method is applied in the syntheses of the alkoxyamines **I**−**IV.** The experiments with unlabeled analogues of nitroxyl radicals **XII** and **XIII** have shown that it is advantageous to decrease reaction times to periods of 2−3 h instead of 4−12 h reported by the authors of this method. It is known that −OH-containing solvents accelerate the Cu^{I}-catalyzed cleavage of the C−Br bond located on the α carbon of 2-bromoesters.[8,9] This fact is utilized in the preparation of the thermally unstable product **I**. Substitution of benzene by 2-ethoxyethanol as solvent allowed the reaction temperature to be decreased to 20 °C.

(3) Peroxide decomposition has been applied in the preparation of **V** and **VII.** 1-(2,2,6,6,-Tetramethyl-4-hydroxypiperidin-1-oxy)-1-phenylethane **(V)** has been prepared according to the procedure applied by Hawker.[10] The 1-phenylethyl radicals have been generated by the thermal decomposition of di-*tert*-butyl peroxide and subsequent reaction of the *tert*-butoxy radicals with the

(4) Yost, Y.; Polnaszek, C. F.; Mason, R. P.; Holtzman, J. L. *J. Labelled Comput. Radiopharm.* **1981**, *18*, 1089.
(5) Lutz, W. B.; Lazarus, S.; Meltzer, R. I. *J. Org. Chem.* **1962**, *27*, 1695.
(6) Rosantsev, E. G. *Free Nitroxyl Radicals*; Plenum Press: New York, London, 1970; Chapter IX.
(7) Matyjaszewski, K.; Woodworth, B. E.; Zhang, X.; Gaynor, S. G.; Metzner, Z. *Macromolecules* **1998**, *31*, 5955.
(8) Chambard, G.; Klumperman, B.; German, A. L. *Macromolecules* **2000**, *33*, 4417.
(9) Haddleton, D. M.; Shooter, A. J.; Heming, A. M. et al. *ACS Symp. Ser.* **1998**, *685*, 284.
(10) Hawker, C. J.; Barclay, G. G.; Orelana, A.; Dao, J.; Devonport, W. *Macromolecules* **1996**, *29*, 5246.

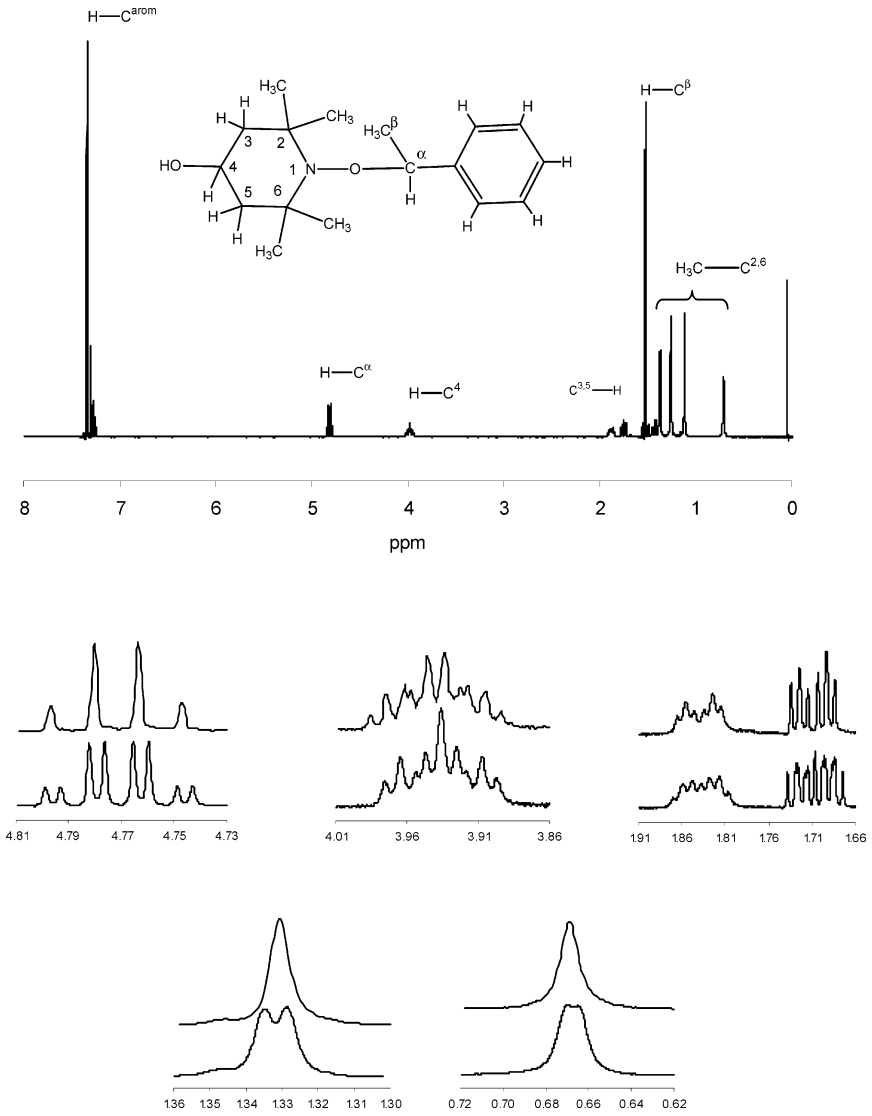

FIGURE 1. ^{1}H NMR spectrum of the alkoxyamine (**VII**). Insets: lower line, spectrum of ^{15}N-labeled compound; upper line, spectrum of the unlabeled analogue.

ethylbenzene. The authors of this procedure recommend the preparation at the temperature of ethylbenzene reflux (ca. 136 °C). A mixture of alkoxyamines is obtained at this temperature. The ^{1}H NMR spectrum contains peaks, which can be ascribed to the unlabeled analogue of **V**[11] and another group of peaks corresponding to 1-methoxy-4-hydroxy-2,2,6,6-tetramethylpiperidine.[12] The latter compound is formed by coupling of **XII** with a methyl radical generated by β scission of the *tert*-butoxy radical at 136 °C. Decrease of the reaction temperature to 115 °C suppresses this side reaction. The preparation of the thermally less stable 2-(2,2,6,6,-tetramethyl-4-hydroxypiperidin-1-oxy)-2-phenylpropane **(VII)** is performed according to Connoly et al.[13] using photolytic decomposition of *tert*-butyl peroxide at ambient temperature in the presence of 2-phenylpropane and **XII**.

The compounds **II** and **VI** are prepared by esterification of the 4-hydroxy functional group of the corresponding alkoxyamine.

The presence of the hydroxyl or *p*-methylphenylsulfonyl functional group in the position 4 of the piperidine ring affects advantageously the melting points of the prepared alkoxyamines. They are in the range of 73−135 °C. This feature enables to purify the studied compounds efficiently by a combination of flush chromatography and recrystallization.

Effect of the ^{15}N Labeling on ^{1}H and ^{13}C NMR Spectra of the Alkoxyamines. The synthesized alkoxyamines were characterized by routine ^{1}H and ^{13}C NMR at first. The effect of the labeling with the ^{15}N isotope on the spectra can be revealed by the comparison of labeled and unlabeled compounds. The spectra are measured under conditions that enable the detection of spin−spin coupling of the ^{15}N nucleus with the nuclei of hydrogen or carbon. The ^{1}H and ^{13}C NMR spectra of the 2,2,6,6-tetramethyl-1-(1-phenylethoxy)piperidin-*^{15}N*-4-ol (**VII**) are compared with its unlabeled analogue in Figures 1 and

(11) Hawker, C. J.; Barclay, G. G.; Dao, J. *J. Am. Chem. Soc.* **1996**, *118*, 11467.
(12) Richeson, C. E.; Mulder, P.; Bowry, V. W.; Ingold, K. U. *J. Am. Chem. Soc.* **1998**, *120*, 7211.
(13) Connoly, T. J.; Baldoví, M. V.; Mohtat, N.; Scaiano, J. C. *Tetrahedron Lett.* **1996**, *37*, 4919.

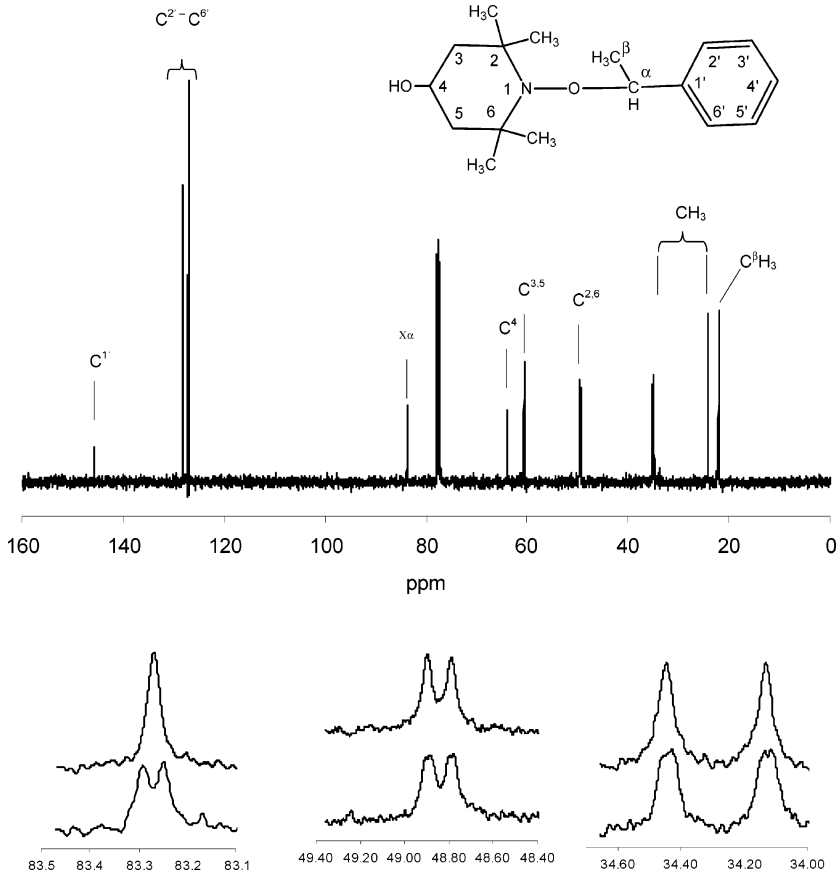

FIGURE 2. ^{13}C NMR spectrum of the alkoxyamine (**VII**). Insets: lower line, spectrum of ^{15}N-labeled compound; upper line, spectrum of the unlabeled analogue.

2. The spectral peaks of both compounds have the same chemical shifts corresponding with the structural units of the molecule. Magnetic properties of ^{15}N and ^{14}N nuclei result in different spin−spin coupling and the multiplicity of some peaks in the same position differs for labeled and unlabeled compounds. The proton located on the α carbon of the alkoxy group resonates at 4.77 ppm. The coupling with the vicinal protons of the neighboring methyl group produces a quartet. This pattern is observed in the spectrum of the unlabeled compound. Labeling with the ^{15}N isotope causes additional splitting of the signal, and eight lines (quartet of doublets) are observed. The absolute value of 2.3 Hz can be estimated for the interaction constant of the heteronuclear N−H spin−spin coupling in this position of the molecule. The bands at 0.67, 1.07, 1.22, and 1.33 ppm are assigned to protons of the methyl groups attached to the piperidin-4-ol ring in the positions 2 and 6. They form broad singlets in the spectrum of the unlabeled **VII**. However, bimodal bands are observed in the spectrum of the labeled compound at 1.33 and 0.67 ppm. The protons in the positions 3, 4, and 5 of the ring form a spin system characterized by multiplets in the ranges 3.89−3.98 ppm (C^4-H) and 1.37−1.51 ppm (C^3-H and C^5-H). The patterns of these multiplets differ for the labeled **VII** and its unlabeled analogue. The differences indicate that the spin of the ^{15}N nucleus affects the NMR resonance of the protons in the entire piperidin-4-ol ring. On the other hand, no effect of the labeling is observed on the signals of the protons attached to the aromatic ring and to the β carbon of the alkoxy group. The strongest effect is observed on the proton present at the α carbon of the alkoxy group. The absolute values of the coupling constants found for the measured alkoxyamines are summarized in Table 1.

The effect of the ^{15}N labeling on the ^{13}C spectra is clearly found on the resonance signal of the α carbon at 83.27 ppm. The splitting in two lines is clearly observed for the ^{15}N-labeled **VII** and corresponds to an absolute value of the interaction constant equal to 4.00 Hz. The unlabeled compound produces only a single line. The resonance signals at 48.80, 48.90, 34.13, and 34.45 ppm are also affected by the nucleus ^{15}N. These lines are not split, but broadened forming peaks with flat tops. The analogous signals of the unlabeled compound are sharp narrow lines resembling Lorenz curves.

^{15}N NMR Spectra of the Alkoxyamines. The ^{15}N nucleus interacts with numerous atoms in the molecule of the alkoxyamine, as the previous comparison has shown. The spin−spin coupling should produce a complicated multiplet on the ^{15}N NMR spectrum. A broad band is found as a result of the overlap of single lines and the limited resolution of the instrument. Application of proton decoupling eliminates the complications caused by N−H heteronuclear interactions. A narrow single peak is obtained under these conditions. The effect of the proton decoupling on the ^{15}N NMR spectrum of alkoxyamines is exemplified in Figure 3.

The previous results show that the ^{15}N nucleus affects the NMR resonance of the proton and ^{13}C isotope at the α position of the alkoxy group. The effect of the substit-

TABLE 1. Chemical Shifts and Absolute Values of Spin−Spin Coupling Constants with ^{15}N Isotope[a]

alkoxyamine	R_1	R_2	X	δ H-C$^{\alpha}$ (ppm)	$\|J_{H-N}\|$ (Hz)	δ C$^{\alpha}$ (ppm)	$\|J_{C-N}\|$ (Hz)
I	$-COOCH_3$	$-CH_3$	−OH	n.a.	n.a.	81.47	3.05
II	$-COOCH_3$	$-CH_3$	−OTs	n.a.	n.a.	81.47	3.06
III	$-COOCH_3$	−H	−OH	4.36	2.6	81.69	4.20
IV	$-COOCH_3$	−H	−OTs	4.28	2.6	81.70	4.20
V	$-C_6H_5$	$-CH_3$	−OH	n.a.	n.a.	80.00	3.05
VI	$-C_6H_5$	$-CH_3$	−OTs	n.a.	n.a.	80.24	3.43
VII	$-C_6H_5$	−H	−OH	4.77	2.3	83.27	4.00
VIII	$-C_6H_5$	−H	−OTs	n.a.[b]	n.a.[b]	83.48	3.80

[a] The quantities are measured for carbons in the α position of the alkoxy group and the adjacent hydrogen if present. [b] Determination not possible due to the peak overlap.

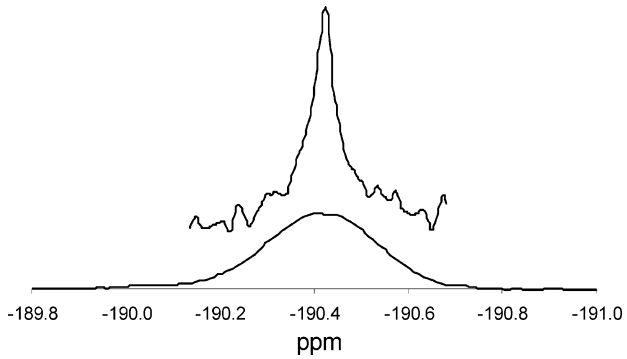

FIGURE 3. Normalized ^{15}N NMR spectrum of the alkoxyamine **(VIII)**. Effect of the proton decoupling on the signal: lower line, without decoupling, 8000 scans; upper line, decoupled, 500 scans.

TABLE 2. ^{15}N NMR Chemical Shifts of the Alkoxyamines I−VIII

alkoxyamine	R_1	R_2	X	chemical shift (ppm)
I	$-COOCH_3$	$-CH_3$	−OH	−198.5
II	$-COOCH_3$	$-CH_3$	−OTs	−200.7
III	$-COOCH_3$	−H	−OH	−177.8
IV	$-COOCH_3$	−H	−OTs	−180.7
V	$-C_6H_5$	$-CH_3$	−OH	−200.9
VI	$-C_6H_5$	$-CH_3$	−OTs	−203.0
VII	$-C_6H_5$	−H	−OH	−188.1
VIII	$-C_6H_5$	−H	−OTs	−190.4

uents present on this atom on the NMR resonance of the ^{15}N isotope can also be anticipated. It is investigated by measurement of the ^{15}N NMR chemical shifts of alkoxyamines having various structural units $-R_1$ and $-R_2$. Since the ^{15}N nucleus affected the ^{1}H NMR resonance of the remote protons located on the piperidin-4-ol ring, it is also expected that remote nuclei will affect the ^{15}N NMR resonance. The effect of the remote group is tested by ^{15}N NMR measurements of alkoxyamines possessing a functional group −X in the 4-position of the piperidine ring.

The set of studied compounds is designed by variation of the structural units R_1, R_2, and X. Two alternatives are chosen for each substituent resulting in eight different compounds. The chemical shifts of the single peak ^{15}N NMR spectra are shown in Table 2. The effect of each substituent on the ^{15}N NMR spectrum can be evaluated by comparison of the pairs of alkoxyamines differing in one substituent of interest and having identical other structural units.

Effect of Substituent −X. The model alkoxyamines having the same substituents R_1 and R_2 are grouped in pairs and the differences in their chemical shifts are related to the difference in the nature of substituent X (Table 3). It is seen, that the substitution of the hydrogen by *p*-toluenesulfonyl in the hydroxyl functional group always results in a decrease of the chemical shift values by 2.1−2.9 ppm. The nature of the substituents R_1 and R_2 has a minor effect on this difference.

TABLE 3. Effect of the Structure of Substituent X on the Position of the Resonance Peak in the ^{15}N NMR Spectrum Measured as the Difference in the Chemical Shifts in Pairs of Model Alkoxyamines

pair of alkoxyamines	−X	$-R_1$	$-R_2$	difference in chemical shift (ppm)
I	−OH	-$COOCH_3$	$-CH_3$	2.2
II	−O-Ts			
III	−OH	$-COOCH_3$	−H	2.9
IV	−OTs			
V	−OH	$-C_6H_5$	$-CH_3$	2.1
VI	−OTs			
VII	−OH	$-C_6H_5$	−H	2.3
VIII	−OTs			

TABLE 4. Effect of the Substituents of the α Carbon on the ^{15}N NMR Chemical Shift

pair of alkoxyamines	$-R_2$	$-R_1$	−X	difference in chemical shift (ppm)
I	−H	$-COOCH_3$	−OH	20.7
III	$-CH_3$			
II	−H	$-COOCH_3$	−OTs	20.0
IV	$-CH_3$			
V	−H	$-C_6H_5$	−OH	12.8
VII	$-CH_3$			
VI	−H	$-C_6H_5$	−OTs	12.6
VIII	$-CH_3$			

Effect of the Substituents R_1 and R_2. The effects of these two functional groups cannot be evaluated separately, in contrast to the substituent X. The largest differences in the ^{15}N NMR chemical shifts are found in pairs of the alkoxyamines differing in structural unit $-R_2$. The extensive effect of the α methyl group is revealed in Table 4. This substitution also affects the quality of the carbon atom localized in the α position with respect to the oxygen atom of the alkyloxy functional group. The observed effect of substituent $-R_2$ can be interpreted as the difference in chemical shift values between the alkoxyamines having a secondary ($-R_2 = -H$) and a tertiary α carbon ($-R_2 = -CH_3$).

The presence or absence of an α methyl group also determines the effect of the substituent $-R_1$ on the ^{15}N NMR chemical shift. Table 5 shows that the effect of $-R_1$ in alkoxyamines with a secondary α carbon is much stronger than in the analogous compounds having a

TABLE 5. Effect of the Substituent $-R_1$ on the ^{15}N NMR Chemical Shifts[a]

pair of alkoxyamines	$-R_1$	$-R_2$	$-X$	difference in chemical shift (ppm)
I	$-COOCH_3$	$-CH_3$	$-OH$	2.4
V	$-C_6H_5$			
II	$-COOCH_3$	$-CH_3$	$-OTs$	2.3
VI	$-C_6H_5$			
III	$-COOCH_3$	$-H$	$-OH$	10.3
VII	$-C_6H_5$			
IV	$-COOCH_3$	$-H$	$-OTs$	9.7
VIII	$-C_6H_5$			

[a] Chemical shift differences found in pairs of alkoxyamines having $-R_1$ methoxycarbonyl or phenyl.

tertiary α carbon. The presence of a phenyl group on the secondary α carbon results in chemical shift values ca. 10 ppm lower compared to compounds having a methoxycarbonyl group in the same position. However, the same structural difference between the compounds with a tertiary α carbon is reflected in a decrease of the chemical shift value by only 2.3−2.4 ppm.

The comparison of chemical shifts described above reveals a high sensitivity of the ^{15}N isotope of the piperidine ring to the structural details of substituents attached in the various positions of the molecule. This result is in accordance with the detection of spin−spin coupling on ^1H and ^{13}C NMR spectra. The strongest effect is observed on the α carbon atom of the alkoxy group. The ^{15}N NMR measurements confirmed that the steric and electronic effects of units $-R_1$ and $-R_2$ impose a combined influence on the ^{15}N NMR chemical shift. The influence of the remote $-X$ functional group is weaker but significant and is in accordance with the remote interactions of the ^{15}N nucleus detected by the observation of N−H spin−spin coupling.

^{15}N NMR spectra of the measured alkoxyamines present narrow single peaks. Differences in chemical shifts are large enough to prevent an overlap of peaks of different alkoxyamines. This feature can be practically exploited in the detection and analysis of various alkoxyamines in a mixture possessing different structural units. The strong effect of the substituents located on the α carbon atom is of special importance. They represent the structure of the reactive site of the original (macro) radical converted into the alkoxyamine in the process of radical trapping (Scheme 2). The efficiency of trapping in the investigation of complex radical reactions is already proven by Rizzardo et al.[14] and by Busfield et al.[15−18] Identification of 8 different radicals formed in the system of ethyl vinyl ether and methyl methacrylate during the initiation is a good example. However, application of liquid chromatography for the analysis restricts their method to low molecular weight trapping products. Our results open the possibility to use ^{15}N NMR as an alternative analytical tool. This method enables to also analyze alkoxyamines that cannot be separated physically. It is expected that this situation will occur after the trapping of macroradicals, because different terminal units of the macromolecular alkoxyamines formed are attached to chains having the same average size and composition. The results obtained by ^{15}N NMR measurements may enable to discriminate among various possible alkoxyamines by extrapolation of the information about the chemical shifts of low molecular weight model compounds to their macromolecular analogues. Low molecular weight model compounds have been applied for the assignment of the characteristic ^1H and ^{13}C NMR chemical shifts to different functional groups of polymers in the work of Kolbert et al.[19,20] The authors have used these assignments to discriminate among vinyl, vinylidene, and vinylene end groups formed during extrusion of ethylene−propylene copolymer. Due to the specific chemical shifts of the end groups, Kolbert and co-workers were able to quantify the occurrence of the various end groups using natural abundance ^{13}C NMR. The polymers in their study had molar masses in the range of $10^4 < M_n < 10^5$. In our work, it is clear that the trapping of the radicals leads to a very specific chemical shift of the α carbon atom of the alkoxy group into an empty part of the (polymer) ^{13}C NMR spectrum. The presence of the electron-withdrawing nitroxide leads to chemical shifts in the range of 80−84 ppm, where the exact peak position is controlled by the nature of the other substituents (see Table 1). This could be used as an additional method to quantify the radical chain ends in a free radical copolymerization. Similarly, the discrimination among five membered and six membered cycles in the structure of the polymer chain formed by the cyclopolymerization of diallyldimethylammonium chloride is performed by assignment of ^{15}N NMR chemical shifts using low molecular weight model compounds. The exclusive formation of five-membered rings has been proven.[21] Bevington[22] has applied an analogous method in the investigation of fragments of AIBN attached to macromolecules during the process of polymerization. He proved that during initiation $(CH_3)_2(CN)C-$ is the only initiator fragment incorporated in the polymer. Our results enable to extend the application of ^{15}N NMR spectroscopy to the investigation of products formed during the trapping of macromolecular radicals.

Conclusions

Synthetic methods developed by various research groups in the past have been optimized for the preparation of ^{15}N labeled derivatives of 1-ethoxy-2,2,6,6-tetramethylpiperidine. These methods enabled to prepare a set of 8 compounds by variation of three structural units. The effects of the units on the ^{15}N NMR spectra are systematically evaluated as relation of the chemical shift differences to the structural differences in pairs of the particular compounds.

(14) Rizzardo, E.; Serelis, A. K.; Solomon, D. *Aust. J. Chem.* **1982**, *35*, 2013.
(15) Busfield, W. K.; Jenkins, I. D.; Van Le, P. *Polymer Bull.* **1996**, *36*, 435.
(16) Busfield, W. K.; Jenkins, I. D.; Monteiro, M. J. *Polymer* **1997**, *38*, 165.
(17) Busfield, W. K.; Jenkins, I. D.; Monteiro, M. J. *J. Polym. Sci.: Part A: Polym. Chem.* **1997**, *35*, 263.
(18) Busfield, W. K.; Jenkins, I. D.; Van Le, P. *J. Polym. Sci.: Part A: Polym. Chem.* **1998**, *36*, 2169.
(19) Kolbert, A. C.; Didier, J. G.; Xu, L. *Macromolecules* **1996**, *29*, 8591.
(20) Kolbert, A. C.; Didier, J. C. *J. Polym. Sci., Part B, Polym. Phys.* **1997**, *35*, 1955.
(21) Masterman, T.C.; Dando, N. R.; Weaver, D. G.; Seyerth, D. *J. Polym. Sci. Part B: Polym. Phys.* **1994**, *32*, 2263.
(22) Bevington, J. C.; Huckerby, T. N.; Hutton, N. W. E. *Eur. Polym. J.* **1982**, *18*, 963.

The most extensive change of the ^{15}N NMR chemical shift is found with the structural variations altering the nature of the α carbon atom of the alkoxy group. Substitution of hydrogen for methyl transforms the secondary carbon into a tertiary one and causes the largest change in the chemical shift in the ^{15}N NMR spectrum. The nature of the functional group (methoxycarbonyl or phenyl) attached to the α carbon has also a significant, but somewhat smaller effect. The ^{15}N isotope is separated from the α carbon only by the oxygen atom in the alkoxyamine and mutual effects of their nuclei on the NMR resonances are not surprising. It is also confirmed by the detection of the N−C and N−H spin−spin coupling between the ^{15}N and α carbon or proton attached to the α carbon, respectively.

The effect of the substituents attached to the α carbon will enable the product analysis after radical trapping. The carbon in the α position represents the reactive center of the trapped radical. The chemical shifts of the trapping products may provide information about the structure of the radical. This sensitivity in ^{15}N NMR is combined with the simplicity of the single peak spectra. It provides possibilities to analyze complex mixtures of trapping products without preliminary separation. The features mentioned above open possibilities to use ^{15}N NMR spectroscopy in the investigation of complex radical reactions.

The ^{15}N isotope also interacts with the remote nuclei in the alkoxyamine molecule as proven by the detection of N−H spin−spin coupling in ^{1}H NMR spectra. The remote functional group attached to the piperidine ring in the 4-position has a relatively small but significant effect on the ^{15}N NMR chemical shift. The difference between the chemical shifts caused by the variation of the remote functional unit is still large enough to avoid overlap of the peaks and can also be utilized for the analysis.

Finally, due to the presence of the nitroxide-substituent in the alkoxyamine, the chemical shifts of the α carbon atom of the alkoxy groups in ^{13}C NMR are in a part of the spectrum (80−84 ppm) that is quite empty. This may provide an additional tool for the identification and quantification of trapped (macro)radical chain ends using natural abundance ^{13}C NMR.

Experimental Section

All experimental details can be found in the Supporting Information.

Acknowledgment. We acknowledge the Dutch Science Foundation (NWO, Council area CW) for financial support of this study.

Supporting Information Available: Experimental details. This material is available free of charge via the Internet at http://pubs.acs.org.

JO034667Q

CHAPTER 3

Chapter 3 entails a study into the terminal monomer unit in a growing copolymer chain. Based on the relative reactivities of growing chains and the two comonomers, there is an equilibrium between the two possible chain ends. Different copolymerization models predict different ratios of the terminal monomer units in growing chains. This work shows that despite some limitations, the experimental determination of the ratio via ^{15}N NMR allows for model discrimination that is not possible by other techniques.

Determination of the Free Radical Concentration Ratio in the Copolymerization of Methyl Acrylate and Styrene. Application of Radical Trapping and ^{15}N NMR Spectroscopy

Peter Kelemen[†] **and Bert Klumperman***

Laboratory of Polymer Chemistry, Department of Chemical Engineering, Eindhoven University of Technology, P.O. Box 513, 5600 MB, Eindhoven, The Netherlands

Received June 7, 2004; Revised Manuscript Received September 28, 2004

ABSTRACT: ^{15}N-labeled nitroxides are employed to trap propagating radicals in the copolymerization of styrene and methyl acrylate. The resulting polymeric alkoxyamines are analyzed by ^{15}N NMR. The assignment of the observed bands to the two possible end groups of the propagating copolymer chain is achieved by comparison of the spectra with the homopolymer alkoxyamines. Copolymers in the suitable molar mass range for the current investigation are obtained by the formation of initiating radicals and nitroxyl radical traps in situ, from a low molar mass ^{15}N-labeled alkoxyamine.

Introduction

The elucidation of the mechanism of free radical copolymerization remains an open problem. Comparison of experimental data (average propagation rate constant $\langle k_p \rangle$ and copolymer composition (F)) with model predictions reveals that different models describe the data equally well.[1] It is not possible to discriminate among the models that are based on qualitatively different mechanistic assumptions. The problem of the discrimination among the models originates from the fact that two types of reactants play a role in the process, i.e., radicals and monomers.

$$P^{\bullet}_{A} + M_{A(S)} \rightarrow P^{\bullet}_{A(S)}$$

$$P^{\bullet}_{S} + M_{A(S)} \rightarrow P^{\bullet}_{A(S)}$$

It should be noted that the subscripts A and S refer to acrylate and styrene, respectively. The applicability of the presented technique will not be limited to this comonomer combination. However, readability is enhanced by using A and S instead of indexes like 1 and 2.

The concentrations of comonomers in the copolymerization reaction are determined experimentally and are related to the experimental data of F and $\langle k_p \rangle$. However, there are no experimental data characterizing the concentrations of radicals [$P^{\bullet}_{A}$] or [$P^{\bullet}_{S}$]. They are commonly calculated from the model equations. The validity of the particular model is implicitly assumed in such an approach, and model discrimination becomes inefficient.

Measurement of experimental assumption-free concentrations of the free radicals participating in the copolymerization is the objective of our work. It is focused on the measurement of the concentration ratio of the macroradicals possessing different terminal groups.

$$A = \frac{[P^{\bullet}_{A}]}{[P^{\bullet}_{S}]}$$

Scheme 1. Formation of the Stable Product—Macromolecular Alkoxyamine—by Trapping Reaction of the (Statistical) Copolymer Macroradical with 2,2,6,6-Tetramethylpiperidine-^{15}N-1-oxyl[a]

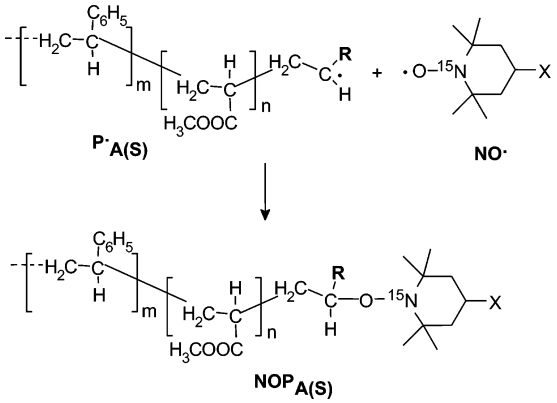

[a] Trapping is applied in the copolymerization of methyl acrylate and styrene. −R = −COOCH$_3$ (P_A, NOP_A) or −C$_6$H$_5$ (P_S, NOP_S).

Knowledge of this quantity for the particular free radical copolymerization should provide additional information for the critical evaluation of copolymerization models.

The main problem in the determination of the ratio A consists of the short lifetime of free radicals and in their low equilibrium concentrations. Our concept of the problem solution is based on the reaction of the propagating macroradicals $P^{\bullet}_{A}$ and $P^{\bullet}_{S}$ with a nitroxide stable free radical [NO$^{\bullet}$]. They are converted into stable macromolecular trapping products NOP_A and NOP_S and subsequently analyzed (Scheme 1). The trapping of the propagating macroradicals in copolymerization and analysis of the macromolecular trapping products are reported here for the first time. The method of radical trapping has been used in the study of complex radical reactions during the initiation of copolymerization,[2−6] but only low molecular weight radicals were involved in that work.

Experimental Section

Materials. The monomers styrene (Aldrich, 99%) and methyl acrylate (Merck, 99+%) were passed through a column containing inhibitor remover and subsequently distilled at reduced pressure under argon. They were stored under an

[†] Present address: VUCHT j.s c., Nobelova 34, 836 03 Bratislava, Slovak Republic.
* Corresponding author. E-mail L.Klumperman@tue.nl.

10.1021/ma048883s CCC: $27.50
Published on Web 11/16/2004

argon blanket at −20 °C and used within 24 h after distillation. The initiator azobis(isobutyronitrile) (AIBN, Merck, >98%) was recrystallized from methanol (Biosolve, p.a.). Alkoxyamine NOR_c (toluene-4-sulfonic acid 2,2,6,6-tetramethyl-1-(1-methyl-1-phenylethoxy)piperidin-^{15}N-4-yl ester) was prepared as described in our previous publication.[7] It was recrystallized from pentane (Biosolve, p.a.) and stored in a closed Schlenk flask under an argon atmosphere. The compound was used within 24 h after recrystallization. Benzene (Biosolve) is purified by distillation. Other solvents of p.a. purity were purchased from Biosolve and used as supplied.

Preparative SEC was carried out as follows. The Injector WISP 710 (Waters) has a maximum injection volume of 200 μL. Six rapid consecutive injections were performed to inject a total volume of 1.2 mL. A Waters pump model 510 operating at a flow rate of 2.0 mL min^{-1} and a Waters differential refractive index detector R401 were employed. As column, a Waters Ultra Styragel 500 Å (19 × 300 mm, bead size 7 μm) was used with THF as the eluent. The experiments were conducted at ambient temperature.

Analytical SEC. The dried polymer was dissolved in tetrahydrofuran (THF, Biosolve) to a concentration of 1 mg/mL. The solution was filtered over a 0.2 μm PTFE syringe filter. Analysis was carried out using a Waters model 510 pump, a Waters model WISP 712 autoinjector, a model 410 refractive index detector, and a model 486 UV detector (at 254 nm). The columns used were a PLgel guard (5 μm particles) 50 × 7.5 mm precolumn, followed by two PLgel mixed-C (5 μm particles) 300 × 7.5 mm columns in series (which were maintained at 40 °C for analysis). The columns used separate polymers in the molecular weight range between 500 and 2 million with high resolution. THF was used as an eluent (flow rate 1.0 mL/min). Data acquisition was performed using waters Millenium 32 (v3.05) software. Calibration was carried out using narrow molecular weight polystyrene (PSTY) standards ranging from 580 to 7 × 10^6 g/mol.

Procedure of Copolymerization and Trapping. The procedure for the copolymerization and trapping can be exemplified by the detailed description of the experiment with a fraction of methyl acrylate f_A = 0.93 in the comonomer mixture. A 10 mL volumetric flask was charged with the alkoxyamine NOR_c (toluene-4-sulfonic acid 2,2,6,6-tetramethyl-1-(1-methyl-1-phenylethoxy)piperidin-^{15}N-4-yl ester) (0.201 g, 0.451 mmol), AIBN (0.026 g, 0.158 mmol), styrene (0.402 g, 3.85 mmol), and methyl acrylate (4.403 g, 51.15 mmol). Benzene was added to a total of the reaction mixture of 10 mL at 20 °C. The solid compounds NOR_c and AIBN were dissolved, and the mixture was transferred into a clean and dry Schlenk flask equipped with magnetic stirrer bar. The Schlenk flask was connected to the vacuum line and the argon inlet. The mixture was degassed by three freeze−pump−thaw cycles. The flask was filled with argon after the last cycle. The Schlenk flask was then transferred into the thermostated bath and heated at 70.0 ± 0.1 °C for 16 min under continuous stirring. The reaction mixture was subsequently cooled to −20 °C.

Separation and Purification of Macromolecular Trapping Products. The flask was opened, and 0.1 g of a nitroxide radical (2,2,6,6-tetramethyl-4-piperidinol-1-oxyl, 0.026 mol) dissolved in 2 mL of benzene was added to the reaction mixture to prevent undesired polymerization during further processing.

The reaction mixture was transferred quantitatively to the preweighted 50 mL round-bottom flask equipped with a magnetic stirrer bar. The flask was mounted in a distillation setup. The condenser of the setup was cooled to −10 °C. This setup allows the evaporation of all volatile constituents of the reaction mixture at temperatures below 25 °C under vacuum. The solid residue was weighed after the evaporation of volatiles (0.518 g), and the mass of the formed copolymer (0.237 g) was estimated by correction for the nonvolatile constituents of the reaction mixture. The copolymer mass corresponded to a comonomer conversion of 4.9%.

The solid residue was redissolved in 10 mL of tetrahydrofuran and purified via preparative SEC. The entire amount was purified in seven runs of 1.2 mL of crude polymer solution.

Table 1. Experimental Conditions of Radical Trapping during the Copolymerization of Methyl Acrylate and Styrene[a]

f_A	[AIBN] (mol L^{-1})	[NOR] (mol L^{-1})	reaction time (min)	conv (%)	$B_{measured}$
0.97	0.05	0.05	25	6.8	0.45
0.96	0.03	0.06	14	4.2	0.30
0.93	0.015	0.045	16	4.9	0.17
0.86	0.015	0.06	14	4.4	∼0
0.28	0.015	0.07	15	3.9	∼0

[a] Values of experimentally determined ratio of macromolecular trapping products B = [NOP_A]/[NOP_S].

Scheme 2. Reaction Scheme of Preparation of the Macromolecular Model Compound Ib

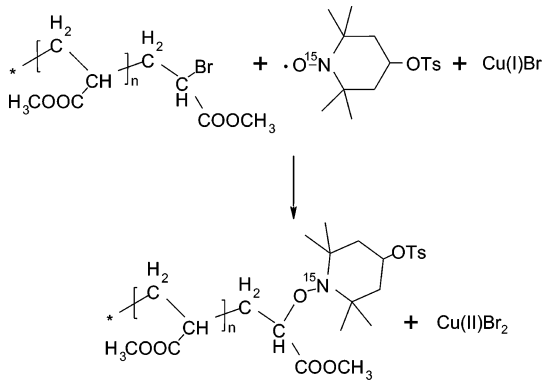

The effluent was divided in 2 mL fractions. Fractions containing copolymer were eluted in time interval corresponding to the elution time of the polymer signal of the RI detector. Fractions containing mainly unreacted NOR_c, AIBN, and further low molecular weight impurities elute later. Fractions of polymer that immediately preceded the first impurity fraction were discarded to ensure the absence of any impurity in the sample. The polymer was isolated by evaporation of tetrahydrofuran in a vacuum at ambient temperature. Seven purification runs were performed to obtain 0.18 g of purified polymer. The polymer was dissolved in 1 mL of the $CDCl_3$, and this solution was used for the ^{15}N NMR measurement.

^{15}N NMR spectra were measured on Unity Inova 500 MHz spectrometer. Conditions of FID acquisition were as follows: transmitter frequency, 50.6 MHz; pulse width, 10.0 ms; spectral width, 8 kHz; filter bandwidth, 4 kHz; acquisition time, 2 s; number of data points, 32 000; delay in pulse sequence, 10 s. Proton decoupling in asynchronous mode was applied using the WALTZ 16 modulation. Nitromethane was used as a chemical shift standard. The signals of 5000 pulses were accumulated for further processing.

Signal Processing. The FID signals were weighted using an exponential window function $\exp(-t\pi l)$ with line broadening parameter l = 1 Hz. Subsequent Fourier transformation provided the NMR spectrum. Phase and baseline of the spectra were corrected. The signal intensities in the regions corresponding to different structures of the terminal segments were integrated. The results obtained for various f_A are given in Table 1.

Preparation of Model Compounds. The preparation of low molecular weight model compounds **Ia**, **IIa**, and **IIIa** was described in our previous publication.[7] Macromolecular model compounds were prepared as follows:

*Poly(methyl acrylate) Capped with ^{15}N-Labeled Alkoxyamine Group **Ib**.* The preparation scheme is depicted in Scheme 2. The preparation is based on the procedure of Matyjaszewski et al.[8]

The ethyl 2-bromoisobutyrate (0.9753 g, 5.03 mmol), ethyl acrylate (9.35 g, 109 mmol), and xylene (16.35 g, 18.9 mL) were mixed in a three-necked flask equipped with condenser, magnetic stirrer bar, and argon inlet. The mixture was flushed with argon for 60 min, and then CuBr (0.29 g, 2.0 mmol), $CuBr_2$ (0.11 g, 0.5 mmol), and *N*,*N*′,*N*″,*N*″-pentamethyldieth-

ylenetriamine (0.43 g, 2.5 mmol) were added. The reaction proceeded at 65 °C for 6 h. The mixture was then diluted with tetrahydrofuran and passed through a layer of basic alumina to remove the copper complex. The solvents were subsequently evaporated. The resulting polymer was analyzed by SEC and found to possess an M_n = 1850 g/mol and PDI = 1.06.

The polymer prepared in the previous step was used as a precursor in the preparation of the model compound **Ib**. The polymer (1 g, 0.54 mmol) was dissolved in benzene (10 mL). Toluene-4-sulfonyl-(2,2,6,6-tetramethylpiperidin-^{15}N-1-oxyl)-4-1-yl (213 mg, 0.65 mmol), copper triflate (72 mg, 0.2 mmol), copper (700 mg, 11 mmol), and 2,2′-di-*tert*-butylbipyridyl (109 mg, 0.4 mmol) were added. The reaction mixture was degassed by three freeze−vacuum−thaw cycles and stirred at 75 °C for 16 h. Benzene was evaporated in vacuum. The polymer was redissolved in tetrahydofuran and passed through a layer of basic alumina. The polymer was separated from low molecular weight impurities using preparative SEC under the conditions described in the section Purification and Isolation of Trapping Compounds.

The yield of the substitution was estimated from the comparison of the theoretical number of alkoxyamine end groups calculated from the M_n determined by SEC and the total number of end groups determined from the ^{1}H NMR spectrum of the prepared polymer. Four aromatic protons of the 4-methylphenylsulfonyl group present two doublets in the region of 7.26−7.32 and 7.68−7.74 ppm. They do not overlap with other peaks of the polymer spectrum. The relative contents of the end groups can be calculated from the ratio of their integral and the integral of the peak corresponding with the protons of the methoxy carbonyl side groups in the poly(methyl acrylate) polymer (3.50−3.64 ppm). The measured ratio of these integrals (4.82×10^{-2}) corresponds with a ratio of 36.2 alkoxyamine end groups per 1000 monomer units. The theoretical ratio calculated from the M_n measured by SEC is 46.5 per 1000 units. Their comparison provides a yield of substitution of 78%.

*Polystyrene Capped with ^{15}N-Labeled Alkoxyamine Groups **IIb** and **IIIb***. Model compound **IIb** (polystyrene capped with the alkoxyamine end group, substituent = −OH) was prepared by nitroxide-mediated living radical polymerization of styrene initiated with 2,2,6,6-tetramethyl-1-(1-phenylethoxy)piperidin-^{15}N-4-ol.

Initiator (80 mg, 0.29 mmol), styrene (1.50 g, 14.4 mmol), and toluene (1.1 g) were mixed in a three-necked flask equipped with condenser, magnetic stirrer bar, and argon inlet to obtain a solution of reactants of total volume 2.9 mL. The solution was flushed with argon for 45 min and stirred at 105 °C for 26 h. After the reaction time was over, the reaction mixture was poured into methanol (150 mL). The precipitate was filtered, washed with another 100 mL of methanol, dried, and weighed to determine the yield of 260 mg of the polymer. The monomer conversion of 17.3% corresponds with a theoretical $M_{n,th}$ = 900 g/mol. The M_n found by SEC was substantially higher ($M_{n,exp}$ = 2300 g/mol, PDI = 1.04). The difference can be explained from the method employed for the polymer isolation. Because of the relatively low molar mass of the polymer, there will be a fraction that does not precipitate upon pouring the reaction mixture into methanol. This results in an underestimated conversion and $M_{n,th}$ calculated from the conversion. In addition, the predominant loss of the lower molecular weight fraction increases the apparent $M_{n,exp}$ as measured from the precipitate. The kinetic measurements of the nitroxide-mediated free radical polymerization were not the goal of our work, and the obtained amount of the sample was sufficient for ^{15}N NMR measurement. However, all other samples were isolated by preparative SEC instead of by precipitation.

Model compound **IIIb** (polystyrene capped with the alkoxyamine end group, substituent −OTs) was prepared by the radical trapping technique as described in the section Procedure of Copolymerization and Trapping. A solution of styrene (5.73 g, 55.0 mmol), AIBN (49.3 mg, 0.3 mmol), and toluene-4-sulfonic acid 2,2,6,6-tetramethyl-1-(1-methyl-1-phenylethoxy)piperidin-^{15}N-4-yl ester (0.134 mg, 0.3 mmol) in benzene possessing a total volume of 10 mL was degassed by three freeze−vacuum−thaw cycles and heated at 70 °C. Monomer conversion was 3.9% after 22 min. The polymer was analyzed by SEC and found to have an M_n = 3350 g/mol and PDI = 1.8.

Scheme 3. Structure of the Low Molecular Weight Model Compound of the Trapping Products NOP[a]

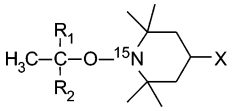

[a] $-R_1 = -C_6H_5$ or $-COOCH_3$; $-R_2 = -Ch_3$ or $-H$; $-X = -OH$ or $-O-SO_2-C_6H_4-CH_3$.

Scheme 4. General Structure of the Macromolecular Model Compound

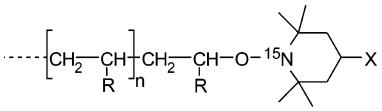

Results and Discussion

Use of ^{15}N NMR in the Analysis of Macromolecular Trapping Products. The macromolecular nature of the trapping products complicates their analysis. They differ only in the structure of their terminal unit. Other properties (average composition, molecular weight, etc.) are practically the same and do not allow an analysis based on physical separation.

The described method of analysis of the macromolecular trapping products is based on ^{15}N NMR spectroscopy of the obtained alkoxyamines. We have measured the ^{15}N NMR spectra of low molecular weight alkoxyamines in previous work.[7] Their general structure (Scheme 3) shows that they are low molecular weight models of the macromolecular trapping products NOP.

The ^{15}N NMR spectrum of any low molecular weight model alkoxyamine consists of a single sharp peak.[7] The chemical shift of the peak is affected by structural details of the alkoxyamine. The most significant effect has been observed with the functional groups $-R_1$ and $-R_2$. The simplicity of the ^{15}N NMR spectra and the differences in the chemical shifts provide a possibility to analyze the mixture of the low molecular weight alkoxyamines without their previous separation.

The expected trapping products NOP_A and NOP_S are of macromolecular nature. It was therefore necessary to investigate also macromolecular model compounds (Scheme 4). Higher complexity of their ^{15}N NMR spectra is revealed when compared with the spectra of the low molecular weight alkoxyamines (Figure 1). The spectra consist of multiple broad bands instead of single peaks. The spectral bands of each macromolecular alkoxyamine are located in the region of chemical shifts that corresponds well with the chemical shift of the single peak in the spectrum of its low molecular weight analogue.

The chemical shifts of the low molecular alkoxyamine having the functional group $-R = -C_6H_5$ are 9.7 ppm lower than that of the alkoxyamine having $-R = -COOCH_3$. Spectra of the macromolecular alkoxyamines are compared in a similar manner. Lower and upper limits of the ranges where the spectral bands occur are taken into account. The values of the lower and upper limit of the macromolecular alkoxyamine with $-R = -C_6H_5$ are 11.4 and 10.7 ppm lower, respectively, than the limits found in the spectrum of the alkoxyamine with $-R = -COOCH_3$.

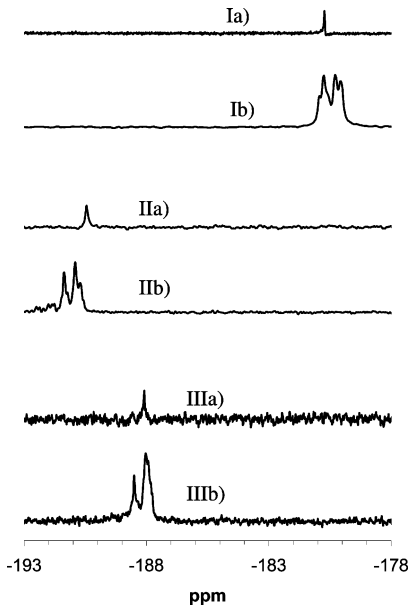

Figure 1. ^{15}N NMR spectra of macromolecular model compounds compared with the spectra of low molecular weight model compounds. **Ia**: low molecular weight, $-R_1 = -H$, $-R_2 = -COOCH_3$, $-X = -OTs$. **Ib**: macromolecular, $-R = -COOCH_3$, $-X = -OTs$. **IIa**: low molecular weight, $-R_1 = -H$, $-R_2 = -C_6H_5$, $X = -OTs$. **IIb**: macromolecular, $-R = -C_6H_5$, $-X = -OTs$. **IIIa**: low molecular weight, $-R_1 = -H$, $-R_2 = -C_6H_5$, $-X = -OH$. **IIIb**: macromolecular, $-R = -C_6H_5$, $-X = -OH$.

The functional group $-X = -OTs$ is present in the alkoxyamines compared above. It is also possible to compare the spectra of macromolecular alkoxyamines with $-R = -C_6H_5$ and differing in their functional group $-X$. The values of the lower and upper limits of the macromolecular alkoxyamine with $-X = -OTs$ are 3.4 and 2.9 ppm lower, respectively, than those in the spectrum of the macromolecular alkoxyamine with $-X = -OH$. A similar comparison between low molecular weight model compounds resulted in a chemical shift difference of 2.3 ppm.[7]

This comparison shows that the differences in the structure of the functional groups $-R$ and $-X$ affect the chemical shifts of the ^{15}N NMR spectra of macromolecular alkoxyamines in the same manner as in the spectra of their low molecular weight analogues. Their complicated nature can be explained by the effect of functional groups located at larger distance from the ^{15}N nucleus. It is well-known from ^{13}C and ^{1}H NMR spectroscopy that the chemical shifts of particular nuclei are affected by the steric configuration of adjacent units. The chemical shift of the macromolecular alkoxyamine in the ^{15}N NMR spectrum is similarly affected by the configuration of groups on the α carbon (terminal unit) and also on more distant atoms (penultimate and antepenultimate units). The macromolecular alkoxyamines are formed by a radical process which is not stereospecific, and they represent a complicated mixture of many stereoisomers. This complexity in the stereochemistry is consequently reflected in the complexity of the ^{15}N NMR spectrum.

The structure of the functional group $-R$ controls the chemical shifts substantially, and spectral bands of alkoxyamines differing in this group are well separated from each other despite their multiplicity and broadening. This result is of high practical importance for our work because it confirms that ^{15}N NMR spectroscopy can be applied in the analysis of macromolecular trapping products.

Scheme 5. Structure of the Thermally Unstable Alkoxyamine NOR$_c$ and Its Decomposition into Trapping Radical NO• and Initiating Radical R$_c^•$

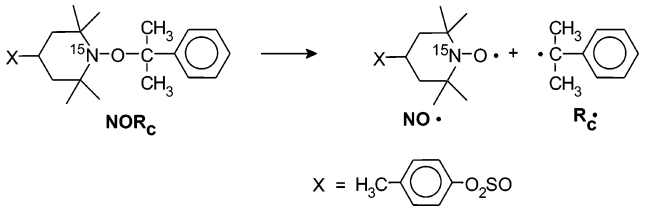

Trapping of Macroradicals by Nitroxyl Radicals Formed "in Situ". The experiments with macromolecular model compounds of the trapping products have shown that the amount of the sample necessary for one measurement is about 10^{-4} mol (sample volume is 1 mL) to achieve sufficient signal-to-noise ratio (SNR) in a reasonable measurement time (12−15 h). The method of radical trapping should allow obtaining this required minimum amount under realistic experimental conditions. The low concentration of macroradicals ($c \approx 10^{-7}$ mol/L) under the conditions of free radical copolymerization sets the necessity to apply a procedure, which enables to accumulate trapping products in the course of the copolymerization.

We have designed a trapping method which is based on the formation of the nitroxide radical in situ from a thermally labile alkoxyamine (Scheme 5)

The process of copolymerization and simultaneous formation of the macromolecular trapping products can be described as follows.

A thermally labile alkoxyamine NOR$_c$ decomposes and forms trapping agent NO$^•$ and initiating radical R$_c^•$.

$$\mathrm{NOR_c} \xrightarrow{k_{dN}} \mathrm{NO^•} + \mathrm{R_c^•}$$

The initiating radical R$_c^•$ reacts quickly with monomer A or S to form propagating radical P$_A^•$ or P$_S^•$.

$$\mathrm{R_c^•} + \mathrm{M_{A(S)}} \rightarrow \mathrm{P_{A(S)}^•}$$

The degree of polymerization of the propagating radicals P$_A^•$ and P$_S^•$ increases as they add more monomer molecules. The equilibrium concentration ratio

$$A = \frac{[\mathrm{P_A^•}]_e}{[\mathrm{P_S^•}]_e}$$

is established due to the cross-propagation reactions

$$\mathrm{P_A^•} + \mathrm{M_S} \xrightarrow{\bar{k}_{AS}} \mathrm{P_S^•}$$

$$\mathrm{P_S^•} + \mathrm{M_A} \xrightarrow{\bar{k}_{SA}} \mathrm{P_A^•}$$

A certain fraction of radicals P$_A^•$ and P$_S^•$ undergoes bimolecular termination to form dead polymer:

$$\mathrm{P_{A(S)}^•} + \mathrm{P_{A(S)}^•} \xrightarrow{\langle k_t \rangle} \mathrm{D}$$

Additional initiator I is present to compensate the loss of the propagating radicals P$_A^•$ and P$_S^•$ by bimolecular

termination. New propagating radicals are formed by fast reaction of the initiating radicals $R_I^\bullet$ with monomers A and S:

$$I \xrightarrow{k_{dI}} 2R_I^\bullet + M_{A(S)} \xrightarrow{2fk_{dI}} P_{A(S)}^\bullet$$

The formation of trapping products proceeds in the reaction of propagating radicals $P_A^\bullet$ and $P_S^\bullet$ with nitroxide radicals $NO^\bullet$ formed in situ:

$$P_{A(S)}^\bullet + NO^\bullet \xrightarrow{k_{cNA(S)}} NOP_{A(S)}$$

The radical trapping must be performed under thermal conditions, where the decomposition of the precursor NOR_c produces a sufficiently large concentration of the trapping agent $NO^\bullet$, and the trapping products NOP_A and NOP_S are still stable enough, so that their eventual decomposition will not interfere with the measured quantity of the radical concentration ratio. Both requirements are fulfilled at a temperature of 70 °C. The estimation of the kinetic data of the decomposition of the alkoxyamines NOR_c, NOP_A, and NOP_S is given in the Supporting Information for the system methyl acrylate−styrene. It proves the fast decomposition of NOR_c as well as the good thermal stability of NOP_A and NOP_S at 70 °C.

The applied trapping with nitroxide radicals formed in situ differs significantly from nitroxide-mediated controlled radical polymerization. In the latter process, the alkoxyamine decomposition, addition of monomers, and nitroxide coupling is repeated many times during the growth of one macromolecule. In contrast, one macromolecular trapping product is formed by one sequence of the elemental reactions mentioned above; i.e., radical trapping is irreversible.

The "in situ" formation of the trapping agent $NO^\bullet$ proceeds homogeneously in the entire reaction volume without any local variation. Its concentration can be simply adjusted by the concentration of precursor NOR_c. Good control over the process of the radical trapping enables to perform it under the conditions, where the macroradicals are predominantly trapped.

It enables to extend the application of the radical trapping to the investigation of the copolymerization process. This is the main advantage of our method in comparison with the trapping performed by direct addition of the trapping agent into the reaction mixture.[2−6] Only low molecular weight trapping products can be prepared by the latter way. The maximum value of their degree of polymerization is eight, and it was achieved by a very cautious tuning of the trapping agent addition.[9]

The details of the importance of the polymerization degree for the determination of the radical concentration ratio A are given in the Supporting Information. The analysis shows, that the ratio A in the presence of the trapping agent $NO^\bullet$ is given by the relation

$$A = \frac{[P_A^\bullet]_e}{[P_S^\bullet]_e} = \frac{\frac{\bar{k}_{SS}}{\bar{r}_S}[M_A] + pk_{cNS}[NO^\bullet]}{\frac{\bar{k}_{AA}}{\bar{r}_A}[M_S] + (1-p)k_{cNA}[NO^\bullet]}$$

where p is the probability that a primary radical adds to monomer A.

When the average degree of polymerization of the trapping products exceeds a lower limit, the ratio A will be independent of the concentration of trapping agent. The ratio A will be then approximated with the equation

$$A = \frac{\bar{k}_{SS}[A]\bar{r}_A}{\bar{k}_{AA}[S]\bar{r}_S}$$

The minimum value of the average polymerization degree depends on particular composition of the monomer feed. It varies from 24 to 50 in the composition range $f_A = 0.15-0.97$ when the system of methyl acrylate−styrene is investigated.

The upper limit of the average polymerization degree is determined by the conditions of the analysis of the trapping products by ^{15}N NMR spectroscopy. The analysis is focused on the alkoxyamine end groups in the sample. The concentration of the end groups decreases with increasing degree of polymerization, and the upper limit of the degree of polymerization is determined by the minimum concentration of the end groups in the sample required for the analysis. Calculations given in the Supporting Information show that the upper limit of the polymerization degree depends on the monomer feed and varies from 51 to 58.

When the trapping proceeds under the conditions of quasi-equilibrium, then the rate of accumulation of the trapping products is determined by the rate of trapping reactions of the two different chain end radicals ($P_A^\bullet$ and $P_S^\bullet$):

$$\frac{\partial[NOP_A]}{\partial t} = k_{cNA}[P_A^\bullet][NO^\bullet]$$

$$\frac{\partial[NOP_S]}{\partial t} = k_{cNS}[P_S^\bullet][NO^\bullet]$$

The ratio of trapping products accumulated during the experiment is then

$$B = \frac{[NOP_A]}{[NOP_S]} = \frac{k_{cNA}[P_A^\bullet]}{k_{cNS}[P_S^\bullet]} = \frac{k_{cNA}}{k_{cNS}}A$$

^{15}N NMR Spectra of Trapping Products. Trapping of macroradicals formed during the copolymerization of methyl acrylate and styrene is performed at various fractions of methyl acrylate (f_A) in the monomer feed. The ^{15}N NMR spectra of the trapping products obtained in these experiments are shown in Figure 2. The appearance of the spectrum depends on the composition of the monomer feed f_A.

Two separate groups of bands can be distinguished in the spectrum of trapping products formed when $f_A = 0.93$ or higher. They are compared with the spectra of trapping products obtained in the homopolymerization of methyl acrylate and styrene (spectra I and VII of Figure 2, respectively). The first group of peaks corresponds with products obtained by trapping of macroradicals possessing a terminal methyl acrylate unit (product NOP_A). They can be found in the region of −179.6 to −181.1 ppm. The relative intensity of these spectral bands decreases significantly with decreasing f_A and cannot be distinguished from the noise line when $f_A \leq 0.86$. The second group can be ascribed to the trapping products derived from macroradical having

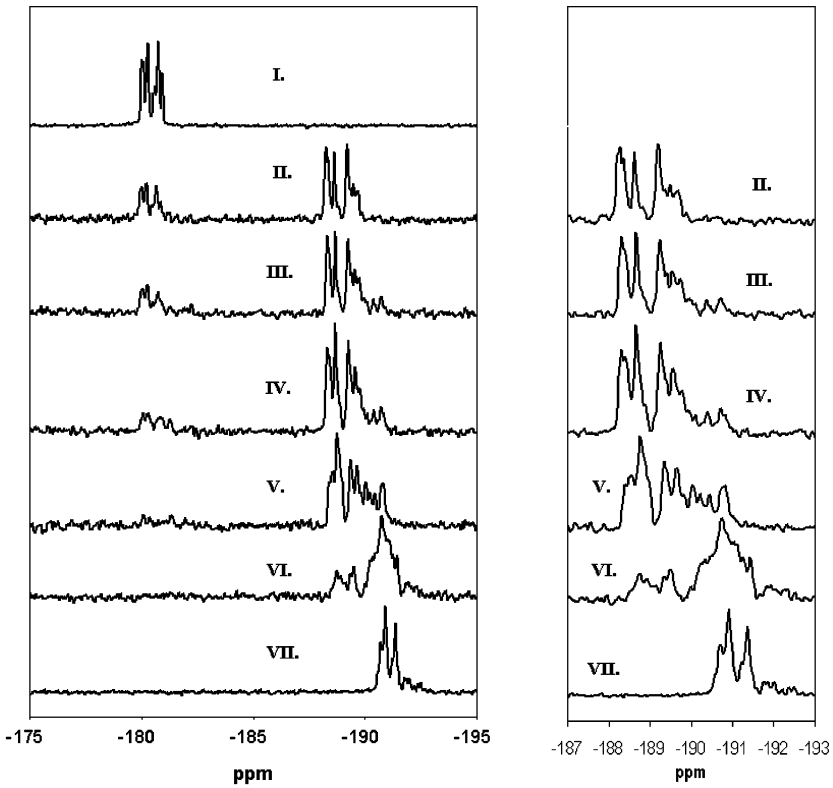

Figure 2. ^{15}N NMR spectra of the trapping products obtained during the copolymerization at various compositions of the monomer feed f_A. I: $f_A = 1.00$; II: $f_A = 0.97$; III: $f_A = 0.96$; IV: $f_A = 0.93$; V: $f_A = 0.86$; VI: $f_A = 0.28$; VII: $f_A = 0.00$. The right-hand side depicts the expanded parts of the spectra in the region −187 to −193 ppm.

styryl terminal unit (product NOP_S). It is located in the region of −192.7 to −188.1 ppm.

The spectral bands ascribed to the products NOP_S are well distinguished from the noise level. Their shape changes with changing f_A. The bands are located in the range from −192.7 to −190.5 ppm when $f_A = 0$. New bands in the range from −190.5 to −188.2 ppm are observed in the spectra when methyl acrylate is present in the monomer feed during the trapping. Their relative intensity increases with increasing f_A, and the intensity of bands in the former region decreases. The spectrum of trapping products obtained at $f_A = 0.97$ has spectral bands related to product NOP_S solely in the region from −190.0 to −188.0 ppm.

This change is explained when the effect of the distant units is taken into account. The spectrum VII is measured for the trapping product having all units (terminal, penultimate, and antepenultimate) derived from styrene. Conversely, trapping products NOP_S formed in the presence of methyl acrylate will possess part of penultimate and antepenultimate units derived from this monomer. These units will affect the ^{15}N NMR spectra of the NOP_S products in a way different from the units derived from styrene. This difference is reflected by change in the location and intensity of the bands in the region from −192.7 to −188.2 ppm.

Radicals $P^{\bullet}_S$ having the penultimate unit derived from styrene ($P^{\bullet}_{SS}$) or from methyl acrylate ($P^{\bullet}_{AS}$) can therefore be identified from the ^{15}N NMR spectra of their trapping products. The mutual concentration ratio of these radicals is given by the equation

$$C = \frac{[P^{\bullet}_{SS}]}{[P^{\bullet}_{AS}]} = r_{SS}s_S\frac{[S]}{[A]}$$

Table 2. Fraction of Radicals $P^{\bullet}_{AS}$ Present in the Reaction Mixture When $f_A = 0.97$ Calculated for Various Values of s_S[a]

s_S	$[P^{\bullet}_{SS}]/[P^{\bullet}_{AS}]$	fraction of $P^{\bullet}_{AS}$ (mol %)
0.94[10]	0.021	97.9
1.10[11]	0.024	97.6
0.59[11]	0.013	98.7
0.41[8]	0.009	99.1

[a] Value of parameter $r_{SS} = 0.73$.

The outcome of the calculation will generally depend on parameters r_{SS} and s_S. The value of parameter s_S is not unambiguously determined, and there are four different values published in the literature. However, in any case this calculation predicts that 97.6−99% of all radicals $P^{\bullet}_S$ will possess a penultimate unit derived from methyl acrylate when f_A is equal to 0.97 (Table 2).

It follows from the above calculation that within the accuracy of the measurement all trapping products NOP_S obtained at $f_A = 0.97$ will possess penultimate units derived from methyl acrylate. They are characterized with ^{15}N NMR spectral bands recorded in the region from −190.0 to −188.0 ppm. On the other hand, spectrum of NOP_S products collected at $f_A = 0$ identifies trapped radicals $P^{\bullet}_S$ having all the penultimate and antepenultimate units derived from styrene. They are located in a separate region from −192.7 to −190.5 ppm. Spectra of trapping products NOP_S obtained at $0.27 \le f_A \le 0.96$ are spread over the entire range −192.7 to −188.2 ppm. Their complexity does not allow an exact assignment to the particular products obtained from radicals $P^{\bullet}_{AS}$ or $P^{\bullet}_{SS}$.

The terminal units in the products NOP_A and NOP_S can be clearly detected from the ^{15}N NMR spectrum because the corresponding spectral bands are located

Table 3. Experimentally Determined Estimates of the Radical Concentration Ratio *A* in the Copolymerization of A and St at 70 °C and Their Comparison with Values Predicted by the Implicit Penultimate Model Using Two Different Sets of Parameters

f_A	$A_{measured}$	A_{calcd} (set 1)	A_{calcd} (set 2)
0.97	≤0.45	2.70	0.106
0.96	≤0.30	2.31	0.083
0.93	≤0.17	1.72	0.051
0.86	∼0	1.14	0.003

in separate regions for any value of f_A. The concentration ratio $B = [NOP_A]/[NOP_S]$ is obtained by integration of the spectral bands. The results are collected in Table 1. As indicated above, the radical ratio A could be estimated if the values of the constants k_{cNA} and k_{cNS} are known. Accurate values of the constants are not measured yet, but they can be estimated from the rate constants measured for the low molecular weight analogues of macroradicals $P^{\bullet}_{MA}$ and $P^{\bullet}_{S}$.[12] The coupling of the methoxycarbonylethyl radical (analogue of $P^{\bullet}_{MA}$) with nitroxide proceeds faster than coupling of the phenyl ethyl radical (analogue of $P^{\bullet}_{S}$). This comparison leads us to the conclusion that

$$\frac{k_{cNA}}{k_{cNS}} \geq 1 \quad \text{and} \quad B \geq A$$

Values of B determined experimentally represent an estimation of the upper limit of the radical concentration ratio A.

The information about the value of A provides a useful tool for the critical evaluation of copolymerization models. A brief illustration of its discriminating power can be exemplified, when two sets of parameters are tested and their ability to predict correct values of A is compared. Both sets predict the copolymer composition and average propagation rate constants equally well in the copolymerization of methyl acrylate and styrene at 50 °C. The first set of parameters is determined by Davis et al.[10] The implicit penultimate model is applied for the description of the copolymerization:

set 1:

$$r_{AA} = r_{SA} = 0.19;\ r_{SS} = r_{AS} = 0.73;\ s_A = 0.11;$$
$$s_S = 0.94;\ k_{AAA} = 1500\ \text{L/(mol s)};$$
$$k_{SSS} = 218\ \text{L/(mol s)}$$

The same process is described by Schoonbrood[11] using another set of parameters:

set 2:

$$r_{AA} = r_{SA} = 0.19;\ r_{SS} = r_{AS} = 0.73;$$
$$s_A = s_S = 0.41;\ k_{AAA} = 10700\ \text{L/(mol s)};$$
$$k_{SSS} = 258\ \text{L/(mol s)}$$

The authors have used different methods for the determination of the homopropagation rate constant of methyl acrylate (k_{AAA}).

Values of A calculated using both sets are compared with the experimentally determined upper limit for various f_A.

It is seen from Table 3 that the first set of parameters overestimates the A value. The second one provides A values lower than the upper limit and is therefore closer to reality.

Application of the experimentally determined upper limit of A in a more detailed analysis of several copolymerization models will be the subject of a separate publication.

Conclusion

Trapping of macroradicals in the process of free radical copolymerization is possible when the trapping agent—a stable nitroxyl radical—is formed in situ from a thermally labile precursor, i.e., an alkoxyamine. This method is applied in the trapping of macroradicals formed during the copolymerization of styrene and methyl acrylate.

The macromolecular trapping products are accessible for analysis via ^{15}N NMR spectroscopy. This method enables to distinguish the structure of the terminal segments of trapped macroradicals. Peaks corresponding to the styrene and methyl acrylate terminal segments are well separated. Their correct assignment is performed by comparison with the ^{15}N NMR peaks of model compounds prepared by independent methods. Integration of the spectrum enables to estimate the upper limit of the concentration ratio of propagating radicals having different terminal units.

Acknowledgment. The authors thank the Chemistry Division of the Dutch National Science Foundation (NWO-CW) for financial support. Prof. J. Lugtenburg (Univ. Leiden) is gratefully acknowledged for stimulating discussions.

Supporting Information Available: Calculations that support the experimental study and indicate the boundary conditions on a kinetic basis. This material is available free of charge via the Internet at http://pubs.acs.org.

References and Notes

(1) Manders, L. G. Pulsed Initiation Polymerization. Ph.D. Thesis, Eindhoven University of Technology, 1997.
(2) Rizzardo, E.; Serelis, A. K.; Solomon, D. *Aust. J. Chem.* **1982**, *35*, 2013.
(3) Busfield, W. K.; Jenkins, I. D.; Van Le, P. *Polym. Bull. (Berlin)* **1996**, *36*, 435.
(4) Busfield, W. K.; Jenkins, I. D.; Monteiro, M. J. *Polymer* **1997**, *38,* 165.
(5) Busfield, W. K.; Jenkins, I. D.; Monteiro, M. J. *J. Polym. Sci., Part A: Polym. Chem.* **1997**, *35*, 263.
(6) Busfield, W. K.; Jenkins, I. D.; Van Le, P. *J. Polym. Sci., Part A: Polym. Chem.* **1998**, *36*, 2169.
(7) Kelemen, P.; Lugtenburg, J.; Klumperman, B. *J. Org. Chem.* **2003**, *68*, 7322.
(8) Matyjaszewski, K.; Woodworth, B. E.; Zhang, X.; Gaynor, S. G.; Metzner, Z. *Macromolecules* **1998**, *31*, 5955.
(9) Zetterlund, P. B.; Busfield, W. K.; Jenkins, I. D. *Macromolecules* **1999**, *32*, 8041.
(10) Davis, T. P.; O'Driscoll, K. F.; Piton, M. C.; Winnik, M. A. *Polym. Int.* **1991**, *24*, 65.
(11) Schoonbrood, H. A. S. Emulsion co- and terpolymerization: monomer partitioning, kinetics and control of the microstructure and material properties. Ph.D. Thesis, Eindhoven University of Technology, 1994.
(12) Sobek, J.; Martschke, R.; Fischer, H. *J. Am. Chem. Soc.* **2001**, *123*, 2849, Table 3.

MA048883S

CHAPTER 4

Chapters 4-7 deal with the early stages of Reversible Addition-Fragmentation Chain Transfer (RAFT) mediated polymerization. It turns out that in many cases a very selective reaction takes place in which the original RAFT agent is converted into a single monomer adduct. We coined the name *initialization* for this process. In chapter 4, the dithiobenzoate-mediated polymerization of styrene is investigated via *in situ* ^{1}H NMR spectroscopy. In this study, the leaving group of the RAFT agent was identical to the primary radical from AIBN decomposition, *i.e.* cyano isopropyl radical.

Reprinted with permission from *Macromolecules* **2004**, *37*, 2383-2394.

Beyond Inhibition: A ^{1}H NMR Investigation of the Early Kinetics of RAFT-Mediated Polymerization with the Same Initiating and Leaving Groups

J. B. McLeary,[†] F. M. Calitz,[†] J. M. McKenzie,[‡] M. P. Tonge,*[,†] R. D. Sanderson,[†] and B. Klumperman*[,†,§]

UNESCO Centre for Macromolecules and Materials, Department of Chemistry and Polymer Science, University of Stellenbosch, Private Bag X1, Matieland 7602, South Africa; Nuclear Magnetic Resonance Laboratories, University of Stellenbosch, Private Bag X1, Matieland 7602, South Africa; and Laboratory of Polymer Chemistry, Eindhoven University of Technology, P.O. Box 513, 5600 MB Eindhoven, The Netherlands

Received October 1, 2003; Revised Manuscript Received January 27, 2004

ABSTRACT: In situ ^{1}H nuclear magnetic resonance (NMR) spectroscopy has been used to directly investigate the processes that occur during the early stages (typically the first few monomer addition steps) of an AIBN-initiated reversible addition−fragmentation chain transfer polymerization of styrene in the presence of the RAFT agent cyanoisopropyl dithiobenzoate at 70 and 84 °C. The change in concentration of important dithiobenzoate species as a function of time has been investigated. It was found that the reaction was extremely selective during the period of consumption of the initial RAFT agent (defined as the initialization period), with almost no production of RAFT-capped chains of degree of polymerization greater than unity until all of the cyanoisopropyl dithiobenzoate was converted to its single monomer adduct. The rate-determining step for this process was found to be the addition (propagation) of the cyanoisopropyl radicals to styrene. During the period where the initial RAFT agent was consumed, fragmentation of formed intermediate radicals strongly favored the production of the tertiary cyanoisopropyl radicals, which were the only significant propagating species during that period. This led to a greater rate of propagation during that period, since the propagation rate coefficient for the cyanoisopropyl radical is greater than that of polystyryl radicals. It was found that inhibition effects can occur in the presence of RAFT agents in homogeneous media when the k_p for initiator fragments is smaller than for long chain radicals, which is a result of this aspect of the RAFT mechanism.

Introduction

Nuclear magnetic resonance spectroscopy is a powerful tool for product analysis. In situ NMR is an elegant way to investigate the kinetics of free radical polymerization reactions. Some pioneering work has been carried out,[1−4] but the limitations of kinetic experiments are usually associated with the complexity of the system to be investigated.

In situ NMR investigation of free radical polymerization is normally extremely complicated due to the nature of a conventional free radical polymerization reaction. High molecular weight polymer forms very rapidly, resulting in peak broadening (two factors often contribute to this: overlap of peaks of many slightly different species and high system viscosities) and difficulty in identifying and examining specific species (usually for the same reasons and also because the very low concentrations of polymer end groups are often below the detection limit of NMR spectroscopy).

In living radical polymerization this situation is significantly different. Living radical polymerization is characterized by a linear increase in molecular weight with monomer conversion and consequently does not usually involve high molecular weight polymer formation early in the reaction.

There are a number of living radical polymerization techniques that are commonly used, each having its own unique characteristics and specific advantages and/or disadvantages. Two of the most well-established techniques are stable free radical mediated polymerization (SFRP)[5,6] and atom transfer radical polymerization (ATRP),[7−10] both of which are reversible end-capping techniques. Recently, there has been a renewed interest in transfer methodology.

Reversible addition−fragmentation chain transfer, or RAFT,[11−16] is a living radical polymerization technique that is extremely versatile and robust. It is compatible with almost all monomers and most conditions that are applicable to conventional free radical polymerization. The RAFT process and its benefits are achieved simply by the addition of a suitable RAFT agent to the polymerization mixture.

In Scheme 1 the elementary reactions for the central exchange process of the RAFT mechanism are depicted. (The main focus of this paper will be on the reactions preceding the central RAFT exchange process, but the central exchange process is used to demonstrate the importance of considering the transfer reactions as bimolecular processes.) The process requires the interaction of two species. The first species is the incoming radical, which adds to the sulfur, across the carbon−sulfur double bond of the thiocarbonyl species. The second species is the thiocarbonyl thio compound, the

[†] Department of Chemistry and Polymer Science, University of Stellenbosch.
[‡] Nuclear Magnetic Resonance Laboratories, University of Stellenbosch.
[§] Eindhoven University of Technology.
* Authors for correspondence: e-mail mptonge@sun.ac.za, fax +27-21-808 4967; e-mail l.klumperman@tue.nl, fax +31 (40) 2463966.

10.1021/ma035478c CCC: $27.50
Published on Web 03/04/2004

Scheme 1. Elementary RAFT Process as Commonly Accepted in the Literature[11]

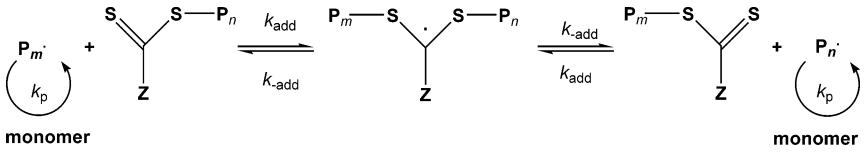

mediating species in the polymerization, which is referred to as the RAFT agent.

There are a number of mysteries regarding the details of the mechanism of the RAFT process. If the central exchange process is all that controls the RAFT-mediated polymerization reaction, then there are some common observations that cannot easily be explicitly explained by this mechanism. The most significant anomalies in RAFT systems are the inhibition and retardation phenomena that occur in many polymerizations.[17−19] These anomalous phenomena have been investigated by a number of authors, including ourselves, and most investigations have focused on the fate of the intermediate radical species that is formed in the RAFT process and its effects on polymerization kinetics. In this paper the issue of inhibition is addressed directly, with focus on the cause and length of the observed inhibition period with reference to the reaction temperature. In the first part of the study, a system in which both the initial RAFT agent leaving group and the initiator-derived radical are the same will be considered.

The relatively stable intermediate radical (which will be referred to as Y$^\bullet$) that is formed by the addition process can fragment to release one of two radical species, namely, the original incoming radical species ($P_m^\bullet$, a propagating radical of degree of polymerization m) or the homolytic leaving group ($P_n^\bullet$) that was previously a part of the RAFT agent.

The rate of polymerization in a radical polymerization is a function of the concentration and type of radical available for propagation and is a function of all radical generation and loss mechanisms. If an equilibrium exists in a RAFT system, then

$$K_{eq} = \frac{k_{add}}{k_{-add}} = \frac{[Y^\bullet]}{[P^\bullet][PX]} \qquad (1)$$

Here K_{eq} is the equilibrium constant, k_{add} and k_{-add} are the rate coefficients for addition and fragmentation, [Y$^\bullet$] and [P$^\bullet$] are the concentrations of the intermediate and propagating radicals, and [PX] is the concentration of RAFT-capped chains. K_{eq} should be constant for a particular RAFT agent/monomer combination at a particular temperature and independent of other conditions. In previous studies[20] it was observed that, early in the reaction, the apparent K_{eq} varies with time and overall degree of polymerization of propagating chains. This implies that the rate coefficients of addition and fragmentation vary significantly with propagating chain type and degree of polymerization during the first few monomer additions per growing chain in the RAFT polymerization process.

Previously,[20] it was suggested that this could be due to a number of possibilities, including chain length dependence of the addition and fragmentation rate constants and possibly termination of the intermediate radical species, either reversibly or irreversibly. The possibility of termination of the intermediate radicals has also been investigated by Monteiro et al.[17] and Kwak et al.[18] Barner-Kowollik et al.[19] have approached the problem by discounting the possibility of intermediate radical termination and suggesting that the inhibition period that is observed in some particular RAFT polymerizations, which is reported as being RAFT agent dependent, could be explained (from modeling results) by the concept of slow fragmentation. Most recently, Barner-Kowollik et al.[21] proposed a reduced irreversible termination and a potential reversible termination of the intermediate radical.

The models provided by these previous studies do not fully explain all the phenomena that have been observed or have not been experimentally validated. The slow fragmentation approach is contradictory[22] to published ESR experimental data,[20] and the products of the termination of the intermediate radical have only very recently been shown to form during the course of a polymerization,[23] although the relative probability of those termination events has not yet been determined.

To fully understand the RAFT process, it is important to examine the nature of the radical species that are present in each reaction. Radical reactivities for addition and radical leaving group stabilities are very important factors that, together with reactant concentrations, determine the rates of polymerization in a RAFT-mediated polymerization. Moad and Solomon's review provides a deeper examination of the general factors that affect radical stabilities and reactivities.[24] It is instructive to consider that, within a series, tertiary radicals are typically more stable and less reactive than secondary radicals, and by the same token, primary radicals are more reactive than secondary radicals. Within the three classes of radicals, the substituents play a crucial role in determining radical behavior. Both steric and electronic effects are important to determine rates of reactions with specific molecules.[25,26]

The current study addresses the early reaction (the first few monomer addition steps) of AIBN-initiated styrene polymerization in the presence of the RAFT agent cyanoisopropyl dithiobenzoate at 70 and 84 °C. The early reaction period before complete conversion of the initial RAFT agent to include growing polymer chains is addressed, i.e., the first monomer addition step(s). In situ ^{1}H NMR spectroscopy was used to directly investigate the concentration of several characteristic species, and thus the rate of polymerization, in the first steps of dithiobenzoate-mediated polymerizations.

Experimental Section

Chemicals. Styrene monomer (Plascon Research Centre, University of Stellenbosch, estimated purity ~99% ^{1}H NMR) was washed with 0.3 M KOH and then distilled under vacuum prior to use to remove inhibitor and polymer. Azobis(isobutyronitrile) (AIBN, Riedel De Haen) was recrystallized from AR grade methanol and found to be ~99% pure by ^{1}H NMR. Deuterated solvents (C_6D_6 99.6%, 0.1% TMS, both from Sigma-Aldrich) and pyrazine (99%, Sigma-Aldrich) were used as received.

Sample Preparation. Samples were prepared by weighing out the masses as given in Table 1. The samples were then transferred to NMR tubes. The tubes were flushed with

Table 1. Composition of Reaction Mixtures for in Situ NMR Analysis[a]

	solvent		initiator		styrene		RAFT agent			
sample	mass (g)	mol ($\times 10^{-3}$)	mass (g)	mol ($\times 10^{-5}$)	mass (g)	mol ($\times 10^{-3}$)	mass (g)	mol ($\times 10^{-4}$)	ratio monomer to RAFT agent $[M]_0/[R]_0$	RAFT agent: initiator $\times$ 2 $([R]_0/2[I]_0)$
1[b]	0.300	3.56	0.010	6.75	0.25	2.40	0.107	4.84	4.96	3.96
2[c]	0.300	3.56	0.010	6.10	0.24	2.31	0.100	4.52	5.10	3.70
3[b]	0.365	4.34	0.011	6.71	0.38	3.68	0	0	0	0
4[c]	0.300	3.56	0.010	6.10	0.38	3.68	0	0	0	0

[a] The solvent used was deuterated benzene (99.6%), and the initiator used was AIBN. The RAFT agent is cyanoisopropyl dithiobenzoate (AD). [b] Reaction carried out at 70 °C. [c] Reaction carried out at 84 °C.

ultrahigh-purity nitrogen for 10 min. At this point a sealed glass insert containing the integration reference standard (pyrazine dissolved in C_6D_6) was inserted, and the tubes were sealed. The use of the reference standard was solely for integration purposes.

Analysis. NMR spectra were recorded on a 600 MHz Varian ^{Unity}Inova spectrometer. A 5 mm inverse detection PFG probe was used for the experiments, and the probe temperature was calibrated using an ethylene glycol sample in the manner suggested by the manufacturer using the method of Van Geet.[27] ^{1}H spectra were acquired with a 3 μs (40°) pulse width and a 4 s acquisition time. The chosen pulse angle allowed complete relaxation of all relevant peaks in the sample, the T_1's of the system having been measured and taken into account. For the ^{1}H kinetic experiments, samples were inserted into the magnet at 25 °C, and the magnet was fully shimmed on the sample. A spectrum was collected at 25 °C to serve as a reference. The sample was then removed from the magnet, and the cavity of the magnet was raised to the required temperature (70 or 84 °C). Once the magnet cavity had stabilized at the required temperature, the sample was reinserted (time zero) and allowed to equilibrate for approximately 5 min. Additional shimming was then carried out to fully optimize the system, and the first spectra were recorded approximately 10 min after the sample was inserted into the magnet.

Integration of spectra was carried out both manually and automatically to allow identification of species during formation. Automated integration was carried out using an ACD labs 7.0 ^{1}H processor.

Synthesis of Transfer Agents. The synthesis of bis(thiobenzoyl) disulfide was carried out following the method of Thang et al.,[28] with the modifications of de Brouwer et al.[29] The synthesis of cyanoisopropyl dithiobenzoate was carried out according to the method of Le et al.[11] and purified by liquid chromatography on a silica column using a 4.5:4.5:1 ratio of pentane:heptane:diethyl ether. The product was dried under vacuum to provide the compound with a ^{1}H NMR purity estimated at ~98%.

Results and Discussion

The NMR data that were obtained during the investigation provide instantaneous concentrations of detectable nonradical species in the RAFT reactions. The effect of chemically induced nuclear polarization on the apparent concentrations of the observed NMR signals in the experiments was found to be minimal under the conditions used.

The concentrations and molar ratios of the reaction components used in all of the reactions in this study are summarized in Table 1. A representative selection of ^{1}H NMR peaks that were integrated for this study can be found in Table 2, and a sample spectrum showing the most important peaks after initialization (see below) was completed is shown in Figure 1. Although the styrene peaks in the spectra collected were large in comparison to the species forming, no dynamic range problems were experienced. As can be seen from Figure 1, a good signal-to-noise ratio was achieved, allowing for integration of the smaller peaks in the spectrum.

Table 2. ^{1}H NMR Chemical Shifts of a Representation of Integrated Species Relevant to the Investigation of Initialization in the Cyanoisopropyl Dithiobenzoate-Mediated Polymerization of Styrene[a]

methyl peaks of R groups δ (ppm)	ortho protons of corresponding dithiobenzoate ring δ (ppm)	species
singlet 0.93	N/A	AA
singlet 1.45	doublet 7.71	AD
two peaks 1.01, 0.87	doublet 7.85	ASD
two peaks 0.81, 0.65	doublet 7.90	AS_2D[b]
two peaks 0.89, 0.72	doublet 7.79	

[a] Species AA is tetramethylsuccinonitrile, AD is cyanoisopropyl dithiobenzoate, and AS_nD are the styrene adducts of AD containing n styrene units. [b] Note stereochemistry.

Figure 2 shows the chemical structures of the primary species of interest for this study. For convenience, the following naming convention will be used. Species AD is the initial RAFT agent containing the dithiobenzoate species (D) and the initial cyanoisopropyl leaving group (A), and ASD is the dithiobenzoate species formed by the single styrene (S) adduct of a cyanoisopropyl radical ($A^\bullet$), while AS_2D and AS_3D species are formed by the respective second and third styrene adducts of the cyanoisopropyl radicals. Note that ASD contains one chiral center, and the resonances of the diasterotopic groups in this molecule can be clearly observed (Figure 1). AS_2D is a diastereomer, and consequently while ASD has only two methyl resonances in the ^{1}H NMR spectrum, AS_2D has four.

The assignments of the ^{1}H NMR peaks were confirmed in a number of ways. Initially, the ^{1}H NMR spectrum of each component in the reaction mixture was obtained to ensure the peaks belonging to each component were unambiguously assigned. Observation of AIBN decomposition at 70 and 84 °C by ^{1}H NMR spectroscopy allowed for the assignment of the peak due to tetramethylsuccinonitrile (AA), which forms during this process. Once the reaction had started, AIBN was consumed to produce AA and initiate polymerization. Styrene was consumed to primarily produce ASD, and AD was consumed to produce ASD. The assignment of the ASD peaks was confirmed by comparing the rates of consumption of AD and styrene and the production of the ASD peaks. There was very good agreement in the time evolution of integrated areas of all corresponding peaks. Additionally, it was found that when all of the AD peaks (both methyl and ortho phenyl protons) disappeared, the assigned ASD peaks reached a maximum, and the amount of monomer consumption according to the assigned styrene peaks was in good agreement with the amount required for complete consumption of the AD species. Thus, all assigned peaks showed good consistency in the time dependences of their intensities, and the rate of monomer consumption was internally verified. The assignments of the peaks for AS_2D were similarly made. Further verification of the peak assign-

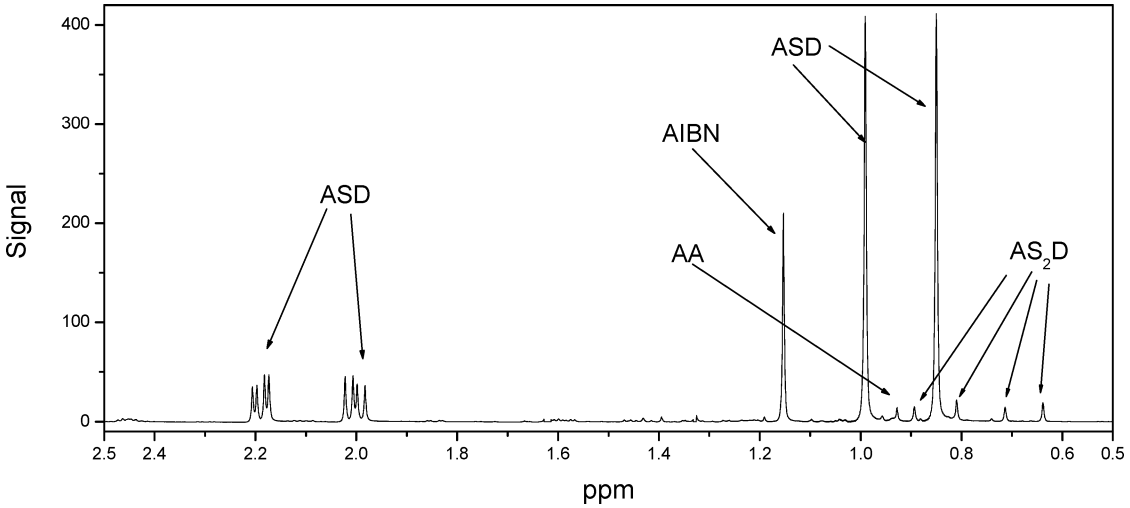

Figure 1. Typical ^{1}H NMR spectrum between 2.5 and 0.5 ppm, directly after initialization, at 70 °C, showing the peaks corresponding to several of the important species studied here. AS_nD are the peaks for the *n*-meric styrene adducts of the cyanisopropyl dithiobenzoate, AA is the product of the termination reaction between two cyanoisopropyl radicals, and AIBN is the initiator. Reactants (reaction 1): 3.56×10^{-3} mol of C_6D_6, 6.75×10^{-5} mol of AIBN, 2.40×10^{-3} mol of styrene, 4.84×10^{-4} mol of cyanoisopropyl dithiobenzoate.

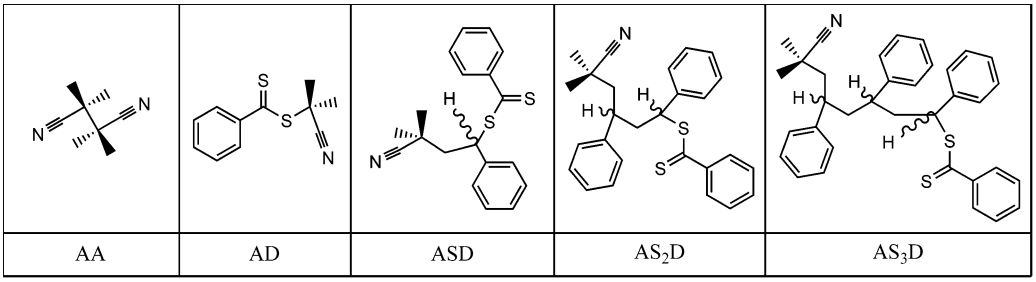

Figure 2. Predominant nonradical species of interest for the investigation of the early period of the free radical polymerization of styrene in the presence of cyanoisopropyl dithiobenzoate, using AIBN as an initiator.

ments was carried out using various NMR experiments on the samples after reaction at room temperature. 2D NMR techniques were investigated, but the most information in regards to confirmation of the peak assignments was obtained by carrying out 1D TOCSY and 1D NOESY experiments. In this way it was possible to identify peaks belonging to a single species and confirm the asssignments. Especially valuable was that the 1D NOESY experiments made it possible to identify the two diastereomers of AS_2D.

This paper addresses, for simplicity, the use of cyanoisopropyl dithiobenzoate as the RAFT agent. The use of this agent, styrene monomer and AIBN as initiator, results in a single active tertiary radical species in the system. This system is far less complex than in the case in which two different tertiary radical species are present, which is discussed in a companion paper.[30] It should be noted that the choice of styrene as a monomer means that the vast majority of radicals formed from propagation reactions should be secondary radicals.

Temperature plays an important role in the rate of reactions in a RAFT-mediated polymerization. For that reason two different temperatures were used to determine whether the results could be explained by the same arguments.

The first experiment was carried out for a period of 4 h at 70 °C, with a reaction mixture containing styrene monomer, cyanoisopropyl dithiobenzoate (species AD), and AIBN initiator (reaction 1, Table 1). Figure 3 shows the time dependence of the concentrations of dithiobenzoate species during this reaction. A rapid decrease in

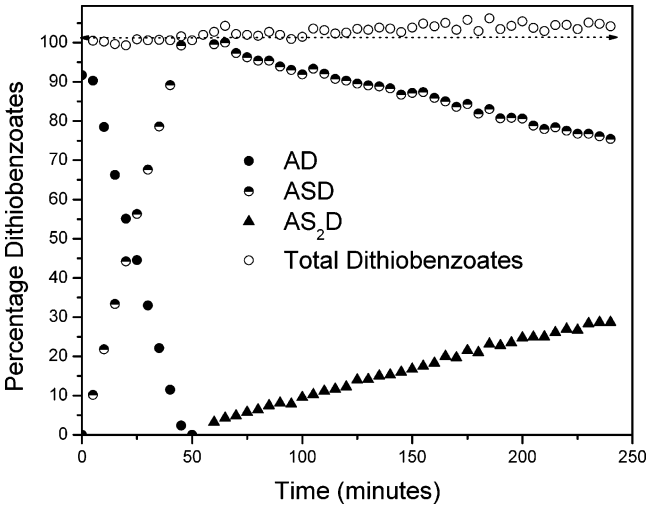

Figure 3. Relative concentrations of methyl protons of dithiobenzoate species vs time in the free radical polymerization of styrene in the presence of cyanoisopropyl dithiobenzoate using AIBN as an initiator polymerized in situ at 70 °C (Table 1, reaction 1: 3.56×10^{-3} mol of C_6D_6, 6.75×10^{-5} mol of AIBN, 2.40×10^{-3} mol of styrene, 4.84×10^{-4} mol of cyanoisopropyl dithiobenzoate).

concentration of the species AD and a buildup of the species ASD until the cyanoisopropyl dithiobenzoate had been completely consumed (after 50 min) were observed. At this point the concentration of species ASD reached a maximum. The nearly linear decrease of [AD] with reaction time is indicative of a pseudo-zero-order reac-

Scheme 2. Steps Involved in the Initialization Period of the RAFT Reaction of Cyanoisopropyl Dithiobenzoate, Styrene Monomer, and AIBN Initiator[a]

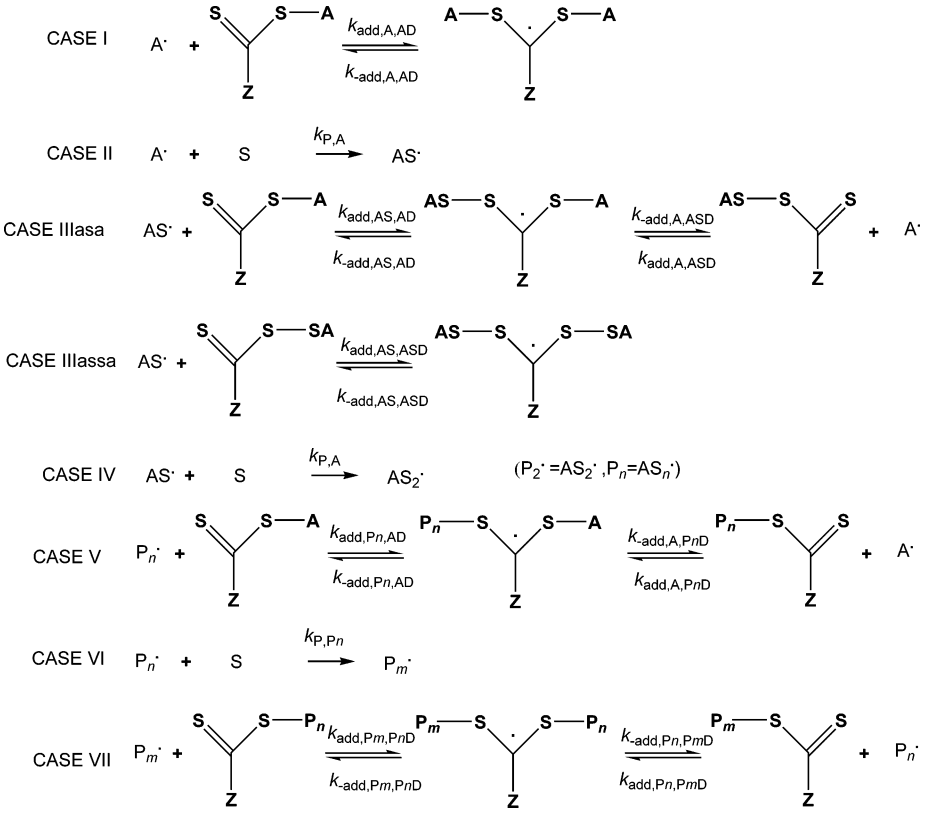

[a] The subcases of case III are variants of reactions of AS• radicals with the two different forms of the RAFT-capped species that are present at that stage of the reaction.

tion in [AD]. Once all of the cyanoisopropyl dithiobenzoate had been converted to ASD (and a very small amount of higher species), the second monomer additions to the radical species begin to increase in frequency (to form species AS_2D). Note that almost no formation of this species occurred before this stage; i.e., the reaction is extremely (although not completely) selective. This will be explained below.

There are several important points to note here. The first is that the conversion of the species AD to ASD is complete, with no detectable "loss" of dithiobenzoate groups to side reactions or the formation of high (detectable) concentrations of intermediate radical species. The termination products for such reactions could not be detected during the course of the reaction (or were below the detection limits of the instrument used), implying that the concentrations of such species were below 10^{-3} M during this reaction. The same was observed for all reactions in this study. The second point to note is that the early reaction is extremely selective. Only one type of radical addition reaction appeared to occur to any significant extent during this initial period (before 50 min), i.e., the propagation of cyanoisopropyl radicals. Very little propagation of longer chain radicals occurred until after this initial period. This also implies that the concentrations of these other propagating radicals and the corresponding thiocarbonylthio-functional dormant chains were very low during this period.

On the basis of the above observations, to facilitate discussion, the following terms are defined: *Initialization* is the process by which the starting RAFT agent is consumed. *Initialization period* is the period in which the starting RAFT agent is consumed. *Initialization time* is the time required for the starting RAFT agent to be completely consumed (converted to other forms). A point to note is that the initialization period is not necessarily the same as a preequilibrium period. "Equilibrium" is not necessarily (probably not) attained immediately following initialization. Also, there are cases where the system might reach a steady state long before initialization is completed. The key point in the current system is that the behavior of the reaction is very different before and after initialization.

Reactions of Radical Species during Initialization. In Scheme 2, the relevant reactions during the polymerization are represented in a way that allows a qualitative discussion on the rate-determining step; termination events are not displayed. The relative probabilities of competing reactions occurring are proportional to their overall rates, which are proportional to the concentrations of reactants and the rate coefficients for the competing processes. The reagent concentrations for this system are a function of a combination of the addition, fragmentation, and propagation rates of the species shown in Scheme 2. It is important to note that there are several different types of intermediate radical species in this period, each of which has different stabilities and (asymmetric) fragmentation rate coefficients. The apparently large differences in addition and fragmentation rate coefficients for the different species involved in this initial period are key to understanding the behavior of the reaction during this period. The most important of these differences is the much faster (preferred) fragmentation rate of intermediates containing a potential tertiary leaving group, to form a RAFT agent and a tertiary radical. This

will be discussed in more detail later. The competing processes and fates of each of the important species in this initial period are now described in detail.

Cyanoisopropyl radicals (A•) generated in the system will undergo one of three main reactions: first, addition to a RAFT agent (relative frequency = k_{add}[RAFT], e.g., $k_{add,AD}$[AD]), for each type of RAFT agent, to form an intermediate radical (these reactions are depicted in cases I, IIIasa, and V; note that case I gives a degenerate product after fragmentation of the formed intermediate radical); second, addition to monomer (propagation, with relative frequency = $k_{p,A}$[M], case II) to give radical species AS•; or third, termination with other radical species.

The radical species AS• can participate in reactions that are similar to the reactions undergone by the A• radicals. These reactions are as follows: first, addition (with different addition rate coefficients) to the RAFT agents (cases IIIasa, IIIassa, or VII); second, propagation with the relevant propagation rate coefficient to form radical species AS_2• (case IV); or third, termination. The products of these processes will be described below.

For the RAFT process to be efficient, propagating radicals must display higher addition rates to the RAFT agent than to monomer.[11] This prevents a possible scenario of rapid propagation to form long chains before the addition−fragmentation process can allow exchange (via the intermediate radical species) between growing chains. Depending on the monomer concentration, a portion of initiator-derived radicals adds directly to the RAFT agent. These reactions cannot be distinguished in the reaction under discussion since when A• adds to AD, eventually resulting in fragmentation to form A•, the overall result is degenerate, and there is no effect on the NMR spectrum. A fraction of A• species will eventually add to a styrene monomer, leading to the formation of AS• in the reaction mixture. The degenerate type of interchange will become evident if the initiating radical is different from the RAFT leaving group (as seen in the second paper of this series[30]).

The fragmentation behavior of each of the formed intermediate radical species is key to the behavior of the early reaction. If the possibility of termination reactions of the intermediate radicals is neglected (probably a good approximation here, since their concentrations during initialization are very small[31]), then each of these intermediate radicals will soon undergo fragmentation, to again produce a propagating radical and RAFT agent. The fragmentation reaction is generally very asymmetric, with a very strong preference to form the more stable propagating radical.

Secondary radical species are more reactive than tertiary radical species with the same substituents (as the reactivity of radical species is inversely related to their stability) when comparing reactions with the same reagents. When radical species with varied substituents are compared, however, care must be taken when making generalizations. Cyanoisopropyl (and cumyl, see the second part of this series[30]) radicals have higher addition rate constants to styrene than the long chain propagation rate constant for styryl radicals.[32,33] These radicals are tertiary and are superior leaving groups and are thus more likely to fragment when attached to a RAFT agent than their respective styryl adducts. For example, in the case of ASDA•, the fragmentation rate, $k_{-add,ASD,A}$, of the tertiary cyanoisopropyl radicals will be much larger than the fragmentation rate, $k_{-add,AD,AS}$, of the secondary AS• radical species (case IIIasa in Scheme 2) due to their higher radical stabilities.[24] This difference in leaving ability generates a large asymmetry in fragmentation rate coefficients for the same intermediate radical (e.g., ASDA•), with the much greater rate coefficient being for the formation of the more stable leaving radical. This implies that the lifetime of intermediate radicals containing at least one tertiary radical will be shorter than for equivalent secondary species, with the large asymmetry in fragmentation rate coefficients leading to a preference for the tertiary radical to result from the fragmentation step. The generated AS• radical species will therefore quickly become end-capped as a thiocarbonyl thio species (ASD) because addition is very fast and will displace tertiary radicals (A• in this case) that are attached to the RAFT agent (case IIIasa). The expelled tertiary radicals can then undergo addition (case I, IIIasa, V) or propagation (case II).

The tertiary radicals (A•) will be unlikely to displace the secondary radical species (e.g., AS•) that are trapped in the dormant state (e.g., case IIIasa) (since the rate coefficient for fragmentation to form the secondary species is much lower than that to form the tertiary species). In such a case, they (A•) will instead begin to behave in a fashion similar to a reversible end-capping reaction such as ATRP or SFRP until such time as they encounter a monomer and propagate, encounter an AD species to form an intermediate radical, before again fragmenting (which has a degenerate end-product after fragmentation), or undergo termination. This means that it is still possible to have a controlled process occurring in the system, but the mechanism by which chains are being activated to allow propagation is different than that of the normal RAFT process.

Almost every cyanoisopropyl dithiobenzoate molecule (AD) in the system is converted to an ASD dormant species before significant concentrations of AS_2• radicals (and therefore any AS_2D or higher dormant species) have the opportunity to develop in the system. This selectivity results from a combination of the fast rates of addition of propagating radicals to the RAFT agent and the extreme asymmetry of the fragmentation step. Accordingly, the formation of AS• radicals (which quickly form the ASD species) becomes the rate-determining step in the process of the formation of ASD from AD. It has been mentioned above that the decrease in RAFT agent concentration initially occurs according to a pseudo-zero-order reaction. ASD cannot form until AS• radicals are formed, which implies that the rate-determining step is the propagation of A• to form AS• (with rate = $k_{p,A}$[M][A•]), since this is much slower than the addition of AS• to AD. The result of this propagation step is visible as the formation of ASD from AD.

As it is unlikely that a secondary radical will be displaced by the addition of a tertiary radical to ASD, the probability of the secondary radical species being reactivated by a transfer step (i.e., case IIIassa, an addition of and then fragmentation to form a secondary species) is dependent on the active concentration of the aforementioned secondary radical species. Since radicals are first formed as tertiary species in this system, which will not activate the secondary radical species by addition to RAFT agents, reactivation of those species depends on both propagation of the cyanoisopropyl radicals and their consequent addition to a RAFT agent

that already contains a dormant secondary species. This will only occur when there is a significant concentration of RAFT agents containing dormant secondary species, which is not the case during the early stages of the initialization period. In the early stages of this period, the rate of addition of AS$^\bullet$ to the initial RAFT agent (containing tertiary species) is too high to allow significant concentrations of AS$^\bullet$ to exist. Thus, the dominant propagating radical will be A$^\bullet$, and the concentration of the secondary radical species (and ASD) will increase until it reaches a maximum after the end of the initialization period (when no AD remains). This has a significant effect on the total concentration of intermediate radical species in the system, since only intermediate radicals with at least two secondary species will be relatively stable. Once a significant concentration of RAFT agents containing dormant secondary species (ASD) is formed at the end of this period, and a significant fraction of secondary radicals are present (AS$^\bullet$), longer chains may form in significant concentrations, and more stable intermediate radicals will form. This should lead to a buildup in intermediate radical concentration, reaching a maximum some time after initialization has been completed. This has indeed been observed in recent ESR spectroscopic studies of this system.[31]

The most prominent criteria for the extremely selective and stepwise behavior in the initialization period, as observed here, are first that the fragmentation of the formed intermediate radicals is very selective toward radicals that have not yet undergone propagation and second that addition of propagating radicals of degree of polymerization of at least unity to the RAFT agent is much faster than to monomer. The first of these criteria will usually hold if the initial leaving group on the RAFT agent is a much better leaving group than that formed after one propagation step, as is the case here. The second criterion will hold if k_{add}[RAFT] $\gg$ $k_{p,1}$[M] (with the appropriate k_{add} for the incoming radical and for all forms of the RAFT agent), which will typically be the case when efficient RAFT agents are used. $k_{p,1}$ (the propagation rate coefficient for a monomeric radical) is chosen here since $k_{p,1}$ is typically greater than k_p. In these systems, most oligomeric radicals will consist of a single monomer unit added to an initiator or RAFT leaving group fragment. If k_{add}[RAFT] $\ll$ $k_{p,1}$[M], then the selective and stepwise behavior will probably not occur since chains of degree of polymerization greater than unity will form before all of the initial RAFT agent has been consumed. Scenarios in which this is likely are when k_{add} (e.g., a low activity RAFT agent, such as a MADIX agent) is small, [RAFT]/[M] is small (e.g., a very high target molar mass), or $k_{p,1}$ is very large (which might occur for some initiators and/or very active monomers). Note that the [RAFT]/[M] ratio can be kept high during initialization, and further monomer added, if this problem arises.

Effects of Temperature. A duplicate reaction was carried out at 84 °C (reaction 2, Table 1). The time dependence of the concentrations of important species is shown in Figure 4. As expected, the reaction rate is substantially faster than in the case of the reaction carried out at 70 °C. In fact, the reaction proceeds so rapidly that the cyanoisopropyl dithiobenzoate is consumed prior to the time the first spectrum was collected. This is presumably due to both the higher radical flux due to initiator decomposition and the higher propagation rate coefficient for the cyanoisopropyl radicals.

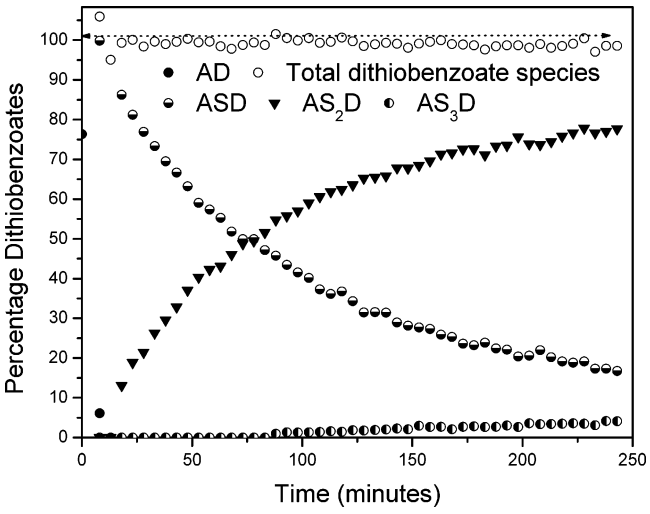

Figure 4. Relative concentrations of ortho protons of the dithiobenzoate rings vs time in the free radical polymerization of styrene in the presence of cyanoisopropyl dithiobenzoate using AIBN as an initiator polymerized in situ at 84 °C (reaction 2, Table 1: 3.56×10^{-3} mol of C_6D_6, 6.1×10^{-5} mol of AIBN, 2.31×10^{-3} mol of styrene, 4.52×10^{-4} mol of cyanoisopropyl dithiobenzoate).

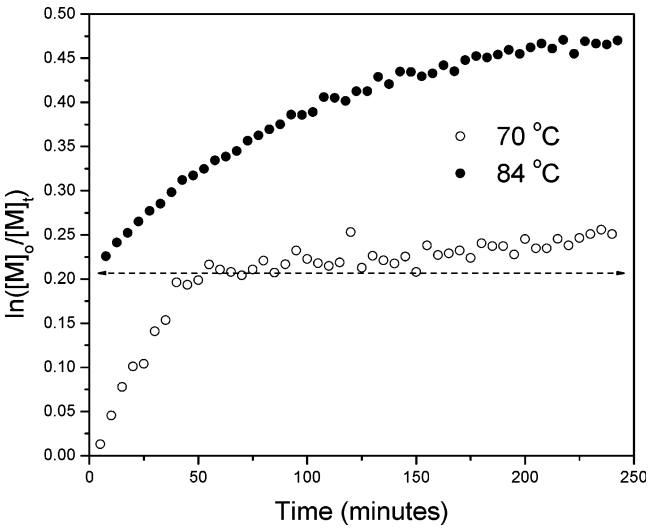

Figure 5. Logarithmic plot of conversion vs time in the reactions of cyanoisopropyl dithiobenzoate with AIBN and styrene in deuterated benzene at 70 and 84 °C. Reactions 1 and 2, Table 1. Reaction 1: 3.56×10^{-3} mol of C_6D_6, 6.75×10^{-5} mol of AIBN, 2.40×10^{-3} mol of styrene, 4.84×10^{-4} mol of cyanoisopropyl dithiobenzoate. Reaction 2: 3.56×10^{-3} mol of C_6D_6, 6.1×10^{-5} mol of AIBN, 2.31×10^{-3} mol of styrene, 4.52×10^{-4} mol of cyanoisopropyl dithiobenzoate.

Overall, the same characteristics were observed at this higher temperature. The reaction showed similar selectivity, with no significant concentrations of AS_2D or higher dormant species formed until after the end of the initialization period, followed by a decrease in rate after the end of the initialization period.

Monomer Consumption. Some interesting observations can be made when comparing the fractional conversion for reactions 1 and 2 in the first-order kinetic plot in Figure 5. The rate of monomer consumption is substantially higher during the initialization period than after this period.

The substantial decrease in rate of reaction after the initialization period at 70 °C is so extreme that after

the initialization period polymerization appears to cease (though it must be noted that it does not, the rate is just so slow that it would not be noticed by most analysis techniques). This is consistent with reports of systems that show little polymerization especially at lower temperatures, even though radicals are being generated in the system.[34]

The rates of polymerization in the reactions, normalized to monomer concentration, are equal to the sum of $k_p[P^\bullet]$ for all propagating species present. The dominant propagating species in the two periods of the polymerization (i.e., initialization and equilibrium) are quite different, namely $A^\bullet$ (cyanoisopropyl radicals) during initialization and $AS_n^\bullet$ (oligostyryl or polystyryl radicals) after initialization. The propagation rate coefficient for the addition of cyanoisopropyl radicals to styrene is 5200 L mol^{-1} s^{-1} at 70 °C,[33] and the propagation rate coefficient for addition of polystyryl radicals to styrene is 480 L mol^{-1} s^{-1} at 70 °C[35] and possibly higher for short oligomeric radicals. The decrease in rate immediately following the end of the initialization period is by a factor of approximately 20. The difference in propagation rate coefficients alone is unable to account for the difference in rates. The only other possibility is that the propagating radical concentration must also have decreased rapidly after initialization, leading to rate retardation that was not present during the initialization period.[23] Thus, the decrease in rate is probably due to a decrease in both the propagating radical concentration (corresponding to the rate retardation commonly observed in dithiobenzoate-mediated free radical polymerization reactions) and the propagation rate coefficient for the dominant propagating radicals in the system. It is important to note that for this reaction there was no apparent inhibition period at the beginning but that the rate of reaction was much higher in the initialization period. This will be discussed further below.

One of the consequences of the initialization period is that the rate of monomer consumption is governed by the rate of conversion of the starting RAFT agent (AD) into the single monomer adduct analogue (ASD). The rate of RAFT agent conversion controls the amount of time taken to change the dominant type of propagating species from that during the initialization period ($A^\bullet$ here) to a different dominant form ($AS_n^\bullet$ here) later. This in turn is governed by the addition rate constants of the R-derived radical (or initiator fragment radical, which is the same in this case) groups to monomer.[32,33] Here it becomes clear that much experimental evidence that has been presented for inhibition in RAFT polymerization[21,36,37] is actually evidence of a slower rate of reaction due to a smaller k_p (than that of the long-chain polymeric radical value) for the R-derived radicals during the initialization period.

In free radical polymerizations, the propagating radical concentration is dependent on the overall rates of initiation and termination and rapidly reaches equilibrium. In a RAFT system there is an extra radical species (intermediate radicals) whose concentration is potentially very significant.[17,20,38] The potential for termination of the intermediate radical, whether reversible or irreversible, is discussed elsewhere.[23] For the purposes of simplification it is assumed that the termination of the intermediate radicals does not significantly change the equilibrium concentration of propagating radicals. This simplification is valid during the initialization period due to the very low concentrations of intermediate radicals in the initialization period; after initialization this assumption may be poor, dependent on the RAFT agent concentration.[23] The discussion will also only consider the case in which the intermediate radical lifetime is not so extensive as to cause rate retardation.

As mentioned earlier, the rate of reaction is significantly faster in the initialization period than after the initialization period for styrene. In contrast, some of the most significant inhibition times that have been reported have been in methyl acrylate (MA) systems.[36] If the methyl acrylate RAFT system using the same RAFT agents used in this study is examined, the following relationship can be derived from literature values:[32,33,39]

$$\frac{k_{p,MA}}{k_{p,A,MA}} \gg 1 \gg \frac{k_{p,STY}}{k_{p,A,STY}} \qquad (2)$$

Here $k_{p,MA}$ and $k_{p,STY}$ refer to the long-chain propagation rate coefficients for MA and STY, and $k_{p,A,MA}$ and $k_{p,A,STY}$ refer to the rate coefficients for the addition of the cyanoisopropyl radical to MA and STY. Assuming, as a first approximation, similar propagating radical concentrations before and after initialization (this is apparently not true here, and usually the propagating radical concentration will be lower after initialization), the relative reaction rates will be primarily dependent on the relevant k_p values. For styrene, this gives a higher rate during initialization than for the period afterward. For MA, a somewhat different rate behavior is predicted, as $k_{p,MA}$ is 13 100 L mol^{-1} s^{-1} [40] at 25 °C and $k_{p,A,MA}$ is 367 L mol^{-1} s^{-1} at 42 °C;[33] i.e., the rate of reaction will be much slower during initialization.

When there is a relatively small amount of RAFT agent present in a reaction (i.e., long chains are targeted), then a very small percentage of the monomer will be consumed during the initialization period. This would be difficult to distinguish from complete inhibition if the target molar mass is high. Monomer to RAFT agent concentration ratios that have been used in the literature are commonly very high,[36] often of the order of a thousand to one. Figure 6 demonstrates this point for both cases where $k_p/k_{p,I}$ (where I is the initiating radical) is greater and less than unity, for different target molar masses. In Figure 6a,b molar ratios of 1:10 RAFT agent to monomer are presented and in Figure 6c,d molar ratios of 1:100 RAFT agent to monomer, assuming constant propagating radical concentrations, in which case the relative reaction rates are proportional to the relevant k_p value. For systems in which the monomer to RAFT agent ratio is not so extreme as to allow for the addition of two monomer units per transfer and in which the transfer rate constant is sufficiently greater than the propagation rate constant, approximately 1 mol of monomer is consumed per mole of RAFT agent during the initialization period. This would be almost indistinguishable from total inhibition (i.e., less than 0.1% conversion would occur during this time), as would cases in which there are oligomers present; e.g., four monomer additions prior to transfer would still be substantially less than 1% of conversion in many systems. It is important to note that examples of systems in which there is supposed to be total inhibition are reported to show color change, which is a well-known indication of polymerization in RAFT-mediated polymerizations. This is consistent with the suggestion

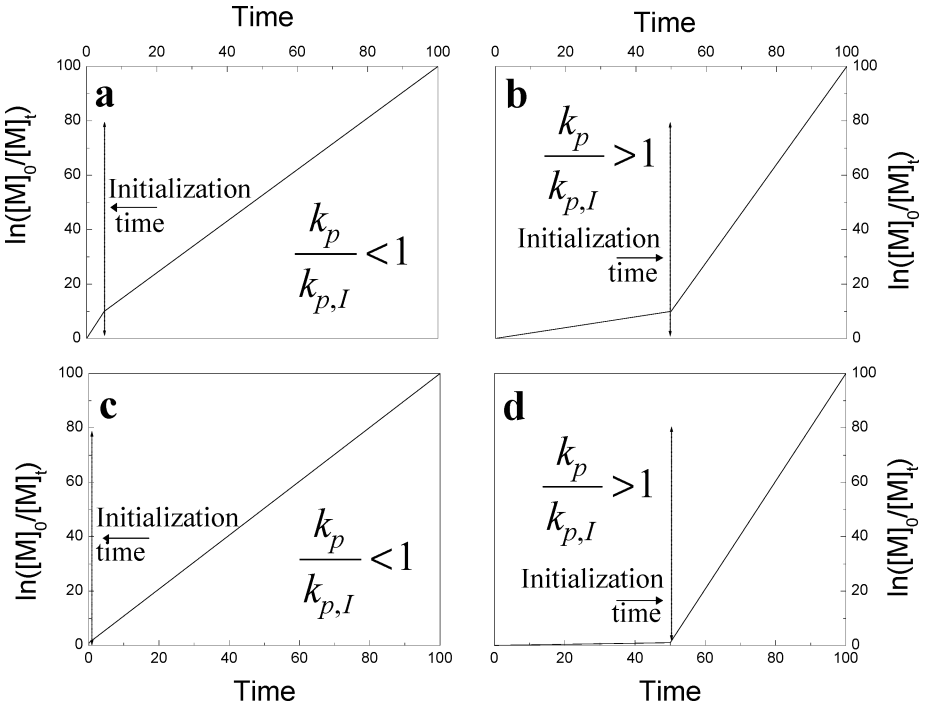

Figure 6. Relationships of the rate of monomer consumption in the two phases of the reaction is indicated in the figures with subscript I referring to equilibrium and initialization, respectively. (a) Case in which the rate of monomer consumption in the equilibrium part of the reaction is higher than in the initialization period (monomer to RAFT agent molar ratio 10:1). (b) Case in which the rate of monomer consumption in the equilibrium part of the reaction is lower than in the initialization period (monomer to RAFT agent molar ratio 10:1). (c) Case in which the rate of monomer consumption in the equilibrium part of the reaction is higher than in the initialization period (monomer to RAFT agent molar ratio 100:1). (d) Case in which the rate of monomer consumption in the equilibrium part of the reaction is lower than in the initialization period (monomer to RAFT agent molar ratio 100:1).

that these systems have an initialization period.[34] Because of the ratios of reagents used in the present study, the initialization period is accentuated.

Radical Generation and Termination Products. The formation of the AA (tetramethyl succinonitrile, TMSN) species in the studied systems was examined in the context of a conventional free radical reaction and initiator (AIBN) decomposition. The AA product is formed by mutual termination of cyanoisopropyl radicals. In Figure 7, the time dependences of the concentrations of AA and AIBN at 84 °C are presented. In reaction 2, the concentration of the AA product shows a slight increase when compared to a control polymerization (reaction 4). The concentration difference appears to be due to an event that generated significant amounts of this product prior to the time of the first scan. This deduction can be made, as the formation of the AA product in reaction 2 appears to be occurring at a slower rate than in reaction 4, suggesting that some event prior to observation caused the different initial concentrations. The higher initial concentration was probably due to the termination behavior of cyanoisopropyl radicals in the initialization period, which could not be examined at the reaction temperature, since initialization was completed before the first scan could be made. The results suggest that the presence of the RAFT agent does not increase the amount of TMSN formation after initialization is complete; i.e., the RAFT agent does not directly promote termination in the system (although it alters the relative populations of propagating radicals, which can change the termination kinetics). The difference in the formed amounts of AA (TMSN) in the RAFT-mediated polymerization and the control lies in the nature of the radical species and the length of the initialization period.

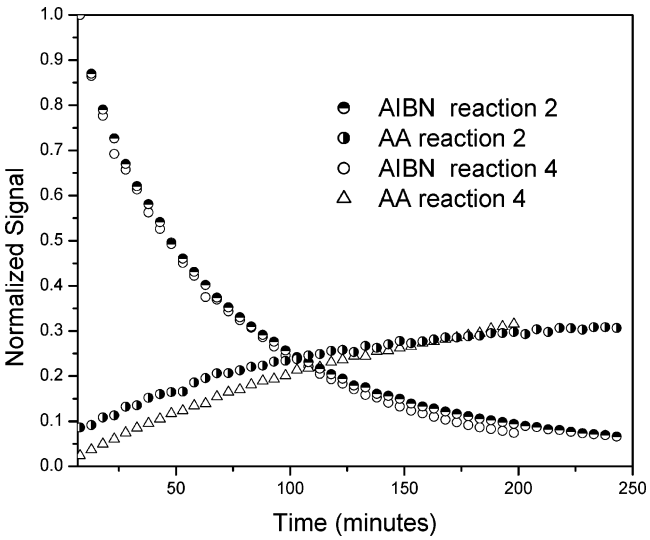

Figure 7. Concentrations of AIBN and AA of reactions 2 and 4 carried out in deuterated benzene at 84 °C. Reaction 2 contains RAFT agent cyanoisopropyl dithiobenzoate, and reaction 4 is a conventional free radical polymerization. Reaction 2: 3.56×10^{-3} mol of C_6D_6, 6.1×10^{-5} mol of AIBN, 2.31×10^{-3} mol of styrene, 4.52×10^{-4} mol of cyanoisopropyl dithiobenzoate. Reaction 4: 3.56×10^{-3} mol of C_6D_6, 6.1×10^{-5} mol of AIBN, 3.68×10^{-3} mol of styrene.

Comparisons between the RAFT-mediated reaction (reaction 2) and the control (reaction 4) at 84 °C (Figure 7) also indicate that the presence of a RAFT agent does not increase the rate of AIBN decomposition.

Figure 8 presents the AIBN and AA product concentrations as determined at 70 °C. The formation of the AA product in reaction 1 occurs at an increased rate throughout the initialization period (lasting approxi-

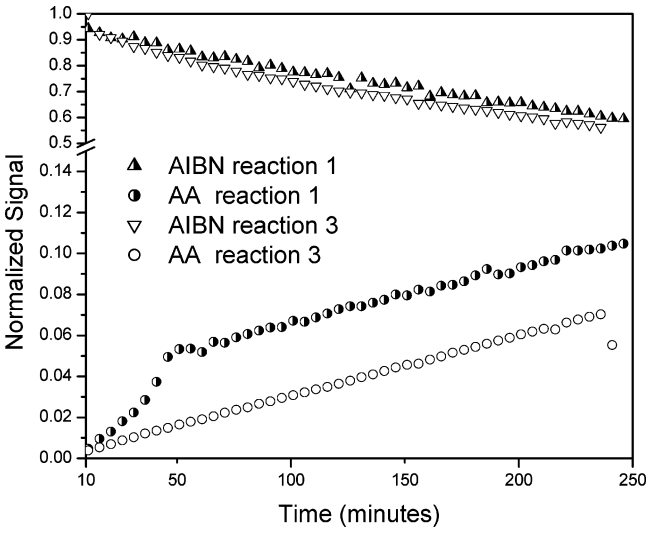

Figure 8. Concentrations of AIBN and AA of reactions 1 and 3 carried out in deuterated benzene at 70 °C. Reaction 1 contains RAFT agent cyanoisopropyl dithiobenzoate, and reaction 3 is a conventional free radical polymerization. Reaction 1: 3.56×10^{-3} mol of C_6D_6, 6.75×10^{-5} mol of AIBN, 2.40×10^{-3} mol of styrene, 4.84×10^{-4} mol of cyanoisopropyl dithiobenzoate. Reaction 3: 4.34×10^{-3} mol of C_6D_6, 6.71×10^{-5} mol of AIBN, 3.68×10^{-3} mol of styrene.

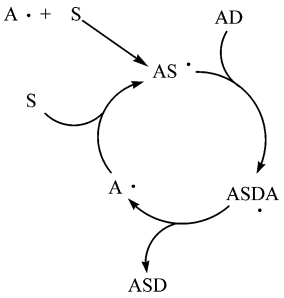

Figure 9. Cycle by which cyanoisopropyl radicals (A•) are rapidly regenerated by addition−fragmentation through a dithioester mediating species, during the early stages of the cyanoisopropyl dithiobenzoate-mediated polymerization of styrene. (A•) adds to styrene (S) to form AS•. AS• adds to AD to generate intermediate radical ASDA• that rapidly fragments to produce A•, which is then once again able to cycle through by adding to styrene.

mately 60 min). This substantiates the above argument presented for the reactions at higher temperatures, namely that the excess AA product is produced during initialization. Following the initialization period the AA product is formed at a similar rate as in a conventional free radical polymerization as evident from comparisons of reactions 1 and 3.

The increased concentrations of the respective termination products in the RAFT-mediated polymerizations are due to an unusual process, in which active chains are kept short (see Figure 9) that occurs during the initialization period. During the initialization period, the A• will add to a monomer unit to form AS•. When these species undergo efficient transfer, a short A• will be expelled. This means that, unlike a conventional radical polymerization, the initialization period replaces the slower terminating AS• species with faster terminating A• radical species. There are significantly higher concentrations of their termination products compared with those in a control reaction because of this replacement during the initialization period. After the initialization period the usual geminate recombination process dominates the formation of the AA species, as can clearly be observed in Figures 7 and 8. The concentration curves for AA are roughly parallel in Figure 8, although in Figure 7 there is a deviation at higher temperature. The reactions at higher temperatures will result in higher conversions and viscosities in the control reaction, leading to a decrease in initiator efficiency and an increase in the geminate recombination product being produced at longer reaction times in reaction 4. A weaker corresponding increase in viscosity is expected in the RAFT system, since both overall conversion and average chain length (on which viscosity depends) are both much lower than in the conventional system.

The chain length dependence of the termination rate coefficients[41−45] means that short species will have a higher rate of termination. The overall termination rate will be higher during initialization than that in a control reaction in which the short chains are quickly converted into longer chains. The higher rate of radical loss through termination implies that reactions with longer initialization periods will consequently have a lower propagating radical concentration after the initialization period, leading to a slower rate of reaction after the initialization period than comparable reactions with shorter initialization periods.

Beyond Initialization. To minimize the length of the initialization period, it is important that the propagation rate constant of the homolytic leaving group of the original RAFT agent with respect to the monomer in use be as high as possible. The only caution is that it should remain a better leaving group than the incoming monomer adduct radicals. To minimize the effect of propagation rate constant differences between initialization and the equilibrium phase of the reaction, a polymeric RAFT agent of the same monomer can be used. In this case the propagation of the initiator fragment, which is unable to displace the polymeric chain until it has propagated, will result in an immediate increase in intermediate radicals equivalent to the end of initialization, as has been seen by ESR spectroscopy.[31] The experimental implication of using the polymeric agent is that the RAFT equilibrium period should be reached very quickly.

Conclusions

This study has provided direct evidence for details of the mechanism of the initialization period of the RAFT process. It was found that the addition−fragmentation process was extremely selective during this period, and because of this, significant quantities of RAFT adducts of degrees of polymerization greater than unity were formed only after complete conversion of the initial RAFT agent to its monomeric adducts. The critical process in the initialization of a dithiobenzoate (RAFT)-controlled polymerization was found to be the formation of the single monomer adduct dithiobenzoate species and, by implication, the propagation of the initial leaving group radicals and the initiator-derived radicals (which are both the cyanoisopropyl radical here).

In situ ^{1}H NMR spectroscopy shows that the first interval of polymerization that could be observed in the studied systems is an initialization period, which has been defined as the period prior to the complete consumption of the initial RAFT agent. In the case of styrene this initialization period shows a more rapid rate of reaction than during the RAFT equilibrium. The rate of polymerization is a function of the values of the

propagation rate constants for the initiator and leaving group fragments. It has been shown that a slower rate of reaction during the initialization period compared to the equilibrium period is expected in the case of methyl acrylate, which is currently under investigation. The initialization period has largely been mistaken for inhibition in the RAFT literature for homogeneous reactions. The lack of previous reports of the rapid rate of reaction during this period is suggested as being due to the long chain lengths targeted in other studies, which means that the initialization period would have been completed before significant conversion had occurred, and thus this period may have gone unnoticed in many systems.

In the system studied, the poorest leaving group was the cyanoisopropylstyryl (i.e., AS$^{\bullet}$) radical although the "long chain" value of addition, propagation, and fragmentation rate coefficients need to be achieved before the system is at equilibrium. This could be for species containing two or more monomer units for both addition and propagation.

The reasons for the behavior observed for the RAFT system are suggested as being dependent on the relative reactivities and radical stabilities and therefore the related addition and fragmentation rate coefficients of the tertiary radical species and their monomer adducts in the system. This can be extended to all efficient RAFT systems, even those where multiple radical species are present and should not be considered as solely an explanation of the cyanoisopropyl dithiobenzoate system.

The main reasons for the extremely selective and stepwise behavior observed in the initialization period are that the fragmentation of the formed intermediate radicals is very selective toward tertiary radicals and that addition of propagating radicals of degree of polymerization of at least unity to the RAFT agent was much faster than to monomer. Cases where this behavior might not occur include the use of RAFT agents with low addition rate coefficients, the use of very high initial ratios of [M]/[RAFT], or systems in which $k_{p,1}$ is very large.

The second part of this investigation addresses the same reaction using cumyl dithiobenzoate, where the initiating and leaving groups are different, and illustrates the similarities and differences in observed behavior.[30]

Acknowledgment. The authors acknowledge the financial assistance of the National Research Foundation of South Africa and the Dutch Polymer Institute. The NMR facilities of the Central Analytical Facility at the University of Stellenbosch are acknowledged for the extensive machine time and expertise required for conducting the experiments.

References and Notes

(1) Barner-Kowollik, C.; Heuts, J. P. A.; Davis, T. P. *J. Polym. Sci., Part A: Polym. Chem.* **2001**, *39*, 656−664.
(2) Haddleton, D. M.; Perrier, S.; Bon, S. A. F. *Macromolecules* **2000**, *33*, 8246−8251.
(3) Aguilar, M. R.; Gallardo, A.; Fernandez, M. D. M.; Roman, J. S. *Macromolecules* **2002**, *35*, 2036−2041.
(4) Barner, L.; Barner-Kowollik, C.; Davis, T. P. *J. Polym. Sci., Part A: Polym. Chem.* **2002**, *40*, 1064−1074.
(5) Hawker, C. J.; Bosman, A. W.; Harth, E. *Chem. Rev.* **2001**, *101*, 3661−3688.
(6) Moad, G.; Rizzardo, E.; Solomon, D. H. *Macromolecules* **1982**, *15*, 909−914.
(7) Kato, M.; Kamigaito, M.; Sawamoto, M.; Higashimura, T. *Macromolecules* **1995**, *28*, 1721−1723.
(8) Ando, T.; Kato, M.; Kamigaito, M.; Sawamoto, M. *Macromolecules* **1996**, *29*, 1070−1072.
(9) Matyjaszewski, K.; Xia, J. *Chem. Rev.* **2001**, *101*, 2921−2990.
(10) Wang, J.-S.; Matyjaszewski, K. *J. Am. Chem. Soc.* **1995**, *117*, 5614−5615.
(11) Le, T. P.; Moad, G.; Rizzardo, E.; Thang, S. H. Polymerization with Living Characteristics WO98/01478, 1998; *Chem. Abstr.* **1998**, *128*, 115390.
(12) Barner-Kowollik, C.; Quinn, J. F.; Nguyen, T. L. U.; Heuts, J. P. A.; Davis, T. P. *Macromolecules* **2001**, *34*, 7849−7857.
(13) Barner-Kowollik, C.; Davis, T. P.; Heuts, J. P. A.; Stenzel, M. H.; Vana, P.; Whittaker, M. *J. Polym. Sci., Part A: Polym. Chem.* **2003**, *41*, 365−375.
(14) Chiefari, J.; Mayadunne, R. T. A.; Moad, C. L.; Moad, G.; Rizzardo, E.; Postma, A.; Skidmore, M. A.; Thang, S. H. *Macromolecules* **2003**, *36*, 2273−2282.
(15) Chong, Y. K. B.; Krstina, J.; Le, T. P. T.; Moad, G.; Postma, A.; Rizzardo, E.; Thang, S. H. *Macromolecules* **2003**, *36*, 2256−2272.
(16) Coote, M. L.; Radom, L. *J. Am. Chem. Soc.* **2003**, *125*, 1490−1491.
(17) Monteiro, M. J.; de Brouwer, H. *Macromolecules* **2000**, *34*, 349−352.
(18) Kwak, Y.; Goto, A.; Tsujii, Y.; Murata, Y.; Komatsu, K.; Fukuda, T. *Macromolecules* **2002**, *35*, 3026−3029.
(19) Barner-Kowollik, C.; Quinn, J. F.; Morsley, D. R.; Davis, T. P. *J. Polym. Sci., Part A: Polym. Chem.* **2001**, *39*, 1353−1365.
(20) Calitz, F. M.; Tonge, M. P.; Sanderson, R. D. *Macromolecules* **2003**, *36*, 5−8.
(21) Barner, L.; Quinn, J. F.; Barner-Kowollik, C.; Vana, P.; Davis, T. P. *Eur. Polym. J.* **2003**, *39*, 449−459.
(22) Barner-Kowollik, C.; Coote, M. L.; Davis, T. P.; Radom, L.; Vana, P. *J. Polym. Sci., Part A: Polym. Chem.* **2003**, *41*, 2828−2832.
(23) Calitz, F. M.; McLeary, J. B.; McKenzie, J. M.; Tonge, M. P.; Klumperman, B.; Sanderson, R. D. *Macromolecules* **2003**, *36*, 9687−9690.
(24) Moad, G.; Solomon, D. H. *The Chemistry of Free Radical Polymerization*, 1st ed.; Elsevier Science Ltd.: Amsterdam, 1995.
(25) Huang, D. M.; Monteiro, M. J.; Gilbert, R. G. *Macromolecules* **1998**, *31*, 5175−5187.
(26) Heuts, J. P. A.; Gilbert, R. G.; Radom, L. *Macromolecules* **1995**, *28*, 8771−8781.
(27) Van Geet, A. L. *Anal. Chem.* **1968**, *40*, 2227−2229.
(28) Thang, S. H.; Chong, Y. K. B.; Mayadunne, R. T. A.; Moad, G.; Rizzardo, E. *Tetrahedron Lett.* **1999**, *40*, 2435−2438.
(29) De Brouwer, H. *RAFT Memorabilia*; Eindhoven University of Technology, ISBN 90-386-2802-1, 2001.
(30) Calitz, F. M.; McLeary, J. B.; Mckenzie, J. M.; Tonge, M. P.; Sanderson, R. D.; Klumperman, B. Manuscript in preparation.
(31) Calitz, F. M.; Tonge, M. P.; Sanderson, R. D. Manuscript in preparation.
(32) Walbiner, M.; Wu, J. Q.; Fischer, H. *Helv. Chim. Acta* **1995**, *78*, 910−924.
(33) Herberger, K.; Fischer, H. *Int. J. Chem. Kinet.* **1993**, *25*, 249−263.
(34) Barner-Kowollik, C.; Vana, P.; Quinn, J. F.; Davis, T. P. *J. Polym. Sci., Part A: Polym. Chem.* **2002**, *40*, 1058−1063.
(35) Buback, M.; Gilbert, R. G.; Hutchinson, R. A.; Klumperman, B.; Kuchta, F. D.; Manders, B. G.; O'Driscoll, K. F.; Russell, G. T.; Schweer, J. *Macromol. Chem. Phys.* **1995**, *196*, 3267−3280.
(36) Perrier, S.; Barner-Kowollik, C.; Quinn, J. F.; Vana, P.; Davis, T. P. *Macromolecules* **2002**, *35*, 8300−8306.
(37) Vana, P.; Davis, T. P.; Barner-Kowollik, C. *Macromol. Theory Simul.* **2002**, *11*, 823−835.
(38) Hawthorne, D. G.; Moad, G.; Rizzardo, E.; Thang, S. H. *Macromolecules* **1999**, *32*, 5457−5459.
(39) Brandrup, J.; Immergut, E. H.; Grulke, E. A. *Polymer Handbook*; John Wiley and Sons: New York, 1999.
(40) Manders, L. G. *Pulsed Initiation Polymerization*, Eindhoven University of Technology, ISBN 90-386-0778-4, 1997.
(41) Heuts, J. P. A.; Davis, T. P.; Russell, G. T. *Macromolecules* **1999**, *32*, 6019−6030.
(42) Buback, M.; Egorovc, M.; Gilbert, R. G.; Kaminsky, V.; Olaj, O. F.; Russell, G. T.; Vana, P. *Macromol. Chem. Phys.* **2002**, *203*, 2570−2582.

(43) Scheren, P. A. G. M.; Russell, G. T.; Sangster, D. F.; Gilbert, R. G.; German, A. L. *Macromolecules* **1995**, *28*, 3637−3649.
(44) Russell, G. T.; Gilbert, R. G.; Napper, D. H. *Macromolecules* **1992**, *25*, 2459−2469.
(45) Russell, G. T.; Gilbert, R. G.; Napper, D. H. *Macromolecules* **1993**, *26*, 3538−3552.

MA035478C

CHAPTER 5

Chapter 5 describes a very similar study to the one in chapter 4, except that the leaving group from the RAFT agent (cumyl) now differs from the primary radical (cyano isopropyl). It turns out that this relatively minor change in the system has a dramatic effect on the initialization behavior.

Reprinted with permission from *Macromolecules* **2005**, *38*, 3151-3161.

A ^{1}H NMR Investigation of Reversible Addition−Fragmentation Chain Transfer Polymerization Kinetics and Mechanisms. Initialization with Different Initiating and Leaving Groups

J. B. McLeary,[†] F. M. Calitz,[†] J. M. McKenzie,[‡] M. P. Tonge,*[,†,§] R. D. Sanderson,[†] and B. Klumperman*[,†,∥]

Dutch Polymer Institute, UNESCO Centre for Macromolecules and Materials, Department of Chemistry and Polymer Science, and Nuclear Magnetic Resonance Laboratories, University of Stellenbosch, Private Bag X1, Matieland 7602, South Africa, and Laboratory of Polymer Chemistry, Eindhoven University of Technology, P.O. Box 513, 5600 MB Eindhoven, The Netherlands

Received November 10, 2004; Revised Manuscript Received February 2, 2005

ABSTRACT: In situ ^{1}H nuclear magnetic resonance spectroscopy was used to directly investigate the processes that occur during the early stages (the first few monomer addition steps) of azobis(isobutyronitrile)-initiated reversible addition−fragmentation chain transfer (RAFT) polymerizations of styrene in the presence of cumyl dithiobenzoate at 70 and 84 °C. The change in concentration of important dithiobenzoate species and monomer as a function of time was investigated. The predominant type of growing chain under the reaction conditions carries a cumyl end group. The initialization period (the period during which the initial RAFT agent is consumed) in the presence of cumyl dithiobenzoate in homogeneous media was significantly longer than for equivalent reactions using cyanoisopropyl dithiobenzoate as RAFT agent, and the rate of monomer conversion was correspondingly slower. Very strong fragmentation selectivity of the formed intermediate radicals (to form the tertiary propagating radical) was observed during the initialization period. The rate-determining step for the initialization process was the addition (propagation) of the initiator-derived and cumyl radicals to styrene, to form the corresponding single-monomer adducts. The greater length of this period with respect to the same reaction using cyanoisopropyl dithiobenzoate as RAFT agent is suggested to be a result of slower propagation due to a smaller addition rate coefficient of the cumyl radical (which was found to be the dominant propagation process during initialization) to styrene, than for the cyanoisopropyl radical, and to a higher average termination rate for the cumyl radicals than for the cyanoisopropyl radicals. The probable (small) difference in intermediate radical concentration is considered to be a less significant contributor to the length of the period.

Introduction

Nuclear magnetic resonance spectroscopy is one of the most powerful modern analytical tools available to molecular scientists. Of relevance here is that it can be a useful technique for the in situ investigation of the kinetics of free radical polymerization reactions. In previous studies we have demonstrated that NMR spectroscopy provides significant insight into the first stages of living (reversible addition−fragmentation chain transfer, RAFT) radical polymerization.[1,2]

Living free radical polymerization has revolutionized the architecture of polymers that can be prepared by free radical polymerization. The ability to chain extend polymers has made it possible to produce tapered gradients and pure block copolymers, providing materials that are of great interest in a wide variety of applications ranging from coatings to biomedical uses. A number of living radical polymerization techniques are currently under investigation, each with its own unique characteristics and specific advantages and/or disadvantages. Two of the most well-established techniques are stable free-radical-mediated polymerization (SFRP)[3,4] and atom transfer radical polymerization (ATRP),[5−8] which are reversible end-capping techniques.

The focus of the current study is the RAFT process,[9−14] another living radical polymerization technique that is extremely versatile and robust. It is compatible with almost all monomers and most conditions that are applicable to conventional free radical polymerization. The benefits of the RAFT process are obtained simply by the addition of the correct choice of RAFT agent to the polymerization mixture.

The RAFT process is a relatively new technique and has recently generated substantial controversy,[15,16] the focus of which is the determination of the precise RAFT mechanism. Being a new technique, there are still some anomalies in the process that at present are not well understood.

Dithioester RAFT agents have the form R−SCSZ, the two main features being the initial leaving group (R) and the "activating" group (Z). Both of these groups have a significant effect on the kinetics and degree of control of the RAFT process. In Scheme 1 the elementary reactions for the central exchange process of the RAFT mechanism are depicted. The relatively stable intermediate radical that is formed (for some RAFT agent/monomer combinations) by the addition process can fragment to release one of two radical species. These are the original incoming radical species (P_m·, a propagating radical of degree of polymerization m), or the homolytic leaving group (P_n·) that was previously a part of the RAFT agent. If this central exchange is the only process that controls the RAFT-mediated polymeriza-

* To whom correspondence should be addressed.
[†] UNESCO Centre for Macromolecules and Materials, Department of Chemistry and Polymer Science, University of Stellenbosch.
[‡] Nuclear Magnetic Resonance Laboratories, University of Stellenbosch.
[§] Current address: Key Centre for Polymer Colloids, School of Chemistry, F11, University of Sydney, NSW 2006, Australia.
[∥] Eindhoven University of Technology.

10.1021/ma047696r CCC: $30.25
Published on Web 03/19/2005

Scheme 1. Elementary Reversible Addition−Fragmentation Chain Transfer Process As Commonly Accepted in the Literature[9]

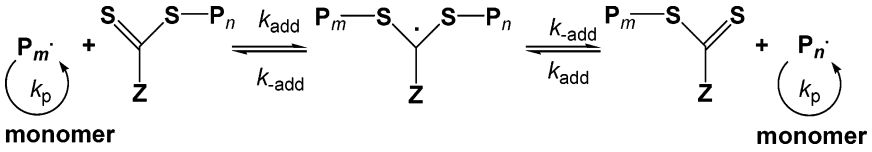

Table 1. Composition of Reaction Mixtures for in Situ NMR Spectroscopic Analysis[a]

	solvent		initiator		styrene		RAFT agent		monomer/RAFT agent ratio, $[M]_0/[R]_0$	RAFT agent/(initiator × 2) ratio, $[R]_0/2[I]_0$
sample	mass (g)	mol × 10^{-3}	mass (g)	mol × 10^{-5}	mass (g)	mol × 10^{-3}	mass (g)	mol × 10^{-4}		
1(CD)[b]	0.250	2.99	0.010	6.3	0.260	2.46	0.100	3.68	6.68	2.92
2(CD)[c]	0.250	2.99	0.010	6.3	0.260	2.46	0.100	3.68	6.68	2.92
3[b]	0.365	4.34	0.011	6.7	0.380	3.68	0	0	0	0
4[c]	0.300	3.56	0.010	6.1	0.380	3.68	0	0	0	0
5(AD)[b]	0.300	3.56	0.010	6.7	0.250	2.40	0.107	4.84	4.96	3.96
6(AD)[c]	0.300	3.56	0.010	6.1	0.240	2.31	0.100	4.52	5.10	3.70

[a] The solvent used was deuterated benzene (99.6%), and the initiator used was azobis(isobutyronitrile). The RAFT agent was cumyl dithiobenzoate (CD) or cyanoisopropyl dithiobenzoate (AD). [b] Reaction carried out at 70 °C. [c] Reaction carried out at 84 °C.

tion reaction, then the inhibition and retardation phenomena that occur in many RAFT-mediated polymerizations cannot easily be fully explained.[17−19]

Previously we reported experimental results that helped to further the understanding of the "inhibition" effect observed in certain RAFT-mediated polymerizations and defined the term "initialization".[1,2] *Initialization* is the process by which the starting RAFT agent is consumed. The *initialization period* is the period in which the starting RAFT agent is consumed. The *initialization time* is the time required for the starting RAFT agent to be completely consumed (converted to other forms). In this paper, the cause and length of the initialization period for azobis(isobutyronitrile)-initiated, *cumyl* dithiobenzoate-mediated polymerization of styrene are investigated at two temperatures. In this case, the initiator-derived and leaving group radicals are different, which has a significant effect on the kinetics of the reaction when compared to the situation where the initiator-derived and leaving group radicals are the same.[1]

The rate of polymerization in a radical polymerization is a function of the radical concentration and type available for propagation, and depends on all radical generation and loss mechanisms. When different types of radicals are present (and thus often competing) in a system, understanding the rate-determining factors for polymerization becomes substantially more complex. We previously reported substantial selectivity during initialization when the only radicals in the system are the tertiary cyanoisopropyl radicals, derived from both initiator and RAFT agent, and secondary radicals derived from monomer addition reactions to the tertiary radical.[1] Very strong addition−fragmentation selectivities have also been observed in RAFT-mediated polymerization of methyl acrylate.[2] This type of selectivity is probably representative of the behavior of many such systems.

The current study addresses, in a manner similar to that of a previous study,[1] the early part of azobis(isobutyronitrile)-initiated styrene polymerization in the presence of the RAFT agent cumyl dithiobenzoate, at 70 and 84 °C, before complete consumption of the initial RAFT agent and the period immediately following initialization. In situ ^{1}H NMR spectroscopy was used to directly determine the variation in concentration of several species during the course of the reaction, with focus being on the early part of the reaction, i.e., the first monomer addition step(s). The effects of using dissimilar initiator and RAFT agent leaving groups on the rate of polymerization and length of the initialization period, and the implication on the RAFT mechanism, are investigated and compared to those of the case where these groups are the same.

Experimental Section

Chemicals. Styrene (Plascon Research Centre, University of Stellenbosch, estimated purity ~99% by ^{1}H NMR) was washed with 0.3 M KOH, and distilled under vacuum prior to use to remove inhibitor and polymer. Azobis(isobutyronitrile) (AIBN, Riedel De Haen) was recrystallized from AR grade methanol and found to be ~99% pure by ^{1}H NMR spectroscopy. Deuterated solvent (C_6D_6, 99.6%, 0.1% tetramethylsilane (TMS), Sigma-Aldrich) and pyrazine (99%, Sigma-Aldrich) were used as received.

Sample Preparation. The masses of the reactants used to make up the various samples are given in Table 1. The samples were transferred to NMR tubes. The tubes were flushed with ultra-high-purity nitrogen for 10 min. At this point a sealed glass insert containing the integration reference standard (pyrazine) was inserted, and the tubes were sealed. The use of the reference standard was solely for integration normalization purposes. A specific example of a reaction is as follows: A stock solution was prepared by weighing 0.250 g (2.99×10^{-3} mol) of C_6D_6, 0.010 g (6.3×10^{-5} mol) of azobis(isobutyronitrile), 0.260 g (2.46×10^{-3} mol) of styrene, and 0.100 g (3.68×10^{-4} mol) cumyl dithiobenzoate into a vial. This stock solution was then transferred into an NMR tube using a pipet and filled to a height of 5 cm. The tube was then flushed with nitrogen (10 min), and the integration reference was inserted. The tube was sealed and refrigerated prior to insertion.

Analysis. NMR spectra were collected on a 600 MHz Varian ^{Unity}Inova spectrometer operating at 600 MHz. A 5 mm inverse detection PFG probe was used for the experiments, and the probe temperature was calibrated using an ethylene glycol sample in the manner suggested by the manufacturer using the method of Van Geet.[20] ^{1}H spectra were acquired with a 3 μs (40°) pulse width and a 4 s acquisition time. The chosen pulse angle allowed complete relaxation of all relevant peaks in the sample, the T_1 values of the system having been measured and taken into account. For the ^{1}H NMR kinetic experiments, samples were inserted into the magnet at 25 °C and the magnet was fully shimmed on the sample. A spectrum was collected at 25 °C to serve as a reference. The sample was then removed from the magnet, and the cavity of the magnet was raised to the required temperature (70 or 84 °C). Once

Table 2. ^{1}H NMR Spectroscopy Chemical Shifts of a Representation of Integrated Species Relevant to the Investigation of Initialization in the Cumyl Dithiobenzoate-Mediated Polymerization of Styrene[a]

δ (ppm), methyl protons of R groups	δ (ppm), ortho protons of corresponding dithiobenzoate ring	species
singlet, 0.93	N/A	AA
singlet, 1.18	N/A	CC
two peaks, 1.10, 1.08	N/A	AC
singlet, 1.45	doublet, 7.71	AD
singlet, 1.81	doublet, 7.81	CD
two peaks, 1.01, 0.87	doublet, 7.85	ASD
two peaks, 1.25, 1.20	doublet, 7.78	CSD
two peaks, 0.81, 0.65	doublet, 7.90	AS_2D[b]
two peaks, 0.89, 0.72	doublet, 7.79	
two peaks, 0.95, 1.02	doublet, 7.81	CS_2D[b]
two peaks, 1.02, 1.14	doublet (not identified)	

[a] Species AA is tetramethylsuccinonitrile, AD is cyanoisopropyl dithiobenzoate, and AS_nD are the styrene adducts of AD containing n styrene units. CD is cumyl dithiobenzoate, and CS_nD are the styrene adducts of CD containing n styrene units. [b] Note stereoisomers.

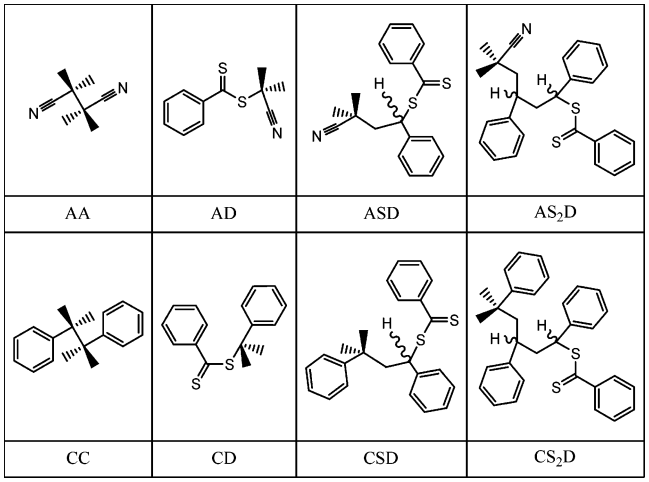

Figure 1. Predominant species of interest for the investigation of the early period of the free radical polymerization of styrene in the presence of cumyl dithiobenzoate, using azobis(isobutyronitrile) as an initiator.

the magnet cavity had stabilized at the required temperature, the sample was reinserted and allowed to equilibrate for approximately 5 min. Additional shimming was then carried out to fully optimize the system, and the experiments were started approximately 10 min after the sample was inserted into the magnet, the exact time being noted.

Integration of spectra was carried out both manually and automatically to allow identification of species during formation. Automated integration was carried out using ACD Labs 7.0 ^{1}H NMR processor.

Synthesis of the RAFT Agent. The synthesis of cumyl dithiobenzoate was carried out according to the method of Le et al.[9] The RAFT agent was purified by successive liquid chromatography on silica and alumina using hexane as eluent. The product crystallized after vacuum removal of solvent and storage below −10 °C. The purity was estimated by ^{1}H NMR to be >95%. Impurities were identified during the integration process and found to be unreactive on the time scale of the reaction.

Results and Discussion

The NMR spectroscopic data that were obtained during the investigation provide instantaneous concentrations of detectable nonradical species in the RAFT-mediated reactions.

The concentrations and molar ratios of the reaction components in all reactions in this study are summarized in Table 1. A representative selection of peaks that were integrated for this study can be found in Table 2. Where two or more peaks are indicated, diastereotopic groups were present.

Figure 1 shows the chemical structures of the primary species of interest for this study. For convenience the following naming convention will be used. Species CD is the initial RAFT agent containing the dithiobenzoate species (D) and the initial cumyl leaving group (C), CSD is the dithiobenzoate species of the single styrene (S) adduct of a cumyl radical (C•), and CS_2D refers to the second styrene adducts of the cumyl radicals. The same naming convention applies for derivatives of the RAFT agent cyanoisopropyl dithiobenzoate (AD), with consecutive monomer adducts ASD, AS_2D, etc., with the cyanoisopropyl group replacing the cumyl group. A sample spectrum showing the most important peaks during initialization is shown in Figure 2. Although the styrene peaks in the spectra collected were large in comparison to the peaks of species containing RAFT groups, no dynamic range problems were experienced. As can be seen from Figure 2, a good signal-to-noise ratio was achieved, allowing for integration of the smaller peaks in the spectrum.

The assignments of the ^{1}H NMR peaks were confirmed in a number of ways. Initially the ^{1}H NMR spectrum of each component in the reaction mixture was individually obtained to ensure the peaks belonging to each component were unambiguously assigned. Observation of azobis(isobutyronitrile) decomposition at 70 and 84 °C by ^{1}H NMR spectroscopy allowed for the assignment of the peak due to tetramethylsuccinonitrile (AA), which forms during this process. To assign peaks due to the combination of two cumyl radical species (CC) as well as the combination of cumyl and cyanoisopropyl radical species (AC), cumyl dithiobenzoate was reacted with azobis(isobutyronitrile) in the absence of monomer. The assignment of the AD, ASD, and AS_2D peaks has been made previously.[1]

The assignment of peaks due to species formed by addition of cumyl radicals to styrene was carried out in a fashion similar to that previously reported.[1] Once a cumyl dithiobenzoate-mediated reaction had begun, initiator-derived radicals allowed consumption of styrene to begin, CD was consumed to produce CSD (and a small amount of ASD and AD), and most AD formed was consumed to produce ASD, as previously observed.[1] The assignment of the CSD peaks was confirmed by comparing the rates of consumption of CD and styrene, and the corresponding formation of peaks assigned to CSD. Additionally, it was found that when all of the CD peaks (both methyl and *o*-phenyl protons) disappeared, the assigned CSD peaks reached a maximum, and the amount of monomer consumption according to the assigned styrene peaks was in good agreement with the amount required for complete consumption of the CD species. Thus, all assigned peaks showed good consistency in the time dependences of their intensities, and the rate of monomer consumption was internally verified. The assignments of the peaks for CS_2D were similarly made. Further verification of the peak assignments was carried out via various NMR spectroscopy techniques, at room temperature, on the samples after reaction. 2D NMR spectroscopic techniques were investigated, but the most information in regard to confirmation of the peak assignments was obtained by carrying

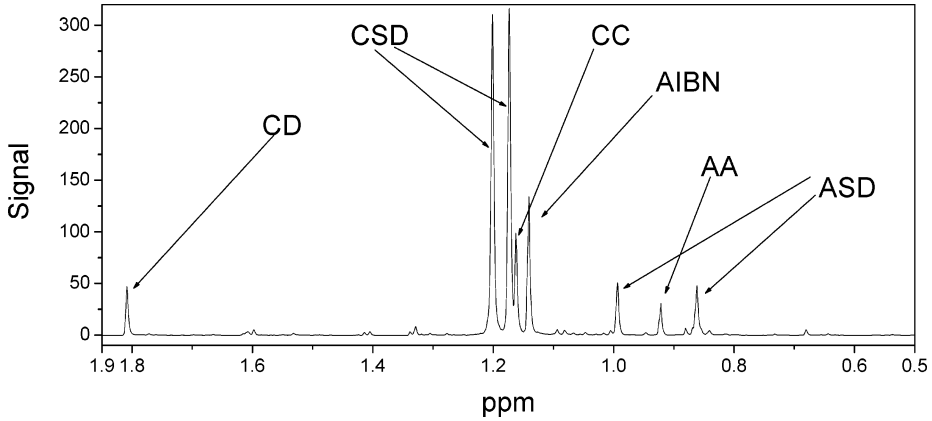

Figure 2. A typical ^{1}H NMR spectrum between 1.9 and 0.5 ppm during initialization, showing the peaks corresponding to several of the important species studied here. Cumyl dithiobenzoate (CD), cumyl styryl dithiobenzoate (CSD), cyanoisopropyl styryl dithiobenzoate (ASD), the geminate cumyl radical product (CC), tetramethylsuccinonitrile (AA), and azobis(isobutyronitrile) (AIBN) are labeled within the spectrum.

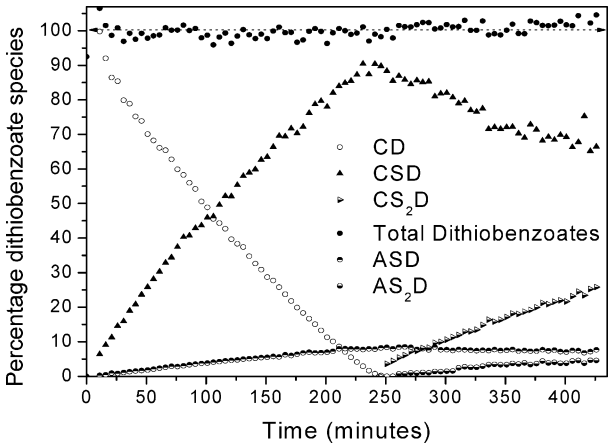

Figure 3. Relative concentrations of the methyl protons of dithiobenzoate species versus time in the in situ free radical polymerization of styrene in the presence of cumyl dithiobenzoate using azobis(isobutyronitrile) as an initiator at 70 °C. Table 1, reaction 1: 2.99×10^{-3} mol of C_6D_6, 6.30×10^{-5} mol of azobis(isobutyronitrile), 2.46×10^{-3} mol of styrene, 3.68×10^{-4} mol of cumyl dithiobenzoate.

out 1D TOCSY and 1D NOESY experiments. In this way it was possible to identify peaks belonging to a single species and confirm the peak assignments.

The use of cumyl dithiobenzoate, styrene monomer, and azobis(isobutyronitrile) as initiator results in a system in which two different tertiary radical species are present. The choice of styrene as monomer results in the vast majority of radicals formed from propagation reactions being secondary radicals.

In a previous study,[1] the radical reactivity for only one type of tertiary initiating radical (cyanoisopropyl) needed to be considered. When a system with two tertiary radical species (cyanoisopropyl and cumyl here) is considered, the polymerization becomes substantially more complex.

The first experimental system examined is the reaction of styrene, cumyl dithiobenzoate, and azobis(isobutyronitrile) at 70 °C (reaction 1, Table 1). Figure 3 shows the time dependence of the concentrations of dithiobenzoate species within the first 7 h of the reaction. Initially, a small but significant amount of AD is formed, due to addition of cyanoisopropyl radicals to CD, followed by fragmentation to produce cumyl radicals and AD. This is the only likely route given existing models for RAFT kinetics that can produce AD from CD at the beginning of the reaction (since almost no CSD exists at this stage). The exchange of end groups is addressed in a later section. Simultaneously, there is a decrease in the concentration of species CD, and a corresponding increase in the concentration of the species CSD and ASD as a single monomer unit is added. This trend continues until the cumyl dithiobenzoate and any cyanoisopropyl dithiobenzoate formed have been completely consumed (after about 240 min). At this point the concentrations of species CSD and ASD have reached a maximum. Once all of the cumyl dithiobenzoate has reacted, the second monomer additions to the radical species begin to increase in frequency (leading to the formation of species CS_2D and AS_2D). The implication of this behavior is that the formation of the CSD and ASD (i.e., addition of A$^\bullet$ and C$^\bullet$ to styrene to form AS$^\bullet$ and CS$^\bullet$) species or the consumption of the starting RAFT agent is the rate-determining step in the process. This behavior is the same as was previously described when the initiating and leaving groups were the same; that is, there is also extremely strong selectivity of the fragmentation of formed intermediate radicals during the initialization period to form the tertiary propagating radicals and the "propagated" form of the RAFT agent (i.e., ASD or CSD). This results in significantly different behavior of the system before and after the completion of initialization.

For clarity in the following discussion, termination reactions (with either propagating or intermediate radicals) are not shown, although they play a significant part in the reaction kinetics. Termination of intermediate radicals is not expected to be significant during initialization, due to the low intermediate radical concentration (as measured by ESR spectroscopy)[21] during most of the initialization period.

The reaction scheme, although similar to, is now substantially more intricate than the scheme reported previously.[1] Scheme 2 shows the types of reactions that are under consideration at the beginning of the reaction (i.e., prior to total consumption of the initial RAFT agent). Those reactions labeled with "c" and "a" are specific to cumyl or cyanoisopropyl radical species, respectively, and those labeled with "as" and "cs" refer to the single-monomer adducts of the cumyl and cyanoisopropyl radical species.

For convenience, the reaction scheme during initialization has been divided into two parts. The first part, as shown in Scheme 2, describes the main processes

Scheme 2. Steps Involved in the Early Part of the Initialization Period (Involving Tertiary Radicals That Have Not Yet Propagated) of the Reversible Addition−Fragmentation Chain Transfer Reaction of Cumyl Dithiobenzoate, Styrene Monomer, and Azobis(isobutyronitrile) Initiator

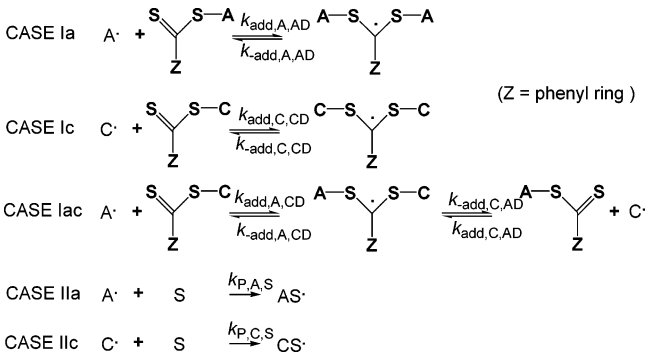

Scheme 3. Additional Steps Involved in the Initialization Period (Including Radicals That Have Propagated Once) of the Reversible Addition−Fragmentation Chain Transfer Reaction of Cumyl Dithiobenzoate, Styrene Monomer, and Azobis(isobutyronitrile) Initiator

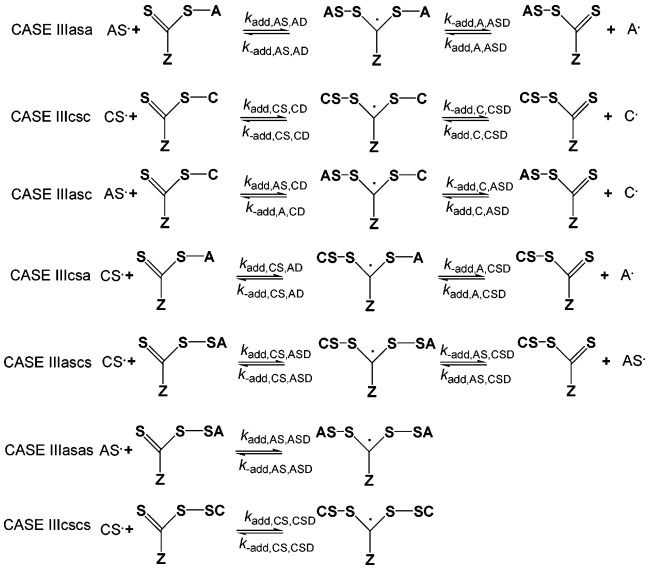

occurring at the start of the reaction, before significant propagation has occurred, and the second part (Scheme 3) the remaining reactions in the initialization period. The species involved in Scheme 2 include RAFT agents that have not added monomer units, propagating radicals that have not undergone propagation, and intermediate radicals formed from the reaction of the aforementioned species. Note that the reactions in Scheme 2 occur throughout the initialization period, until all of the initial RAFT agent has been consumed. The cyanoisopropyl radicals generated by initiator decomposition undergo one of three main reactions: (i) addition to a RAFT agent (case Ia or Iac), (ii) addition to monomer (propagation), to give radical species AS• (case IIa), or (iii) termination. Cumyl radicals generated by fragmentation of the formed intermediate radical in case Iac will either undergo addition to a RAFT agent (case Ic or Iac) or addition to monomer (propagation) to produce CS• (case IIc) or terminate.

The remaining significant reactions of propagating radicals (those that involve at least one species that has previously reacted with monomer) during the initialization period are shown in Scheme 3. The new reactions are as follows: the cyanoisopropyl and cumyl radicals can undergo two other reactions, namely, addition to either cyanoisopropylstyryl or cumylstyryl dithiobenzoate (shown on the right-hand side of either case IIIasa or case IIIcsa (for A•) or case IIIasc or case IIIcsc (for C•)) to form the corresponding intermediate radicals. Similarly, AS• can add to a RAFT agent, i.e., cases IIIasa, IIIasc, IIIcsas, and IIIasas. CS• can also add to a RAFT agent, i.e., cases IIIcsc, IIIcsa, IIIcsas, and IIIcscs. The formed intermediate radicals will predominantly fragment to give the shorter, tertiary radicals.

Scheme 4. Additional Steps Involved toward the End of the Initialization Period (Including Radicals That Have Propagated More Than Once) of the Reversible Addition−Fragmentation Chain Transfer Reaction of Cumyl Dithiobenzoate, Styrene Monomer, and Azobis(isobutyronitrile) Initiator

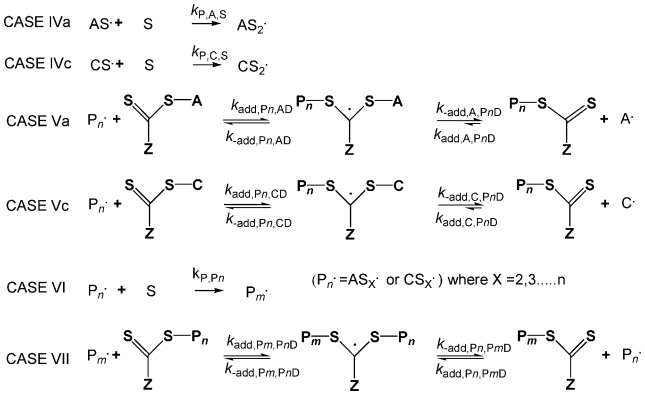

Note that, in this reaction, where the initiating and leaving radicals are different, there are now ten distinct types of intermediate radicals that can form during the initialization period, whereas there are only three such types of intermediates when the two radicals are the same. This can potentially significantly change the kinetics of the system, and makes accurate modeling of these kinetics extremely problematic, since there are then 32 potentially different rate coefficients (all of which are currently unknown) for the addition−fragmentation equilibria in the initialization period alone. However, as for the system previously described,[1] it appears that the most important factors determining the length of the initialization period are the propagation and/or termination rates of the cyanoisopropyl and cumyl radicals and the initial amount of RAFT agent and initiator present in the reaction.

Toward the end of the initialization process the reactions shown in Scheme 4 begin to dominate. AS• and CS• can propagate (cases IVa and IVc, respectively), or alternatively, AS• and CS• can add to any remaining RAFT agent (cases Va and Vc). It is expected that, after initialization, no C• (seen as CD) will be present in the reaction mixture, since all of the initial CD has been consumed. Once significant amounts of CS_nD and AS_nD ($n \geq 2$) have formed, longer chain propagation can occur (case VI), and the system is probably at or approaching steady-state equilibrium. Once the chains have reached a sufficient degree of polymerization, the steady-state (main) addition−fragmentation equilibrium will be reached (case VII). A• radicals formed by initiator decomposition throughout the reaction will be able to add to RAFT chains. However, being unable to displace the longer chains that are attached to RAFT agents (i.e.,

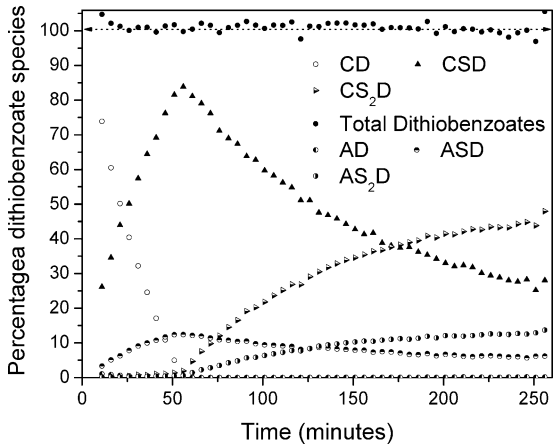

Figure 4. Relative concentrations of the methyl protons of the dithiobenzoate species versus time in the in situ free radical polymerization of styrene in the presence of cumyl dithiobenzoate using azobis(isobutyronitrile) as an initiator at 84 °C. Table 1, reaction 2: 2.99×10^{-3} mol of C_6D_6, 6.30×10^{-5} mol of azobis(isobutyronitrile), 2.46×10^{-3} mol of styrene, 3.68×10^{-4} mol of cumyl dithiobenzoate.

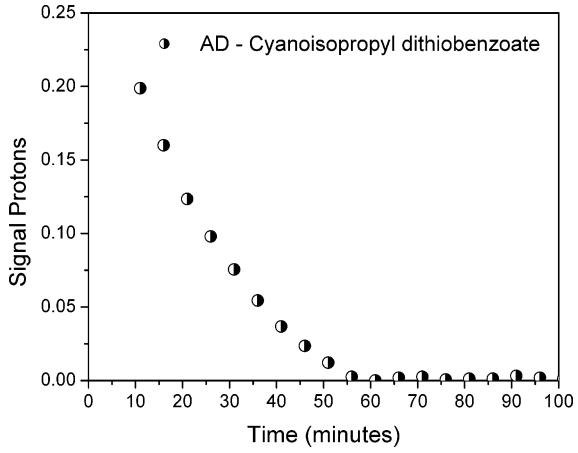

Figure 5. Concentration−time evolution of the AD species in reaction 2 (Table 1) at 84 °C: 2.99×10^{-3} mol of C_6D_6, 6.30×10^{-5} mol of azobis(isobutyronitrile), 2.46×10^{-3} mol of styrene, 3.68×10^{-4} mol of cumyl dithiobenzoate.

the right-hand side of case Va), the A• radicals will instead terminate or propagate to a length at which they can effectively participate in the main addition−fragmentation equilibrium.

Effect of Temperature. The second reaction (reaction 2, Table 1) was a duplicate of reaction 1 (see Table 1) carried out at 84 °C for comparative purposes. The time dependences of the concentrations of important species are shown in Figure 4. The initialization period (about 50 min) was much shorter than that of reaction 1 (about 240 min). The radical flux from the initiator and the temperature dependence of the A• and C• propagation and/or termination reactions clearly play a very important role in the length of the initialization period. It is interesting to note that species AD, which is not an original component of the reaction mixture, reaches a maximum concentration prior to the commencement of spectral data collection at 8 min. This is shown in Figure 5. AD is formed by the addition of A• to CD, and subsequent fragmentation of the formed intermediate radical to eject the C• radical.

It has been shown that the initialization time is temperature dependent in the case of cyanoisopropyl dithiobenzoate.[1] This is again true for the case where cumyl dithiobenzoate is used as RAFT agent. This is because the same factors (propagation and/or termination of A• and C• radicals, and subsequent addition to a RAFT agent) govern the initialization behavior for both RAFT systems. In the initial cyanoisopropyl dithiobenzoate experiments, the initialization time was determined by the rate of addition of a single styrene unit (per RAFT agent) to the cyanoisopropyl radicals (A•) to form AS•, which then added to the initial RAFT agent. In the cumyl dithiobenzoate experiments, the duration of the initialization period is directly dependent on the rate of addition of a single styrene unit to the cumyl and (to a lesser extent) cyanoisopropyl radicals. The length of the initialization period is directly related to monomer conversion, and reasons for differences from the previously studied system will be discussed below.

Monomer Consumption. In RAFT polymerizations in which initiator-derived initiating radicals and initial leaving group radicals (R•) are different, the number of different *propagating* (and intermediate) radicals is increased. It should be noted that in the cumyl dithiobenzoate system there are two main types of propagating radical species present during the initialization period, i.e., C• and A•. In this case the expression for the rate of monomer consumption in the initialization period becomes a composite term (the average "propagation" rate coefficient will be $\langle k_p \rangle = k_{p,A}[A^\bullet] + k_{p,C}[C^\bullet]$, where $k_{p,A}$ and $k_{p,C}$ are the addition rate coefficients of A• and C• radicals to monomer, respectively, assuming that there are no significant side reactions of these radicals) to take into account the fractions of the two types of radicals active in the system. This substantially increases the difficulty in resolving different influences on the propagating radical concentration.

Comparison between the amount of CC and AA termination products formed, which will be discussed below, suggests that the dominant propagating radical through most of the initialization period is C•, which mainly adds to styrene, as evident through the dominance of the CSD (over ASD) product during initialization. This has been confirmed by electron spin resonance (ESR) spectroscopy.[22]

The monomer consumption of the cumyl dithiobenzoate-mediated reactions (1 and 2), as seen in Figure 6, is faster during the initialization period (240 and 50 min) for both reactions than after this period has ended. A decrease in the rate of monomer consumption after the initialization period is seen for the reactions even after correction for initiator decomposition (not shown). However, the change in rate of monomer consumption at the end of initialization is not as clearly evident as was previously seen in the cyanoisopropyl dithiobenzoate-mediated reactions (Figure 6).[1] Since the length of the initialization period is much greater for the CD than for the AD system under similar reaction conditions, then the average termination rates are much higher in the current case (leading to a lower propagating radical concentration), the average propagation rate coefficient (dominated by C•) is lower in the current case, and/or a difference in partitioning of radicals between the intermediate and propagating form is present. The observed differences between the AD- and CD-mediated reactions and the change in monomer consumption rates at the end of the initialization period are consistent with a system not yet having reached steady-state equilibrium during initialization. Since the length of the initialization period is dependent on the rate of mono-

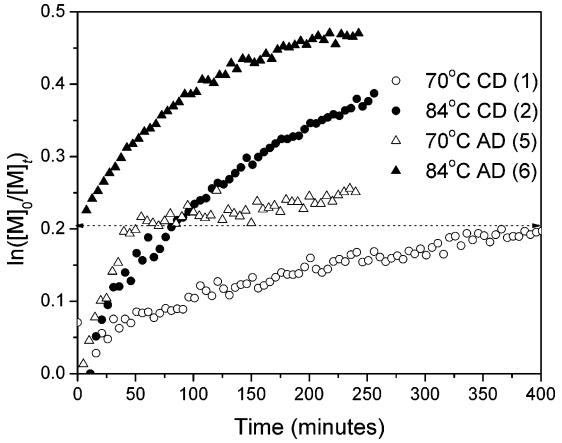

Figure 6. Semilogarithmic plot of fractional conversion versus time in the reactions of cumyl dithiobenzoate and cyanoisopropyl dithiobenzoate with azobis(isobutyronitrile) and styrene in deuterated benzene, respectively, at 84 and 70 °C. Table 1, reactions 1, 2 and 5, 6: (1) 2.99×10^{-3} mol of C_6D_6, 6.30×10^{-5} mol of azobis(isobutyronitrile), 2.46×10^{-3} mol of styrene, 3.68×10^{-4} mol of cumyl dithiobenzoate; (2): 2.99×10^{-3} mol of C_6D_6, 6.30×10^{-5} mol of azobis(isobutyronitrile), 2.46×10^{-3} mol of styrene, 3.68×10^{-4} mol of cumyl dithiobenzoate; (5) 3.56×10^{-3} mol of C_6D_6, 6.75×10^{-5} mol of azobis(isobutyronitrile), 2.40×10^{-3} mol of styrene, 4.84×10^{-4} mol of cyanoisopropyl dithiobenzoate; (6) 3.56×10^{-3} mol of C_6D_6, 6.1×10^{-5} mol of azobis(isobutyronitrile), 2.31×10^{-3} mol of styrene, 4.84×10^{-4} mol of cyanoisopropyl dithiobenzoate.

mer consumption under these conditions, the same reasons for the differences in monomer propagation rates apply to the lengths of the initialization periods.

A possible cause for the rate differences seen in the cumyl and cyanoisopropyl systems during initialization is a difference in partitioning of radicals between the intermediate and propagating forms, resulting in a lower propagating radical concentration and thus more retardation in polymerization rate occurring in the cumyl dithiobenzoate-mediated system. This would imply that there is a substantial concentration of intermediate radicals in the CD-mediated system, but not in the AD-mediated case. This could occur if the addition rate coefficients to the thiocarbonyl thio moiety (and/or the fragmentation rate coefficients of the formed intermediate radicals) of the cumyl and cyanoisopropyl radical species are substantially different.[12] However, ESR data[22] suggest that there is no significant difference in the intermediate radical concentrations during the initialization period for the AD and CD reactions, so although this cannot be completely ruled out as a contributing factor, higher intermediate radical concentrations are unlikely to be the cause of the rate difference. Note that, since low concentrations of intermediate radicals form in these cases, it is predicted that the rate of monomer consumption during initialization, and the length of the initialization period, should be similar to that of analogous reactions using non-retarding RAFT agents. This has indeed been observed.[2]

If the intermediate radical concentration is very low during initialization, then, as a first approximation, the total propagating radical concentration for both cyanoisopropyl and cumyl dithiobenzoate-mediated systems will be proportional to the square root of the rate coefficient of initiator decomposition, and inversely proportional to the square root of the average termination rate coefficients for the systems. The rate of initiator decomposition is identical for the reactions studied. Since the initial rates of monomer consumption (and the resulting initialization time) are about 3−5 times faster when AD is used as the initial RAFT agent, $\langle k_p \rangle / \langle k_t \rangle^{1/2}$ (where these rate coefficients are appropriately weighted averages for the propagation (addition, as described above) and termination of the A$^\bullet$ and C$^\bullet$ radicals for each case) must be larger by the same ratio for the AD case. It is not possible to distinguish between propagation and termination rate coefficients as a cause of the rate difference with the current experiments. Arguments for both cases are now discussed.

As (to a good approximation) only a single styrene unit adds to the cyanoisopropyl radicals for each RAFT species (and cumyl radicals for the cumyl dithiobenzoate case) during initialization, a lower $k_{p,C}$ (propagation rate coefficient of a cumyl radical) will contribute toward a longer initialization period for the cumyl dithiobenzoate case. It has been stated[13] that the value for $k_{p,A}$ (propagation rate coefficient of a cyanoisopropyl radical) (4040−4896 L mol^{-1} s^{-1} depending on the parameters used) is higher than that for $k_{p,C}$, (3800 L mol^{-1} s^{-1}) at 60 °C. The values given above were calculated by Chong et al.[13] using the Arrhenius parameters provided by Herberger et al.[23] and Walbiner et al.,[24] respectively. The value for $k_{p,C}$ was based on the averaged log A value of 7.5 for tertiary radicals and the activation energy provided by Fischer and Radom.[25] When the averaged log A value is used for the cyanoisopropyl with the values provided by Fischer and Radom,[25] the difference in rate coefficients is approximately 20%. It should be noted that the activation energy used in ref 13 for the cumyl radical is based on similar radicals (not the cumyl radical), and thus, the difference in k_p values might be slightly larger than that quoted here. The above difference between $k_{p,A}$ and $k_{p,C}$ alone is however unable to explain the difference in monomer consumption observed for the cyanoisopropyl and cumyl dithiobenzoate reactions. Thus, unless the $k_{p,C}$ value for our reaction is significantly different from the value calculated by Chong et al.[13] and from $k_{p,A}$, it is likely that there is a difference in total propagating radical concentrations between the two systems.

A difference in propagating radical concentrations for the two systems could be due to a difference in termination kinetics. This suggests that the rate coefficients for termination of cumyl radicals with themselves and/or cyanoisopropyl radicals are significantly higher than for the mutual termination of cyanoisopropyl radicals under the same conditions. This is contrary to expectations based on molecular size, since the cumyl radical is larger (and therefore expected to diffuse and terminate[26,27] more slowly) than the cyanoisopropyl radical. Terazima and co-workers have shown that the diffusion of radicals in solution is sometimes significantly slower than for their parent closed shell molecules,[28,29] and the same phenomenon was reported in the case of the cyanoisopropyl radical species ($D = 1.18 \times 10^9$ m^2 s^{-1} in benzene at 22 °C, estimated 70% of predicted value based on volume).[30] Although Fischer et al.[31] reported a $k_{t,C}$ value of 1.2×10^9 M^{-1} s^{-1}, in *tert*-butylbenzene at 297 K, Terazima indicates that the benzyl ($D = 4.1 \times 10^9$ m^2 s^{-1} in hexane,[32] also previously reported by Burkhart et al.[33] as $D = 4.1 \times 10^9$ m^2 s^{-1} in benzene) and 4-aminophenylthiyl radicals do not suffer from the slower rate of diffusion. This was attributed to the stable π electron resonance structure which resulted in less solvent interaction and a faster diffusion rate than those of their parent closed shell molecules.[32,34] It is consid-

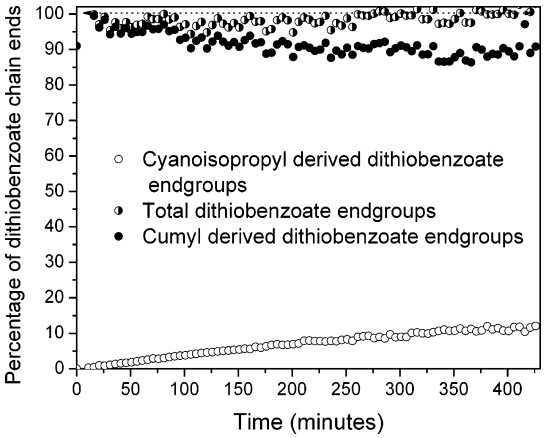

Figure 7. Percentage of cumulative integrated end groups of the dithiobenzoate species, in the polymerization of styrene, mediated by cumyl dithiobenzoate, using azobis(isobutyronitrile) as an initiator at 70 °C.

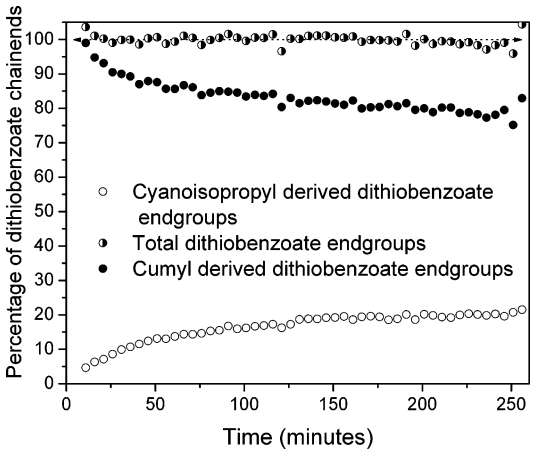

Figure 8. Percentage of cumulative integrated end groups of the dithiobenzoate species, in the polymerization of styrene, mediated by cumyl dithiobenzoate, using azobis(isobutyronitrile) as an initiator at 84 °C.

ered reasonable that the same behavior could potentially be observed in the case of the cumyl radical. Weiner reported that termination rate coefficients for the cumyl radical were ca. 8 times higher than for the cyanoisopropyl radical at room temperature in benzene.[35] This is the only study in which the termination rate coefficients of the cyanoisopropyl and cumyl radicals are directly compared by the same techniques. The estimation technique used is reported to lead to overestimation of the rate coefficients in the case of the cumyl radical; however, their value for the cyanoisopropyl radical is consistent with that of Terazima at 22 °C.[30] Unfortunately, there is a lack of consistency among experiments, temperatures, and reported termination rate coefficients for cumyl and cyanoisopropyl radicals throughout the available literature, so the large difference in termination rate coefficients reported by Weiner when compared to the value of Fischer needs further verification at the reaction temperature with consistent techniques. It is considered that the implied large difference in termination rate coefficients between systems is possible, but not certain. Such differences in termination kinetics (in addition to small differences in propagation kinetics) between the two types of radicals are capable of explaining the observed rate differences during initialization. Moreover, there is also the possibility that there are side reactions that produce undetectably (in these experiments) small amounts of side products that might have kinetic significance during the initialization process. However, it should be noted that there was no detectable loss of dithiobenzoate species throughout the entire duration of the reactions (as shown in Figures 7 and 8).

Radical Generation and Termination Products. The terminated species give insight into the reactions that govern the RAFT mechanism during the early stages of the polymerization process. These can be examined indirectly from the relative concentrations of all of the dithiobenzoate species with cumyl and cyanoisopropyl end groups and directly by the nature and amounts of the formed terminated species.

Figure 7 shows the time dependence of the relative concentrations of all dithiobenzoate species with cumyl (CD, CSD, CS_2D) and cyanoisopropyl (AD, ASD, AS_2D) end groups in reaction 1. There is a gradual displacement of cumyl end groups from the living polymer, with a corresponding equivalent increase in cyanoisopropyl end groups, and no observable overall loss of dithiobenzoate species. All of the dithiobenzoate species with cumyl end groups are present at the beginning of the reaction, resulting in an initial maximum concentration, followed by the observed decrease. Addition of cyanoisopropyl-ended radicals to cumyl-ended RAFT chains, followed by fragmentation of the formed intermediate radical to give cumyl or cumylstyryl radicals that are then terminated, is responsible for this change in end groups.

The number of living chains with a cyanoisopropyl end group increases with time due to two factors: (1) "transfer" is efficient; therefore, species CD will be displaced by any other radical in the system, allowing possible termination of expelled $C^{\bullet}$;[13] (2) there is a limited supply of cumyl groups, whereas $A^{\bullet}$ groups are continually supplied. Under such conditions, the total number of chains with cyanoisopropyl end groups *must* therefore increase. A constant concentration of chains with dithiobenzoate end groups throughout the reaction indicates that very little loss (below the detection limit of the NMR spectrometer) of this type of chain occurs (due to intermediate radical termination, formation of stable intermediates, or degradation) throughout the duration of the reaction.

Figure 8 shows the time dependence of the relative concentrations of all dithiobenzoate species with cumyl and cyanoisopropyl end groups within the first 3 h of reaction 2. As in the reaction at 70 °C, there is a gradual displacement of the cumyl end groups by cyanoisopropyl groups. The rate of increase of cyanoisopropyl end groups is at a maximum early in the reaction. This is because the number of radicals generated by azobis(isobutyronitrile) decomposition is highest early in the reaction, and the number of cumyl-ended chains (which will compete for cyanoisopropyl-ended radicals) is at a maximum at the beginning of the reaction. As all of the dithiobenzoate species with cumyl end groups are present at the beginning of the reaction, a maximum is expected at the beginning of the reaction and a gradual decrease in the concentration of the dithiobenzoate species with cumyl end groups, as some of the cumyl groups are involved in termination. This was observed. It is also interesting to note that the highest rate of decrease is during the earlier part of the reaction, i.e., during the initialization period. The high level of cumyl−cumyl (CC) termination seen during the initial-

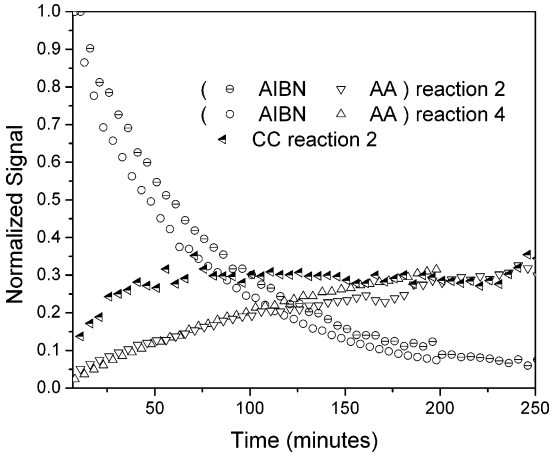

Figure 9. Concentration evolution of the termination products AA and CC formed in the reaction of styrene and azobis(isobutyronitrile) with (reaction 2) and without (reaction 4) cumyl dithiobenzoate in deuterated benzene at 84 °C.

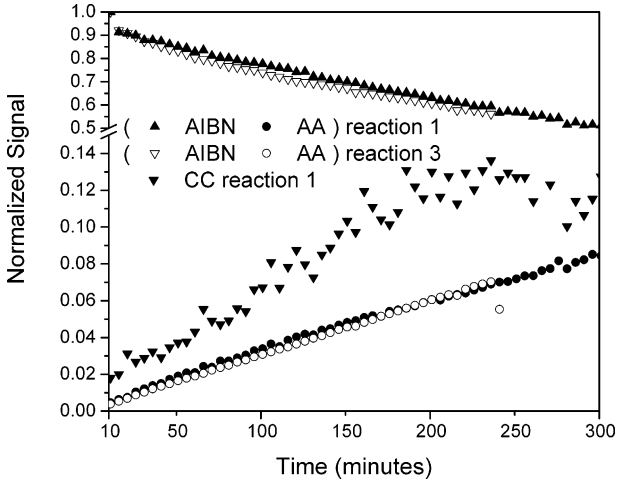

Figure 10. Concentration evolution of the termination products formed in the reaction of styrene and azobis(isobutyronitrile) with (reaction 1) and without (reaction 3) cumyl dithiobenzoate in deuterated benzene at 70 °C.

ization period is also confirmation of this (Figure 8). The increased temperature in reaction 2 compared to reaction 1 increased the radical flux in the system, leading to a higher rate of displacement of cumyl end groups from the dithiobenzoate species. The net result was approximately 20% end group interchange by the end of the monitoring period in reaction 2 and 10−12% in reaction 1. The interchange of end groups is especially important for applications in which specific end groups are required.

There are significantly more (Figure 9) cumyl−cumyl (CC) termination products than products of other termination processes during the initialization period. Production of CC ceases at the end of the initialization period, since (by definition) there are no remaining cumyl leaving groups on RAFT chains. The amount of AA produced by termination is not significantly greater than for the control (conventional) reaction (reaction 4, Table 1) without the RAFT agent; i.e., there is little "excess" reaction between A• radicals, which is quite different from the case when AD was used as RAFT agent.[1] This suggests that the AA termination product is predominantly a geminate recombination product as in the case of the control reaction. Other termination reactions occur (i.e., giving products AC and CSC), but due to their lack of symmetry in structure (leading to fine structure and broad peaks) and small concentrations, these termination products were too small to be integrated accurately and are therefore not shown in Figure 9. This suggests that the concentration of cumyl radicals is much higher than that of the cyanoisopropyl radicals, which is complementary to ESR results.[22] This is also consistent with the dominance of C• propagation during initialization (seen as the predominant formation of CSD). This is due to displacement of cumyl radicals by AS•, CS•, and A• radicals (A• radicals are the next most common propagating species, since insignificant amounts of AS_2D and CS_2D are seen during initialization), although the concentration of the generated species AD is low relative to that of the CD species. The rate of monomer consumption (Figure 6) implies that the concentration of propagating species (primarily C•) is at a maximum at the start of the reaction; consequently, the rate of termination will also be at a maximum as indicated by the initial maximum rate of CC termination products forming during the early parts of the reaction, implying that the cumyl radical will be the most abundant radical during the early reaction.

In Figure 10 the respective termination products for reaction 1 at 70 °C are shown. The very small amounts of termination at the lower temperature complicated analysis, but the same trends were observed as at the higher reaction temperatures. The CC termination product is dominant until the end of initialization, at which time the termination of the CC radicals ceases.

The increased concentrations of the respective termination products in the RAFT-mediated polymerizations during initialization are due to the unique process that is taking place, in which active chains are kept short. During the initialization period A• or C• will add to a monomer unit to form AS• or CS•. When these species undergo efficient transfer, a short A• or C• will be expelled. The chain length dependence of the termination rate coefficients means that short species will have a higher rate of termination, and the overall termination rate will be higher than that in a control reaction in which the short chains are quickly converted into longer chains.[26,27] At the end of initialization, longer chain radicals can form in significant quantities, and thus the resulting average rate coefficient for termination is likely to decrease, leading to a possible increase in the propagating radical concentration (depending on other factors, such as the relative amounts of intermediate radicals). The longer initialization periods with CD as RAFT agent will result in less residual initiator at the end of initialization compared with that in the AD systems. Thus, propagating radical concentrations are expected to be lower at the end of initialization for CD-mediated reactions, compared to analogous AD reactions. The higher rate of radical loss through termination (Figure 11) implies that longer initialization periods will require significantly higher radical fluxes to allow reactions to reach conversions comparable to those of shorter initialization time reactions. This behavior might be a contributing factor to reported increased rate retardation during polymerizations where cumyl dithiobenzoate has been used as a RAFT agent.[36] The increased amount of short chain termination products during the first part of the initialization period (Figure 11) for the CD case is consistent with a higher overall rate of termination during this period, as suggested earlier.

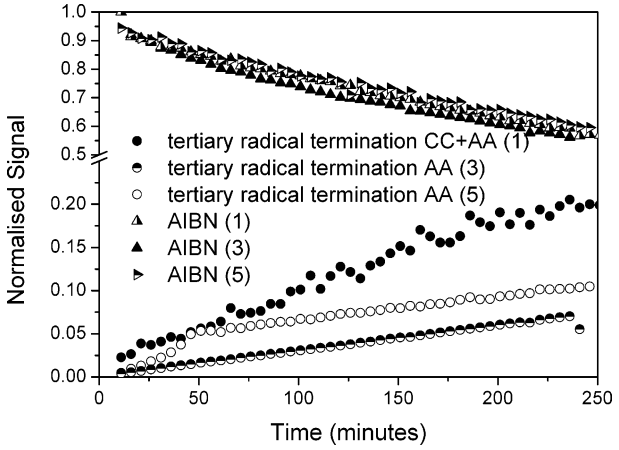

Figure 11. Sum of the concentration evolutions of the termination products AA and CC formed in the reaction of styrene and azobis(isobutyronitrile) without a mediating agent (reaction 3, Table 1), with cumyl dithiobenzoate (reaction 1, Table 1), and with cyanoisopropyl dithiobenzoate (reaction 5, Table 1) at 70 °C.

Beyond Initialization. In the case of an initiator that provides radicals that are unable to displace initial R groups from the initial RAFT agent, the process of initialization will be begun by the propagation of the initiator-derived radicals prior to exchange. This process may result in an initialization period that is less dependent on the initial R group and more dependent on the initiator fragment than the system studied here.

The propagated radicals are often better (as is the case here) able to displace the initial R groups. In the reactions presented in this study of cumyl dithiobenzoate with azobis(isobutyronitrile) as initiator, the relative abilities of the radicals are such that some displacement of the cumyl group (by the cyanoisopropyl radical) can occur before the first propagation step, as has been seen by the formation of the AD species in reactions 1 and 2. The amount of AD produced was however very small with respect to those of ASD and CSD and had no significant effect on the types of chains or kinetics.

However, the use of radical initiator or R group species that are less likely to fragment from the intermediate radical species than the species presented here should be carefully monitored. The initialization period as discussed here is not subject to retardation behavior as reported in the literature.[17,18,37−40] If the initial radical species in the system are such that the intermediate radical concentration begins to increase immediately, retardation will occur and the pseudo-zero-order behavior with respect to the initial RAFT agent concentration is unlikely to hold. The rate-determining processes will then also differ substantially.

Conclusions

In this study, in situ ^{1}H NMR spectroscopy has provided novel insight into the mechanism of the first interval of polymerization that could be observed in the studied systems (the initialization period) of the RAFT process. It was shown that when two efficient radicals were used as initiator and leaving groups, respectively, the addition−fragmentation process was extremely selective during this period, and because of this, significant quantities of RAFT adducts of degrees of polymerization greater than 1 were formed only after complete conversion of the initial RAFT agent to its monomeric adducts. The critical process in the initialization of these RAFT-mediated polymerizations was the formation of the single-monomer adduct dithiobenzoate species, and by implication, the propagation of the leaving and initiator-derived radical groups.

The observed behavior during initialization is suggested to be dependent on the relative reactivities and radical stabilities, and therefore the related addition and fragmentation rate coefficients of the tertiary radical species (and the formed intermediate radicals) in the systems and their monomer adducts. The possibility of termination rate differences between cyanoisopropyl and cumyl radicals based on diffusion differences is also considered as a contributing factor. The potential (small) difference in intermediate radical concentration is considered to play a negligible role.

The selectivity of the addition−fragmentation process during initialization was a result of a bias toward fragmentation to form the cumyl radical, which was responsible for the majority of the monomer consumption (and thus formation of the critical CSD group) and termination reactions. The dominance of this propagating radical was due to efficient transfer from initiator-derived radicals, the relatively high initial concentration of CD, and the fragmentation selectivity. The dominance of the cumyl radical during the initialization period resulted in significantly slower monomer consumption (and a correspondingly increased initialization time) during this period than for the previous[1] analogous AD-mediated reaction. The poorest leaving group was the styryl (i.e., AS$^\bullet$ and CS$^\bullet$) radical. As a result of the selectivity, the initialization period shows behavior different from that during the main RAFT equilibrium.

The dominance of cumyl-ended propagating radicals in this system leads to significant differences in the length of the initialization period with respect to that of the analogous AD-mediated system, and possibly until all chains in the system are "long". The relative amounts of cumyl-ended growing chains decreased throughout the duration of the reaction (due to termination of cumyl-ended chains, and the continuous supply of cyanoisopropyl radicals that eventually form growing chains). This process was more significant at the higher temperature studied, presumably due to the relatively higher rate of generation of cyanoisopropyl radicals and resulting termination of cumyl-ended chains.

The general behavior here is likely to be applicable to many efficient RAFT systems (that show the strong addition−fragmentation selectivity observed here) where multiple radical species are present and should not be considered as solely an explanation of the cumyl dithiobenzoate system. Indeed, the general observations here are similar to those seen when the initiating and leaving groups are the same,[1,2] as expected when the same general mechanisms dominate.

At some time after initialization, the "long chain" values of addition, propagation, termination, and fragmentation rate coefficients will be achieved, at which point the system will reach steady-state equilibrium. This might require each chain to add two or more monomer units.

Acknowledgment. We acknowledge the financial assistance of the National Research Foundation of South Africa and the Dutch Polymer Institute. The NMR facilities of the Central Analytical Facility at the University of Stellenbosch are acknowledged for the

extensive machine time and expertise required for conducting the experiments.

References and Notes

(1) McLeary, J. B.; Calitz, F. M.; McKenzie, J. M.; Tonge, M. P.; Sanderson, R. D.; Klumperman, B. *Macromolecules* **2004**, *37*, 2383−2394.
(2) McLeary, J. B.; Mckenzie, J. M.; Tonge, M. P.; Sanderson, R. D.; Klumperman, B. *Chem. Commun.* **2004**, 1950−1951.
(3) Hawker, C. J.; Bosman, A. W.; Harth, E. *Chem. Rev.* **2001**, *101*, 3661−3688.
(4) Moad, G.; Rizzardo, E.; Solomon, D. H. *Macromolecules* **1982**, *15*, 909−914.
(5) Kato, M.; Kamigaito, M.; Sawamoto, M.; Higashimura, T. *Macromolecules* **1995**, *28*, 1721−1723.
(6) Ando, T.; Kato, M.; Kamigaito, M.; Sawamoto, M. *Macromolecules* **1996**, *29*, 1070−1072.
(7) Matyjaszewski, K.; Xia, J. *Chem. Rev.* **2001**, *101*, 2921−2990.
(8) Wang, J.-S.; Matyjaszewski, K. *J. Am. Chem. Soc.* **1995**, *117*, 5614−5615.
(9) Le, T. P.; Moad, G.; Rizzardo, E.; Thang, S. H. PCT Int. Appl., 1998, WO 98/01478.
(10) Barner-Kowollik, C.; Quinn, J. F.; Nguyen, T. L. U.; Heuts, J. P. A.; Davis, T. P. *Macromolecules* **2001**, *34*, 7849−7857.
(11) Barner-Kowollik, C.; Davis, T. P.; Heuts, J. P. A.; Stenzel, M. H.; Vana, P.; Whittaker, M. *J. Polym. Sci., Part A: Polym. Chem.* **2003**, *41*, 365−375.
(12) Chiefari, J.; Mayadunne, R. T. A.; Moad, C. L.; Moad, G.; Rizzardo, E.; Postma, A.; Skidmore, M. A.; Thang, S. H. *Macromolecules* **2003**, *36*, 2273−2282.
(13) Chong, Y. K. B.; Krstina, J.; Le, T. P. T.; Moad, G.; Postma, A.; Rizzardo, E.; Thang, S. H. *Macromolecules* **2003**, *36*, 2256−2272.
(14) Coote, M. L.; Radom, L. *J. Am. Chem. Soc.* **2003**, *125*, 1490−1491.
(15) Barner-Kowollik, C.; Coote, M. L.; Davis, T. P.; Radom, L.; Vana, P. *J. Polym. Sci., Part A: Polym. Chem.* **2003**, *41*, 2828−2832.
(16) Wang, A. R.; Zhu, S.; Kwak, Y.; Goto, A.; Fukuda, T.; Monteiro, M. J. *J. Polym. Sci., Part A: Polym. Chem.* **2003**, *41*, 2833−2839.
(17) Monteiro, M. J.; de Brouwer, H. *Macromolecules* **2000**, *34*, 349−352.
(18) Kwak, Y.; Goto, A.; Tsujii, Y.; Murata, Y.; Komatsu, K.; Fukuda, T. *Macromolecules* **2002**, *35*, 3026−3029.
(19) Barner-Kowollik, C.; Quinn, J. F.; Morsley, D. R.; Davis, T. P. *J. Polym. Sci., Part A: Polym. Chem.* **2001**, *39*, 1353−1365.
(20) Van Geet, A. L. *Anal. Chem.* **1968**, *40*, 2227−2229.
(21) Calitz, F. M.; McLeary, J. B.; McKenzie, J. M.; Tonge, M. P.; Klumperman, B.; Sanderson, R. D. *Macromolecules* **2003**, *36*, 9687−9690.
(22) Calitz, F. M.; Tonge, M. P.; Sanderson, R. D. Manuscript in preparation.
(23) Herberger, K.; Fischer, H. *Int. J. Chem. Kinet.* **1993**, *25*, 249−263.
(24) Walbiner, M.; Wu, J. Q.; Fischer, H. *Helv. Chim. Acta* **1995**, *78*, 910−924.
(25) Fischer, H.; Radom, L. *Angew. Chem., Int. Ed.* **2001**, *40*, 1340−1371.
(26) Heuts, J. P. A.; Davis, T. P.; Russell, G. T. *Macromolecules* **1999**, *32*, 6019−6030.
(27) Buback, M.; Egorovc, M.; Gilbert, R. G.; Kaminsky, V.; Olaj, O. F.; Russell, G. T.; Vana, P. *Macromol. Chem. Phys.* **2002**, *203*, 2570−2582.
(28) Terazima, M.; Okamoto, K.; Hirota, N. *J. Phys. Chem.* **1993**, *97*, 13387−13393.
(29) Terazima, M.; Hirota, N. *J. Chem. Phys.* **1993**, *98*, 6257−6262.
(30) Terazima, M.; Nogami, Y.; Tominaga, T. *Chem. Phys. Lett.* **2000**, *332*, 503−507.
(31) Sobek, J.; Martschke, R.; Fischer, H. *J. Am. Chem. Soc.* **2001**, *123*, 2849−2857.
(32) Okamoto, K.; Hirota, N.; Terazima, M. *J. Phys. Chem.* **1997**, *101*, 5269−5277.
(33) Burkhart, R. D. *J. Am. Chem. Soc.* **1968**, *90*, 273−277.
(34) Ukai, A.; Hirota, N.; Terazima, M. *Chem. Phys. Lett.* **2000**, *319*, 427−433.
(35) Weiner, S. A.; Hammond, G. S. *J. Am. Chem. Soc.* **1969**, *91*, 986−990.
(36) Moad, G.; Chiefari, J.; Chong, B. Y.; Krstina, J.; Mayadunne, R. T.; Postma, A.; Rizzardo, E.; Thang, S. H. *Polym. Int.* **2000**, *49*, 993−1001.
(37) Kwak, Y.; Goto, A.; Fukuda, T. *Macromolecules* **2004**, *37*, 1219−1225.
(38) Perrier, S.; Barner-Kowollik, C.; Quinn, J. F.; Vana, P.; Davis, T. P. *Macromolecules* **2002**, *35*, 8300−8306.
(39) Souaille, M.; Fischer, H. *Macromolecules* **2002**, *35*, 248−261.
(40) Vana, P.; Davis, T. P.; Barner-Kowollik, C. *Macromol. Theory Simul.* **2002**, *11*, 823−835.

MA047696R

CHAPTER 6

A scientific debate about the interpretation of the kinetic behavior of RAFT-mediated polymerization took place around 2004-2010. The discussion centered around slow fragmentation of the intermediate radical or termination reactions of the intermediate radical as an interpretation for experimental observations. The data sets from chapters 4 and 5 were used in modeling exercises. Chapter 6 describes the way we interpret the data, where the agreement between experimental data and model description is excellent.

Reprinted with permission from *Macromol. Rapid Commun.* **2006**, 27, 1233-1240.

Summary: The presence of strong chain length selectivity behavior during initialization in the RAFT process is an experimental observation. The mechanistic underpinning of the observation is, however, open to interpretation. The rates and concentration profiles for the cyanoisopropyl-dithiobenzoate-mediated polymerization of styrene at 70 °C can be relatively well reproduced by either the slow fragmentation or intermediate radical termination models. The use of modeling that provides a fit to the data is an important tool, but should be considered as additional evidence in support of experimental data rather than as experimental evidence in and of itself.

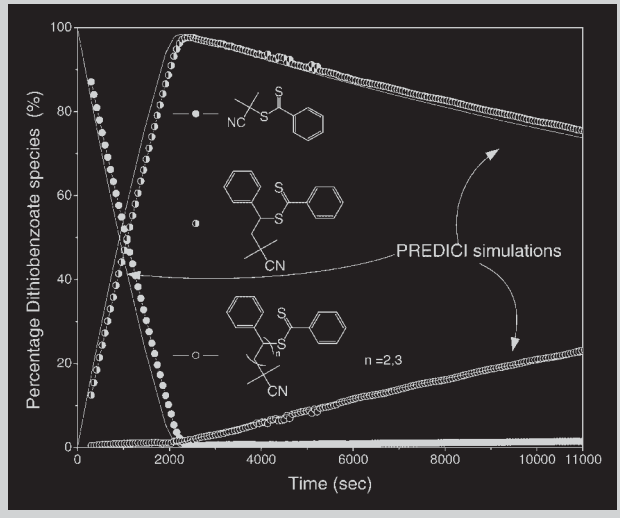

Comparison of the time dependencies of the concentrations of AD, AMD, and AM_2D by PREDICI modeling for the cyanoisopropyl-mediated polymerization of styrene at 70 °C generated by the IRT model (lines) versus experimental data.

A Mechanistic Interpretation of Initialization Processes in RAFT-Mediated Polymerization[a,b]

James B. McLeary,[1] *Matthew P. Tonge,*[1] *Bert Klumperman**[1,2]

[1] UNESCO Centre for Macromolecules and Materials, Department of Chemistry and Polymer Science, University of Stellenbosch, Private Bag X1, Matieland 7602, South Africa
Fax: +31 40 246 3966; E-mail: l.klumperman@tue.nl
[2] Laboratory of Polymer Chemistry, Eindhoven University of Technology, PO Box 513, 5600 MB Eindhoven, The Netherlands

Received: April 7, 2006; Revised: May 16, 2006; Accepted: May 29, 2006; DOI: 10.1002/marc.200600238

Keywords: initialization; kinetics (polym.); mechanism; NMR; reversible addition fragmentation chain transfer (RAFT)

Introduction

The reversible addition fragmentation chain transfer (RAFT)-mediated polymerization process has been shown to be a highly versatile and widely applicable living radical polymerization method that lends itself to complex architectural design. The RAFT process has been developed to the point where it is starting to be applied for the production of polymers on a commercial scale. However, the mechanisms underlying the process are still subject to significant debate.[1,2]

The occurrence of inhibition and retardation in RAFT-mediated polymerizations has led to the rise of two different modeling approaches that are difficult to reconcile. These two different explanations for observable phenomena are commonly referred to as the 'slow fragmentation'[3] (SF) and 'intermediate radical termination'[4] (IRT) models. Both these models have large unresolved issues. A large body of general polymerization rate data, and developed molar mass data, has been presented that can be

[a] The present work was inspired by a recent publication by M. L. Coote et al. entitled '*Quantum Chemical Mapping of Initialization Processes in RAFT Polymerization*' (*Macromol Rapid Commun*. **2006**, *27(13)*, 1015.)

[b] Supporting information for this article is available at the bottom of the article's abstract page, which can be accessed from the journal's homepage at http://www.mrc-journal.de, or from the author.

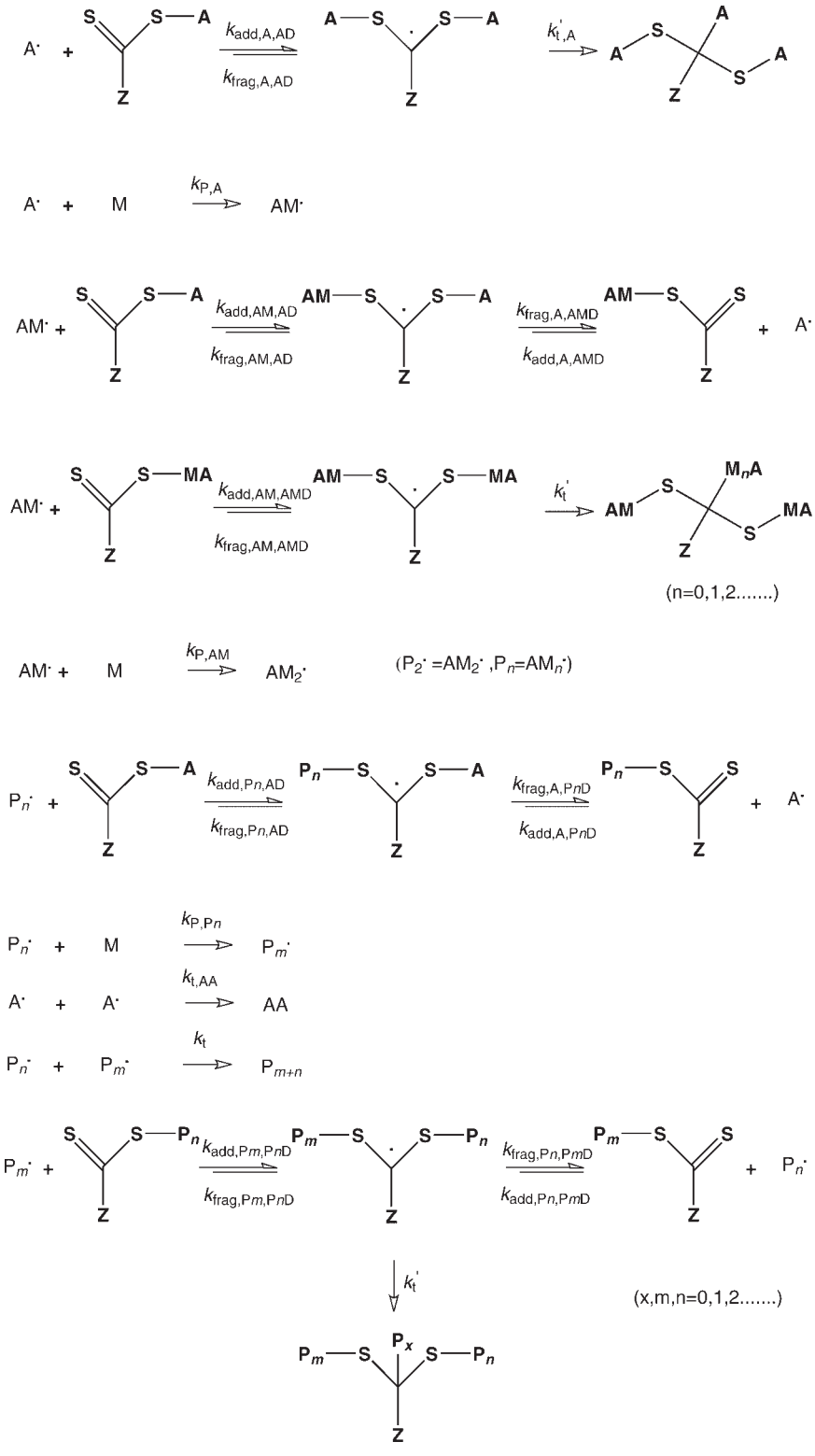

Scheme 1. Elementary reactions and corresponding rate coefficients used for the modeling of the RAFT process.

adequately described by the SF model.[2,3,5] The inclusion of chain-length dependence allows proper description of the initialization processes, but it omits the contribution of the very high intermediate radical concentration that the model predicts for RAFT-mediated reactions, which differs substantially from the experimentally observed values.[6–8] The possibility of these radicals being present as reversibly terminated species[9] is potentially a solution to this dilemma, but then the problem is closely related to the perceived flaw of the IRT model in that the concentrations of species that would be expected are such that experimental observation should be possible. In much the same fashion as the SF model, a number of groups have published data and explained their results using the IRT model.[4,6,10,11] The IRT model has, however, also yet to be justified by the practical observation of a concentration of terminated products of the intermediate radical of the RAFT process that would explain the retardation that occurs in these reactions, and this model differs substantially from that based on the quantum chemical calculations performed by Coote and co-workers.[12]

Recently McLeary et al.[13–15] showed via in-situ NMR spectroscopy that the RAFT process has an extreme selectivity at short chain lengths on the basis of fragmentation rates from the intermediate radical form of the RAFT agent for initial leaving groups and single monomer adduct leaving groups. One of the observations of these studies was that an apparent pseudo-zero order consumption of initial RAFT agent was occurring. This led to the conclusion that the addition of the initiating radical (leaving group of the original RAFT agent) to the first monomer is rate determining. A consequence of that is the expectation that the rate of monomer consumption during initialization is independent of the stabilizing (Z) group. This was experi-

$$\mathrm{AIBN} \rightarrow \mathrm{A}^{\mathrm{dot}} + \mathrm{A}^{\mathrm{dot}},\ k_{\mathrm{d}} \qquad \mathrm{A}^{\mathrm{dot}} + \mathrm{M} \rightarrow \mathrm{AM}^{\mathrm{dot}},\ k_{\mathrm{am}} \qquad \mathrm{AM}^{\mathrm{dot}} + \mathrm{M} \rightarrow \mathrm{AM_2}^{\mathrm{dot}},\ k_{\mathrm{p}}$$

$$\mathrm{AM_2}^{\mathrm{dot}} + \mathrm{M} \rightarrow \mathrm{AM_3}^{\mathrm{dot}},\ k_{\mathrm{p}} \qquad \mathrm{A}^{\mathrm{dot}} + \mathrm{A}^{\mathrm{dot}} \rightarrow \mathrm{AA},\ k_{\mathrm{t,aa}} \qquad \mathrm{A}^{\mathrm{dot}} + \mathrm{AM}^{\mathrm{dot}} \rightarrow \mathrm{AMMA},\ k_{\mathrm{t,ama}}$$

$$\mathrm{A}^{\mathrm{dot}} + \mathrm{AM_2}^{\mathrm{dot}} \rightarrow \mathrm{AMMA},\ k_{\mathrm{t,ama}} \qquad \mathrm{A}^{\mathrm{dot}} + \mathrm{AM_3}^{\mathrm{dot}} \rightarrow \mathrm{AMMA},\ k_{\mathrm{t,ama}} \qquad \mathrm{AM}^{\mathrm{dot}} + \mathrm{AM}^{\mathrm{dot}} \rightarrow \mathrm{AMMA},\ k_{\mathrm{t,2}}$$

$$\mathrm{AM}^{\mathrm{dot}} + \mathrm{AM_2}^{\mathrm{dot}} \rightarrow \mathrm{AMMA},\ k_{\mathrm{t,2}} \qquad \mathrm{AM}^{\mathrm{dot}} + \mathrm{AM_3}^{\mathrm{dot}} \rightarrow \mathrm{AMMA},\ k_{\mathrm{t,2}} \qquad \mathrm{AM_2}^{\mathrm{dot}} + \mathrm{AM_2}^{\mathrm{dot}} \rightarrow \mathrm{AMMA},\ k_{\mathrm{t}}$$

$$\mathrm{AM_3}^{\mathrm{dot}} + \mathrm{AM_2}^{\mathrm{dot}} \rightarrow \mathrm{AMMA},\ k_{\mathrm{t}} \qquad \mathrm{AM_3}^{\mathrm{dot}} + \mathrm{AM_3}^{\mathrm{dot}} \rightarrow \mathrm{AMMA},\ k_{\mathrm{t}} \qquad \mathrm{A}^{\mathrm{dot}} + \mathrm{AD} \rightarrow \mathrm{ADA},\ k_{\mathrm{add}}$$

$$\mathrm{A}^{\mathrm{dot}} + \mathrm{AMD} \rightarrow \mathrm{AMDA},\ k_{\mathrm{add}} \qquad \mathrm{A}^{\mathrm{dot}} + \mathrm{AM_2D} \rightarrow \mathrm{AM_2DA},\ k_{\mathrm{add}} \qquad \mathrm{A}^{\mathrm{dot}} + \mathrm{AM_3D} \rightarrow \mathrm{AM_3DA},\ k_{\mathrm{add}}$$

$$\mathrm{AM}^{\mathrm{dot}} + \mathrm{AD} \rightarrow \mathrm{AMDA},\ k_{\mathrm{add,1}} \qquad \mathrm{AM}^{\mathrm{dot}} + \mathrm{AMD} \rightarrow \mathrm{AMDMA},\ k_{\mathrm{add,1}} \qquad \mathrm{AM}^{\mathrm{dot}} + \mathrm{AM_2D} \rightarrow \mathrm{AMDM_2A},\ k_{\mathrm{add,1}}$$

$$\mathrm{AM}^{\mathrm{dot}} + \mathrm{AM_3D} \rightarrow \mathrm{AMDM_3A},\ k_{\mathrm{add,1}} \qquad \mathrm{AM_2}^{\mathrm{dot}} + \mathrm{AD} \rightarrow \mathrm{AM_2DA},\ k_{\mathrm{add,2}} \qquad \mathrm{AM_2}^{\mathrm{dot}} + \mathrm{AMD} \rightarrow \mathrm{AM_2DMA},\ k_{\mathrm{add,2}}$$

$$\mathrm{AM_2}^{\mathrm{dot}} + \mathrm{AM_2D} \rightarrow \mathrm{AM_2DM_2A},\ k_{\mathrm{add,2}} \qquad \mathrm{AM_2}^{\mathrm{dot}} + \mathrm{AM_3D} \rightarrow \mathrm{AM_2DM_3A},\ k_{\mathrm{add,2}} \qquad \mathrm{AM_3}^{\mathrm{dot}} + \mathrm{AD} \rightarrow \mathrm{AM_3DA},\ k_{\mathrm{add,3}}$$

$$\mathrm{AM_3}^{\mathrm{dot}} + \mathrm{AMD} \rightarrow \mathrm{AM_3DMA},\ k_{\mathrm{add,3}} \qquad \mathrm{AM_3}^{\mathrm{dot}} + \mathrm{AM_2D} \rightarrow \mathrm{AM_3DM_2A},\ k_{\mathrm{add,3}} \qquad \mathrm{AM_3}^{\mathrm{dot}} + \mathrm{AM_3D} \rightarrow \mathrm{AM_3DM_3A},\ k_{\mathrm{add,3}}$$

$$\mathrm{A}^{\mathrm{dot}} + \mathrm{ADA} \rightarrow \mathrm{ADAterm},\ k_{\mathrm{t}}^{\mathrm{prime}} \qquad \mathrm{A}^{\mathrm{dot}} + \mathrm{AMDA} \rightarrow \mathrm{ADAterm},\ k_{\mathrm{t}}^{\mathrm{prime}} \qquad \mathrm{A}^{\mathrm{dot}} + \mathrm{AM_2DA} \rightarrow \mathrm{ADAterm},\ k_{\mathrm{t}}^{\mathrm{prime}}$$

$$\mathrm{A}^{\mathrm{dot}} + \mathrm{AM_3DA} \rightarrow \mathrm{ADAterm},\ k_{\mathrm{t}}^{\mathrm{prime}} \qquad \mathrm{A}^{\mathrm{dot}} + \mathrm{AMDMA} \rightarrow \mathrm{ADAterm},\ k_{\mathrm{t}}^{\mathrm{prime}} \qquad \mathrm{A}^{\mathrm{dot}} + \mathrm{AM_2DMA} \rightarrow \mathrm{ADAterm},\ k_{\mathrm{t}}^{\mathrm{prime}}$$

$$\mathrm{A}^{\mathrm{dot}} + \mathrm{AM_3DMA} \rightarrow \mathrm{ADAterm},\ k_{\mathrm{t}}^{\mathrm{prime}} \qquad \mathrm{A}^{\mathrm{dot}} + \mathrm{AM_2DM_2A} \rightarrow \mathrm{ADAterm},\ k_{\mathrm{t}}^{\mathrm{prime}} \qquad \mathrm{A}^{\mathrm{dot}} + \mathrm{AM_3DM_2A} \rightarrow \mathrm{ADAterm},\ k_{\mathrm{t}}^{\mathrm{prime}}$$

$$\mathrm{A}^{\mathrm{dot}} + \mathrm{AM_3DM_3A} \rightarrow \mathrm{ADAterm},\ k_{\mathrm{t}}^{\mathrm{prime}} \qquad \mathrm{AM}^{\mathrm{dot}} + \mathrm{ADA} \rightarrow \mathrm{ADAterm},\ k_{\mathrm{t}}^{\mathrm{prime}}{}_{\mathrm{long}} \qquad \mathrm{AM}^{\mathrm{dot}} + \mathrm{AMDA} \rightarrow \mathrm{ADAterm},\ k_{\mathrm{t}}^{\mathrm{prime}}{}_{\mathrm{long}}$$

$$\mathrm{AM}^{\mathrm{dot}} + \mathrm{AM_2DA} \rightarrow \mathrm{ADAterm},\ k_{\mathrm{t}}^{\mathrm{prime}}{}_{\mathrm{long}} \qquad \mathrm{AM}^{\mathrm{dot}} + \mathrm{AM_3DA} \rightarrow \mathrm{ADAterm},\ k_{\mathrm{t}}^{\mathrm{prime}}{}_{\mathrm{long}} \qquad \mathrm{AM}^{\mathrm{dot}} + \mathrm{AMDMA} \rightarrow \mathrm{ADAterm},\ k_{\mathrm{tp}}^{\mathrm{rime}}{}_{\mathrm{long}}$$

$$\mathrm{AM}^{\mathrm{dot}} + \mathrm{AM_2DMA} \rightarrow \mathrm{ADAterm},\ k_{\mathrm{t}}^{\mathrm{prime}}{}_{\mathrm{long}} \qquad \mathrm{AM}^{\mathrm{dot}} + \mathrm{AM_3DMA} \rightarrow \mathrm{ADAterm},\ k_{\mathrm{t}}^{\mathrm{prime}}{}_{\mathrm{long}} \qquad \mathrm{AM}^{\mathrm{dot}} + \mathrm{AM_2DM_2A} \rightarrow \mathrm{ADAterm},\ k_{\mathrm{t}}^{\mathrm{prime}}{}_{\mathrm{long}}$$

$$\mathrm{AM}^{\mathrm{dot}} + \mathrm{AM_3DM_2A} \rightarrow \mathrm{ADAterm},\ k_{\mathrm{t}}^{\mathrm{prime}}{}_{\mathrm{long}} \qquad \mathrm{AM}^{\mathrm{dot}} + \mathrm{AM_3DM_3A} \rightarrow \mathrm{ADAterm},\ k_{\mathrm{t}}^{\mathrm{prime}}{}_{\mathrm{long}} \qquad \mathrm{AM_2}^{\mathrm{dot}} + \mathrm{ADA} \rightarrow \mathrm{ADAterm},\ k_{\mathrm{t}}^{\mathrm{prime}}{}_{\mathrm{long}}$$

$$\mathrm{AM_2}^{\mathrm{dot}} + \mathrm{AMDA} \rightarrow \mathrm{ADAterm},\ k_{\mathrm{t}}^{\mathrm{prime}}{}_{\mathrm{long}} \qquad \mathrm{AM_2}^{\mathrm{dot}} + \mathrm{AM_2DA} \rightarrow \mathrm{ADAterm},\ k_{\mathrm{t}}^{\mathrm{prime}}{}_{\mathrm{long}} \qquad \mathrm{AM_2}^{\mathrm{dot}} + \mathrm{AM_3DA} \rightarrow \mathrm{ADAterm},\ k_{\mathrm{t}}^{\mathrm{prime}}{}_{\mathrm{long}}$$

$$\mathrm{AM_2}^{\mathrm{dot}} + \mathrm{AMDMA} \rightarrow \mathrm{ADAterm},\ k_{\mathrm{t}}^{\mathrm{prime}}{}_{\mathrm{long}} \qquad \mathrm{AM_2}^{\mathrm{dot}} + \mathrm{AM_2DMA} \rightarrow \mathrm{ADAterm},\ k_{\mathrm{t}}^{\mathrm{prime}}{}_{\mathrm{long}} \qquad \mathrm{AM_2}^{\mathrm{dot}} + \mathrm{AM_3DMA} \rightarrow \mathrm{ADAterm},\ k_{\mathrm{t}}^{\mathrm{prime}}{}_{\mathrm{long}}$$

$$\mathrm{AM_2}^{\mathrm{dot}} + \mathrm{AM_2DM_2A} \rightarrow \mathrm{ADAterm},\ k_{\mathrm{t}}^{\mathrm{prime}}{}_{\mathrm{long}} \qquad \mathrm{AM_2}^{\mathrm{dot}} + \mathrm{AM_3DM_2A} \rightarrow \mathrm{ADAterm},\ k_{\mathrm{t}}^{\mathrm{prime}}{}_{\mathrm{long}} \qquad \mathrm{AM_2}^{\mathrm{dot}} + \mathrm{AM_3DM_3A} \rightarrow \mathrm{ADAterm},\ k_{\mathrm{t}}^{\mathrm{prime}}{}_{\mathrm{long}}$$

$$\mathrm{AM_3}^{\mathrm{dot}} + \mathrm{ADA} \rightarrow \mathrm{ADAterm},\ k_{\mathrm{t}}^{\mathrm{prime}}{}_{\mathrm{long}} \qquad \mathrm{AM_3}^{\mathrm{dot}} + \mathrm{AMDA} \rightarrow \mathrm{ADAterm},\ k_{\mathrm{t}}^{\mathrm{prime}}{}_{\mathrm{long}} \qquad \mathrm{AM_3}^{\mathrm{dot}} + \mathrm{AM_2DA} \rightarrow \mathrm{ADAterm},\ k_{\mathrm{t}}^{\mathrm{prime}}{}_{\mathrm{long}}$$

$$\mathrm{AM_3}^{\mathrm{dot}} + \mathrm{AM_3DA} \rightarrow \mathrm{ADAterm},\ k_{\mathrm{t}}^{\mathrm{prime}}{}_{\mathrm{long}} \qquad \mathrm{AM_3}^{\mathrm{dot}} + \mathrm{AMDMA} \rightarrow \mathrm{ADAterm},\ k_{\mathrm{t}}^{\mathrm{prime}}{}_{\mathrm{long}} \qquad \mathrm{AM_3}^{\mathrm{dot}} + \mathrm{AM_2DMA} \rightarrow \mathrm{ADAterm},\ k_{\mathrm{t}}^{\mathrm{prime}}{}_{\mathrm{long}}$$

$$\mathrm{AM_3}^{\mathrm{dot}} + \mathrm{AM_3DMA} \rightarrow \mathrm{ADAterm},\ k_{\mathrm{t}}^{\mathrm{prime}}{}_{\mathrm{long}} \qquad \mathrm{AM_3}^{\mathrm{dot}} + \mathrm{AM_2DM_2A} \rightarrow \mathrm{ADAterm},\ k_{\mathrm{t}}^{\mathrm{prime}}{}_{\mathrm{long}} \qquad \mathrm{AM_3}^{\mathrm{dot}} + \mathrm{AM_3DM_3A} \rightarrow \mathrm{ADAterm},\ k_{\mathrm{t}}^{\mathrm{prime}}{}_{\mathrm{long}}$$

$$\mathrm{AM_3}^{\mathrm{dot}} + \mathrm{AM_3DM_3A} \rightarrow \mathrm{ADAterm},\ k_{\mathrm{t}}^{\mathrm{prime}}{}_{\mathrm{long}} \qquad \mathrm{ADA} \rightarrow \mathrm{A}^{\mathrm{dot}} + \mathrm{AD},\ k_{\mathrm{frag,I\_I}} \qquad \mathrm{AMDA} \rightarrow \mathrm{AM}^{\mathrm{dot}} + \mathrm{AD},\ k_{\mathrm{frag,IM\_I}}$$

$$\mathrm{AM_2DA} \rightarrow \mathrm{AM_2}^{\mathrm{dot}} + \mathrm{AD},k_{\mathrm{frag,IMM\_I}} \qquad \mathrm{AM_3DA} \rightarrow \mathrm{AM_3}^{\mathrm{dot}} + \mathrm{AD},\ k_{\mathrm{frag,macro\_I}} \qquad \mathrm{AMDA} \rightarrow \mathrm{AMD} + \mathrm{A}^{\mathrm{dot}},\ k_{\mathrm{frag,I\_sec}}$$

$$\mathrm{AM_2DA} \rightarrow \mathrm{AM_2D} + \mathrm{A}^{\mathrm{dot}},\ k_{\mathrm{frag,I\_sec}} \qquad \mathrm{AM_3DA} \rightarrow \mathrm{AM_3D} + \mathrm{A}^{\mathrm{dot}},\ k_{\mathrm{frag,I\_sec}} \qquad \mathrm{AMDMA} \rightarrow \mathrm{AMD} + \mathrm{AM}^{\mathrm{dot}},\ k_{\mathrm{frag,Im\_sec}}$$

$$\mathrm{AM_2DMA} \rightarrow \mathrm{AM_2D} + \mathrm{AM}^{\mathrm{dot}},\ k_{\mathrm{frag,Im\_sec}} \qquad \mathrm{AM_3DMA} \rightarrow \mathrm{AM_3D} + \mathrm{AM}^{\mathrm{dot}},\ k_{\mathrm{frag,Im\_sec}} \qquad \mathrm{AM_2DMA} \rightarrow \mathrm{AMD} + \mathrm{AM_2}^{\mathrm{dot}},\ k_{\mathrm{frag,Imm\_sec}}$$

$$\mathrm{AM_2DM_2A} \rightarrow \mathrm{AM_2D} + \mathrm{AM_2}^{\mathrm{dot}},\ k_{\mathrm{frag,Imm\_sec}} \qquad \mathrm{AM_3DM_2A} \rightarrow \mathrm{AM_3D} + \mathrm{AM_2}^{\mathrm{dot}},\ k_{\mathrm{frag,Imm\_sec}} \qquad \mathrm{AM_3DMA} \rightarrow \mathrm{AMD} + \mathrm{AM_3}^{\mathrm{dot}},\ k_{\mathrm{frag,macro\_sec}}$$

$$\mathrm{AM_2DM_3A} \rightarrow \mathrm{AM_2D} + \mathrm{AM_3}^{\mathrm{dot}},\ k_{\mathrm{frag,macro\_sec}} \qquad \mathrm{AM_3DM_3A} \rightarrow \mathrm{AM_3D} + \mathrm{AM_3}^{\mathrm{dot}},\ k_{\mathrm{frag,macro\_sec}}$$

Scheme 2. The complete PREDICI scheme used to generate the profiles provided in this paper. All the reactions were defined as elementary reactions for the purposes of simply representing the initialization period.

mentally confirmed by comparisons of polymerizations of methyl acrylate mediated by cumyl dithiobenzoate and by cumyl phenyldithioacetate,[13] although some deviation occurs towards the end of this period for specific monomer and retarding RAFT-agent combinations as a result of the formation of more stable intermediate radicals towards the end of the initialization period, which would also create some retardation in the system.

The application of PREDICI to the modeling of polymerization data has been fairly common for the RAFT process.[16] The implementation of the IRT model or 'fast fragmentation' without chain-length dependence lacks the selectivity required for the observed large kinetic differences during and after initialization to occur, as does a chain-length independent implementation of the SF model. This feature is a function of the fact that a constant addition rate coefficient and equilibrium constant will simply provide the same fragmentation rate coefficient for all species. However, the selectivity observed during initialization via in-situ NMR spectroscopy can very rapidly be reproduced via PREDICI if chain-length dependence is included in either model. Previously this behavior has been discussed at length (without simulations) for the fast fragmentation approach.[14,15] Coote et al. show clearly how chain-length dependence can be used to improve the SF model.[17] Chain-length dependence of the equilibrium constant was also suggested by Calitz et al. in 2003 for the IRT model for short chain lengths on the basis of electron spin resonance spectroscopy data,[7] and on the basis of the large number of potentially different addition-fragmentation rate coefficients as a function of chain length by McLeary et al.[15] Calitz et al. suggested that the equilibrium constant would increase from initial values of less than $10\,L \cdot mol^{-1}$ for the dithiobenzoate-mediated polymerization of styrene with an increase in chain length regardless of temperature. The difficulty in reconciling the two models comes from the significant differences in the fragmentation rates used by the two arguments. Kwak et al. suggested that at 60 °C a reasonable long chain value for the equilibrium constant at long chain lengths was around $55\,L \cdot mol^{-1}$.[11] Recently an independent determination of the equilibrium constant for the cyanoisopropyl dithiobenzoate-mediated polymerization of styrene was conducted by Luo et al using miniemulsion polymerization. The value that was calculated for the long chain equilibrium constant by these authors was $314\,L \cdot mol^{-1}$ at 75 °C.[18] As the nature of the determination was quite different from that of Kwak et al., the correspondence (less than an order of magnitude difference) is quite good. The SF model, using chain-length dependence and based on quantum chemical calculations in

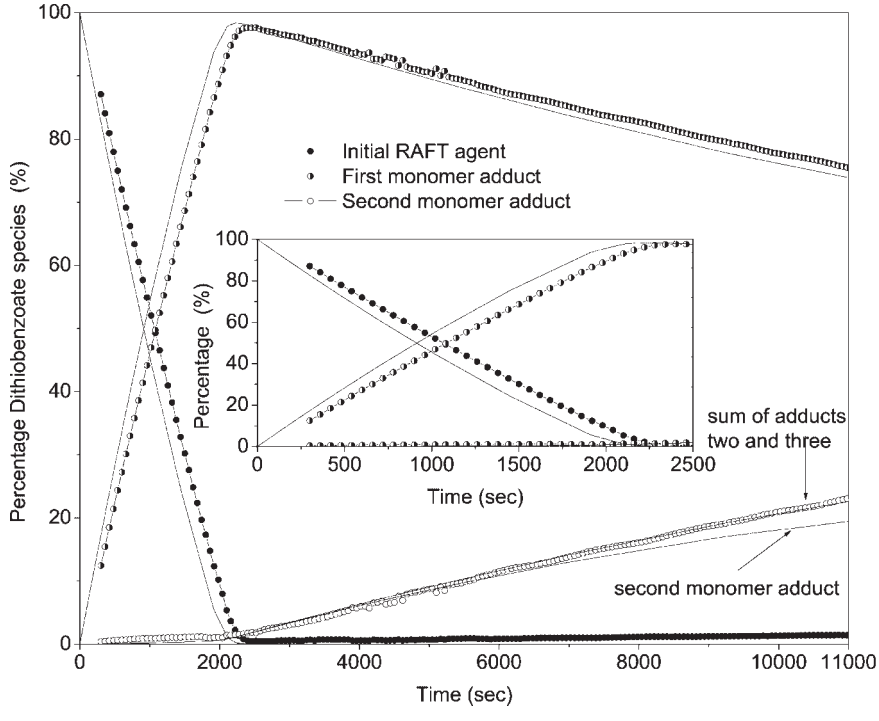

Figure 1. Comparison of the time dependencies of the concentrations of AD, AMD, and AM_2D by PREDICI modeling for the cyanoisopropyl-mediated polymerization of styrene at 70 °C generated by the IRT model (lines) versus experimental data obtained in precisely the same fashion as McLeary et al. with a one-minute data point interval.[14] The implementation of the PREDICI model provided in Scheme 2 used the rate coefficients for IRT as provided in Table 1 (solid lines). Starting reactant concentrations were: AD 0.695 M, 2,2′-azoisobutyronitrile (AIBN) 0.137 M, and styrene 3.82 M.

Coote and co-workers[17] provides equilibrium constants between 1.5×10^5 and 3.8×10^9 $L \cdot mol^{-1}$, which are consistent with equilibrium constants previously published by that group. The difference in equilibrium constants (and since both models agree on addition rate coefficients, the same difference applies to the resulting fragmentation rate coefficients) between the two models has commonly been referred to as six orders of magnitude.

Here we show that the implementation of the IRT model is also capable of modeling reaction kinetics with chain-length dependent fragmentation of the intermediate radical using independently determined equilibrium constant values. The values are on the order of those calculated by Calitz et al. for the cumyl dithiobenzoate-mediated polymerization of styrene for short chains and reach the equilibrium constants estimated by Luo et al. for long chain intermediate radicals.

Results and Discussion

The RAFT polymerization process model and the complete PREDICI scheme used to generate the profiles provided in this paper are given in Scheme 1 and 2, respectively. When modeling the data using the intermediate radical termination model, the linearity of the monomer consumption and initial RAFT agent loss data during the initialization period is comparable to the experimental data previously reported as shown in Figure 1.[14] All rate coefficients are given in Table 1. Note that the monomer consumption and initial RAFT agent loss are strongly coupled here, since almost all monomer consumption results in the production of AMD from AD, where AD is cyanoisopropyl dithiobenzoate and AMD is its *n*-meric styryl adduct (Scheme 1 and 2). The addition rate coefficients have been taken as 10^6 $L \cdot mol^{-1} \cdot s^{-1}$ in the same fashion as Coote et al. except for the addition of cyanoisopropyl radicals to the RAFT agent, which have been taken as half that value.[17] Termination rate coefficients have been used that are somewhat higher for short chain termination than the termination rate coefficients used by Coote et al.[17] The self-termination rate coefficient for cyanoisopropyl radicals is reported to be 1.2×10^9 $L \cdot mol^{-1} \cdot s^{-1}$ at room temperature, which makes a rate coefficient of six times that value (as used here, see Table 1) realistic at 70 °C.[19,20] The use of this coefficient is justified by examining the tetramethylsuccinonitrile peak intensity in the PREDICI models and comparing it

Table 1. A comparison of rate coefficients used in the PREDICI (provided in Scheme 2) implementations at 70 °C[a].

Intermediate radical termination (Scheme 1)	PREDICI rate coefficient (Scheme 2)	Rate coefficient	Slow fragmentation (ref. [17])	Rate coefficient
$k_{add,A,AD}$; $k_{add,A,PnD}$; $k_{add,A,AMD}$	k_{add}	5×10^5 $L \cdot mol^{-1} \cdot s^{-1}$	(k_{add})	5×10^5 $L \cdot mol^{-1} \cdot s^{-1}$
$k_{add,AM,AD}$; $k_{add,AM,AMD}$	$k_{add,1}$	1×10^6 $L \cdot mol^{-1} \cdot s^{-1}$	k_{add}	1×10^6 $L \cdot mol^{-1} \cdot s^{-1}$
$k_{add,Pn,AD}$; $k_{add,Pn,PmD}$ $n=2$	$k_{add,2}$	1×10^6 $L \cdot mol^{-1} \cdot s^{-1}$	k_{add}	1×10^6 $L \cdot mol^{-1} \cdot s^{-1}$
$k_{add,Pn,AD}$; $k_{add,Pn,PmD}$ $n>2$	$k_{add,3}$	1×10^6 $L \cdot mol^{-1} \cdot s^{-1}$	k_{add}	1×10^6 $L \cdot mol^{-1} \cdot s^{-1}$
$k_{fragA,PmD}$	k_{frag,I_sec}	2×10^6 s^{-1}	k_{fragI_sec}	5.8 s^{-1}
$k_{fragAM,PmD}$	k_{frag,IM_sec}	3×10^3 s^{-1}	k_{fragIM_sec}	0.3 s^{-1}
$k_{fragPn,PmD}$ $n=2$	k_{frag,IMM_sec}	3×10^3 s^{-1}	$k_{fragIMM\_sec}$	3.7×10^{-4} s^{-1}
$k_{fragPn,PmD}$ $n>2$	$k_{frag,macro\_sec}$	3×10^3 s^{-1}	$k_{fragmacro\_sec}$	2.5×10^{-4} s^{-1}
$k_{fragA,AD}$	k_{frag,I_I}	1×10^6 s^{-1}	k_{fragI_I}	4.3 s^{-1}
$k_{fragAM,AD}$	k_{frag,IM_I}	3×10^2 s^{-1}	k_{fragIM_I}	2.9×10^{-3} s^{-1}
$k_{fragPn,AD}$ $n=2$	k_{frag,IMM_I}	3×10^2 s^{-1}	$k_{fragIMM\_I}$	1.1×10^{-5} s^{-1}
$k_{fragPn,AD}$ $n>2$	$k_{frag,macro\_I}$	3×10^2 s^{-1}	$k_{fragmacro\_I}$	4.9×10^{-6} s^{-1}
k_{tAA}	k_{tAA}	8×10^9 $L \cdot mol^{-1} \cdot s^{-1}$	k_{tAA}	1×10^9 $L \cdot mol^{-1} \cdot s^{-1}$
k_t	k_t	1.2×10^8 $L \cdot mol^{-1} \cdot s^{-1}$	k_t	1.2×10^8 $L \cdot mol^{-1} \cdot s^{-1}$
k_t $n,m=1,(1,2,3)$	k_{t2}	6×10^8 $L \cdot mol^{-1} \cdot s^{-1}$	(k_{t2})	6×10^8 $L \cdot mol^{-1} \cdot s^{-1}$
k_t $n,m=0,(1,2,3)$	k_{tAMA}	1×10^9 $L \cdot mol^{-1} \cdot s^{-1}$	(k_{tAMA})	1×10^9 $L \cdot mol^{-1} \cdot s^{-1}$
$k'_{t,A}$	k'_t	1.2×10^8 $L \cdot mol^{-1} \cdot s^{-1}$	$k'_{t,A}$	0
k'_t	k'_{tlong}	6×10^7 $L \cdot mol^{-1} \cdot s^{-1}$	k'_t	0
k_d	k_d	3.6×10^{-5} s^{-1}	k_d	3.6×10^{-5} s^{-1}
$k_{p,A}$	k_{am}	5 200 $L \cdot mol^{-1} \cdot s^{-1}$	k_I	5 200 $L \cdot mol^{-1} \cdot s^{-1}$
k_p; $k_{p,AM}$	k_p	480 $L \cdot mol^{-1} \cdot s^{-1}$	k_p	480 $L \cdot mol^{-1} \cdot s^{-1}$
f	f	0.7	f	0.7

[a] The SF rate coefficients are taken from Coote et al.[17] The rate of cyanoisopropyl radical self-termination has been increased to compensate for temperature from the data of Terazima et al.[20] Termination rates for cyanoisopropyl radicals and other species have been scaled by chain length taking into account the limits of long chain termination in styrene polymerization and the self-termination of cyanoisopropyl radicals. Fragmentation rate coefficients have been calculated via the equilibrium constants of Luo et al.[18] with no compensation for chain length differences with chain growth. The differences between the preferential and nonpreferential fragmentation have been created using an order of magnitude difference between the rates for the fragmentation paths. Addition rates have been taken as 10^6 $L \cdot mol^{-1} \cdot s^{-1}$ for comparison purposes, while addition of cyanoisopropyl radicals has been halved because of the different nature of the radical. SF coefficients provided in parentheses were only implemented via the model presented here. The implementation of the model of Coote et al. is identical to that published.[17] All other rate coefficients are taken from Coote et al.[17]

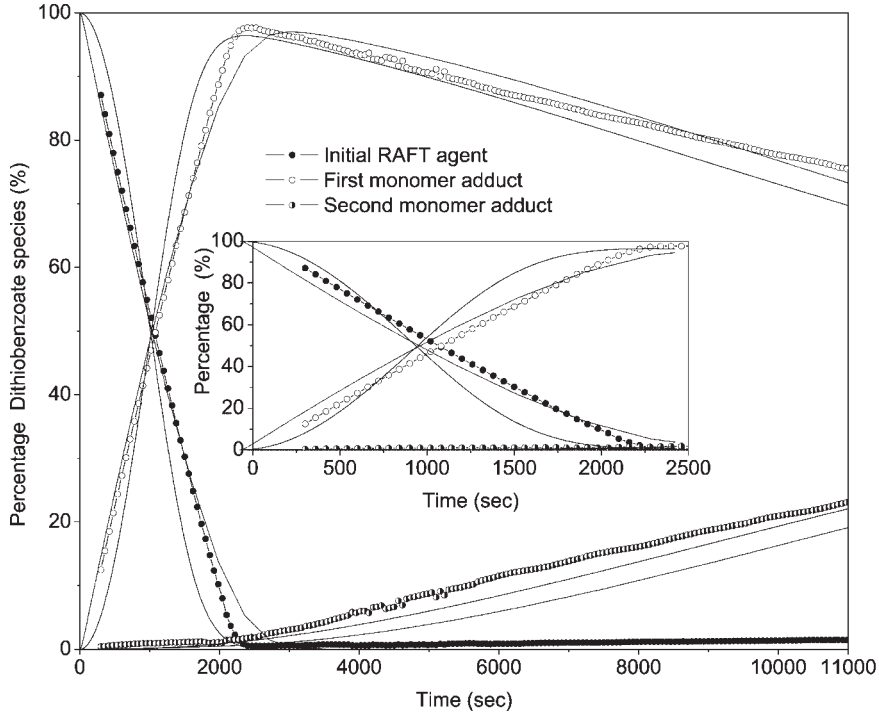

Figure 2. Comparison of the time dependencies of the concentrations of AD, AMD, and AM_2D obtained by PREDICI modeling (using the model in Scheme 2), for the cyanoisopropyl-mediated polymerization of styrene at 70 °C versus experimental data obtained in precisely the same fashion as McLeary et al. with a one minute data point interval.[14] Data obtained using the rate coefficients for SF as provided in Table 1 are indicated by solid lines, while the dotted lines indicate the use of the faster termination rate coefficients as listed under the IRT and SF models for the self-termination reaction of cyanoisopropyl radicals and a lower addition rate coefficient for the addition of the cyanoisopropyl radical to RAFT agents. Starting reactant concentrations were: AD 0.695 M, AIBN 0.137 M, styrene 3.82 M.

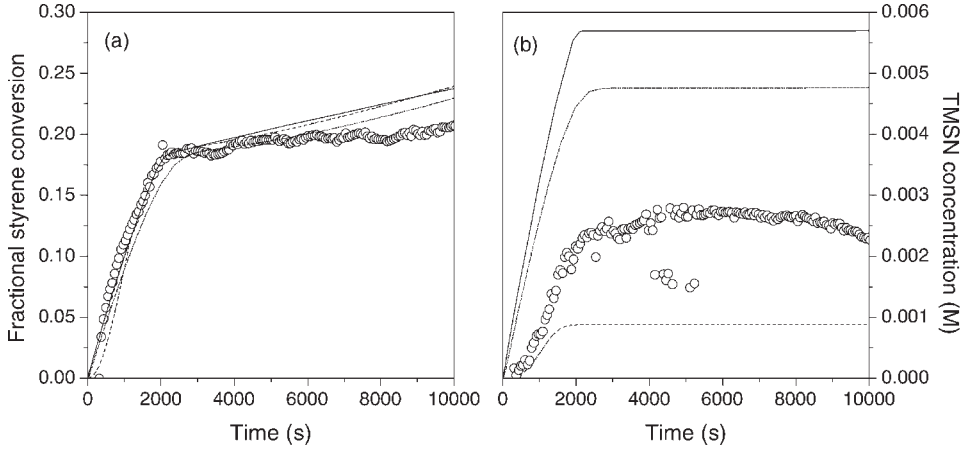

Figure 3. Comparison of the time dependencies of the concentrations of a) styrene and b) tetramethylsuccinonitrile (TMSN) obtained by PREDICI modeling (using the model in Scheme 2), for the cyanoisopropyl-mediated polymerization of styrene at 70 °C versus experimental data obtained in precisely the same fashion as McLeary et al. with a one minute data point interval.[14] The results using the rate coefficients for SF are indicated by dotted and dashed lines: the dotted lines indicate the use of the faster termination rate coefficients as listed under the IRT model in Table 1 for the self-termination reaction of cyanoisopropyl radicals and a lower addition rate coefficient for the addition of the cyanoisopropyl radical to RAFT agents, while the dashed lines are for the rate coefficients provided by Coote et al. The solid lines indicate the IRT implementation. Starting reactant concentrations were: AD 0.695 M, AIBN 0.137 M, styrene 3.82 M.

to the experimental data, which suggest a correspondence within a factor of two. The rate of intermediate radical termination has been taken as one half of the propagating radical termination on the basis that the termination is dominated by the diffusion of the small radical species in the reaction.[11] The deviations from the experimental data in terms of the initialization time predicted by the model are largely a function of the addition rate coefficient for cyanoisopropyl radicals to styrene, which are reported as being accurate to within a factor of two.[21] In addition, there is also uncertainty in the values of the termination rate coefficients and their dependence on chain length for such short radical chains. The predicted rate of monomer and AD consumption can readily be made to better fit the experimental data by reasonable adjustment of either of the above rate coefficients (to both of which the rate data are sensitive). Such a 'curve fitting' approach is, however, unnecessary for the purposes of showing that the intermediate radical termination model is capable of reproducing the features of the experimental data. As the rate coefficients for the fragmentation and addition of the second and third monomer adducts of the RAFT agents are identical for the purposes of the demonstration, the second monomer adduct in the model begins to deviate at longer times, but by simply adding the second and third monomer adducts a very good correlation is obtained. Figure 1 shows that the linearity generated by the IRT model is much closer to that of the experimental data than the curvature generated by the SF model shown in Figure 2 (using the model of Coote et al.), which was based on quantum-chemically calculated rate coefficients. However, using faster termination rate coefficients and the PREDICI implementation provided here for the SF model with the quantum-calculated rate coefficients shows an improved linearity of the PREDICI implementation (see Figure 2). The curvature of the SF modeling is partially a function of the fact that this model generates non-equilibrium conditions in radical species concentrations for each chain length. It has been shown that leaving groups that may be expected to show small differences in initialization behavior, such as cumyl and cyanoisopropyl radicals, may actually provide widely different behavior.[15] Despite the deviations from experimental results, qualitative selectivity can be generated for both models via PREDICI implementation.

Figure 3 provides the conversion of monomer and the formation of tetramethylsuccinonitrile. All three PREDICI implementations provide a very similar monomer conversion profile, while the deviations from the tetramethylsuccinonitrile profile are roughly within a factor of two in all cases.

The primary problem that both models have is the concentration of the 'missing' species, which is accompanied by PREDICI implementation of SF and IRT. In the case of the IRT model, the concentration of terminated intermediate species at the end of the modeled reaction time is on the order of a few percent of the thiocarbonylthio species, while in the SF model the intermediate radical concentration is of a similar order. It should be noted that in-situ ^{13}C NMR spectroscopy has successfully been used to monitor the formation of terminated intermediate radical species with time, although quantification was not possible.[22] The suggestion that the SF model can be adapted by adopting the reversible termination of the RAFT agent as a viable radical sink has been suggested by Coote et al.[17] The concentration of these species would, however, be of an order that it should be possible to observe these species during in-situ reaction monitoring. The decomposition rate of these species would also need to be such that radical decay of the intermediate signal can be fitted by following the square root of initiator concentration, which has been observed for the time dependence of the intermediate radical signal via electron spin resonance spectroscopy.

More detailed information is available in Supporting Information.

Conclusion

As both models still suffer from 'missing species' it is important to reflect on the fact that these systems are both models that appear to qualitatively reflect some of the behavior of the experimental systems. The fits are not, however, a mechanistic proof, although they can be used as supporting evidence for a prevailing mechanism. As pointed out by Coote et al.,[17] chain-length-dependent behavior at short chain lengths is likely to affect addition, fragmentation, propagation, and termination kinetics, which leads to an extremely complex reaction with many variables that may be tuned to fit any number of models.

The ideal evidence for either model would be to identify and observe the required concentrations of the 'missing species'.

Acknowledgements: The NMR facilities of the NMR laboratories of the *University of Stellenbosch* are acknowledged for the experimental data used in this communication.

[1] A. R. Wang, S. Zhu, Y. Kwak, A. Goto, T. Fukuda, M. J. Monteiro, *J. Polym. Sci., Part A: Polym. Chem.* **2003**, *41*, 2833.
[2] C. Barner-Kowollik, M. L. Coote, T. P. Davis, L. Radom, P. Vana, *J. Polym. Sci., Part A: Polym. Chem.* **2003**, *41*, 2828.
[3] C. Barner-Kowollik, J. F. Quinn, D. R. Morsley, T. P. Davis, *J. Polym. Sci., Part A: Polym. Chem.* **2001**, *39*, 1353.
[4] M. J. Monteiro, H. de Brouwer, *Macromolecules* **2001**, *34*, 349.
[5] [5a] C. Barner-Kowollik, P. Vana, J. F. Quinn, T. P. Davis, *J. Polym. Sci., Part A: Polym. Chem.* **2002**, *40*, 1058; [5b] C. Barner-Kowollik, T. P. Davis, J. P. A. Heuts, M. H. Stenzel, P.

Vana, M. Whittaker, *J. Polym. Sci., Part A: Polym. Chem.* **2003**, *41*, 365; [5c] A. Feldermann, M. L. Coote, M. H. Stenzel, T. P. Davis, C. Barner-Kowollik, *J. Am. Chem. Soc.* **2004**, *126*, 15915.

[6] Y. Kwak, A. Goto, Y. Tsujii, Y. Murata, K. Komatsu, T. Fukuda, *Macromolecules* **2002**, *35*, 3026.

[7] F. M. Calitz, M. P. Tonge, R. D. Sanderson, *Macromolecules* **2003**, *36*, 5.

[8] A. Alberti, M. Benaglia, M. Laus, D. Macciantelli, K. Sparnacci, *Macromolecules* **2003**, *36*, 736.

[9] C. Barner-Kowollik, J. F. Quinn, T. L. U. Nguyen, J. P. A. Heuts, T. P. Davis, *Macromolecules* **2001**, *34*, 7849.

[10] A. Goto, K. Sato, Y. Tsujii, T. Fukuda, G. Moad, E. Rizzardo, S. H. Thang, *Macromolecules* **2001**, *34*, 402.

[11] Y. Kwak, A. Goto, T. Fukuda, *Macromolecules* **2004**, *37*, 1219.

[12] [12a] M. L. Coote, L. Radom, *J. Am. Chem. Soc.* **2003**, *125*, 1490; [12b] M. L. Coote, D. J. Henry, *Macromolecules* **2005**, *38*, 1415.

[13] J. B. McLeary, J. M. McKenzie, M. P. Tonge, R. D. Sanderson, B. Klumperman, *Chem. Commun.* **2004**, 1950.

[14] J. B. McLeary, F. M. Calitz, J. M. McKenzie, M. P. Tonge, R. D. Sanderson, B. Klumperman, *Macromolecules* **2004**, *37*, 2383.

[15] J. B. McLeary, F. M. Calitz, J. M. McKenzie, M. P. Tonge, R. D. Sanderson, B. Klumperman, *Macromolecules* **2005**, *38*, 3151.

[16] M. Wulkow, M. Busch, T. P. Davis, C. Barner-Kowollik, *J. Polym. Sci., Part A: Polym. Chem.* **2003**, *42*, 1441.

[17] M. L. Coote, E. I. Izgorodina, E. H. Krenske, M. Busch, C. Barner-Kowollik, *Macromol. Rapid Commun.* **2006**, *27*(*13*), 1015.

[18] Y. Luo, R. Wang, L. Yang, B. Yu, B. Li, S. Zhu, *Macromolecules* **2006**, *39*, 1328.

[19] A. N. Savitsky, H. Paul, A. I. Shushin, *J. Phys. Chem. A* **2000**, *104*, 9091.

[20] M. Terazima, Y. Nogami, T. Tominaga, *Chem. Phys. Lett.* **2000**, *332*, 503.

[21] H. Fischer, L. Radom, *Angew. Chem. Int. Ed.* **2001**, *40*, 1340.

[22] F. M. Calitz, J. B. McLeary, J. M. McKenzie, M. P. Tonge, B. Klumperman, R. D. Sanderson, *Macromolecules* **2003**, *36*, 9687.

CHAPTER 7

In chapters 4-6, initialization during the RAFT-mediated polymerization of styrene, which is a very well behaved monomer, was described. The situation becomes much more complex if a poorly stabilized monomer such as vinyl acetate or N-vinylpyrrolidone is polymerized. In this case, much less reactive RAFT agents (*e.g*. dithiocarbamates or xanthates) must be used. Chapter 7 shows how *in situ* ^{1}H NMR can be used as a tool to determine the efficiency of RAFT agents. Efficient initialization can be distinguished from situations that are less favorable, such as those where the macro-RAFT agent is more reactive than the initial RAFT agent.

Reprinted with permission from *Macromolecules* **2006**, *39*, 7796-7797.

In-Situ NMR Spectroscopy for Probing the Efficiency of RAFT/MADIX Agents

Gwenaelle Pound,[†] James B. McLeary,[†] Jean M. McKenzie,[‡] Ronald F. M. Lange,[§] and Bert Klumperman*[,†,⊥]

Department of Chemistry and Polymer Science, University of Stellenbosch, Private Bag X1, Matieland 7602, South Africa; Central Analytical Facility, University of Stellenbosch, Private Bag X1, Matieland 7602, South Africa; BASF Research, GKT/U−B1, D-67056 Ludwigshafen, Germany; and Lab of Polymer Chemistry, Eindhoven University of Technology, P.O. Box 513, 5600 MB Eindhoven, The Netherlands

Received August 11, 2006
Revised Manuscript Received September 26, 2006

This Communication shows the first experimental evidence of selective initialization of poorly stabilized monomers in reversible addition fragmentation chain transfer (RAFT)[1] mediated living radical polymerization. Xanthate chain transfer agents[2] (CTAs) of the general formula EtO−C(═S)−SR were used to mediate the polymerization of *N*-vinylpyrrolidone (NVP) and vinyl acetate (VAc). In-situ ^{1}H NMR spectroscopy was performed to follow the concentrations of xanthate and monomer and to identify the nonradical species involved in the RAFT mechanism. Various xanthates were screened (Figure 1), and a direct relationship between a xanthate−monomer system which gives fast and selective initialization and a high degree of control over the molar mass distribution of the polymer was found.

From the concentration profiles of the xanthate, monomer (NVP), and the single monomer adduct of the xanthate shown in Figure 2, we observe that during the first 275 min the reaction is highly selective. There is no significant further polymerization until the xanthate is completely converted into the single monomer adduct. At the end of the initialization process, a slight but sudden change in the rate of monomer consumption occurs.

A selection of four ^{1}H NMR spectra at different reaction times is shown in Figure 3. This figure qualitatively confirms the selectivity during the first monomer addition. Similar behavior was earlier observed for dithiobenzoate-mediated polymerization of styrene.[3] However, for a poorly stabilized monomer such as NVP or VAc, it is quite unexpected to see such high selectivity.

The nature of the leaving group radical (R•) was identified as the determining factor in the initialization process. Until it was directly observed via in-situ ^{1}H NMR spectroscopy monitored polymerizations, slow selective initialization due to a low rate of addition of the leaving group radical to the monomer (slow reinitiation) was often mistaken for inhibition.[4] The slow formation of the single monomer adduct and the abnormally high concentration of the cyanoisopropyl recombination product (R_1R_1) gave evidence of the slow rate of addition of cyanoisopropyl radicals to VAc[5] (VAc-X1) and its effect on the rate of CTA conversion.

The experiment illustrated in Figure 2 was repeated with R = 2-carboxyethyl (X2) and with R = *tert*-butyl (X3). The use

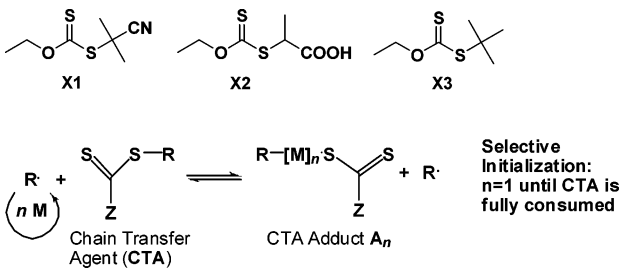

Figure 1. Xanthate chain transfer agents and mechanism of fragmentation of the initial chain-transfer agent.

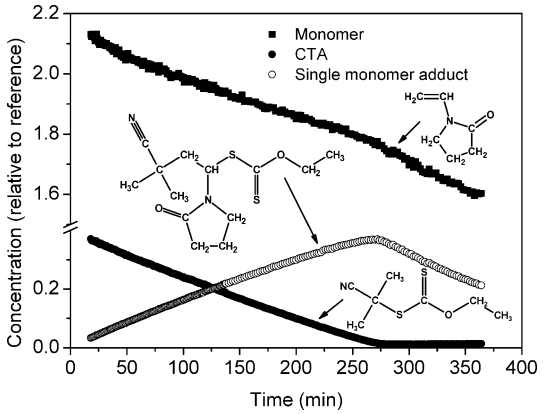

Figure 2. Concentration profiles of the species involved in initialization in the xanthate-mediated polymerization of NVP at 70 °C in C_6D_6, $[monomer]_0/[xanthate]_0 = 5$, probed by in-situ ^{1}H NMR spectroscopy (R = cyanoisopropyl).

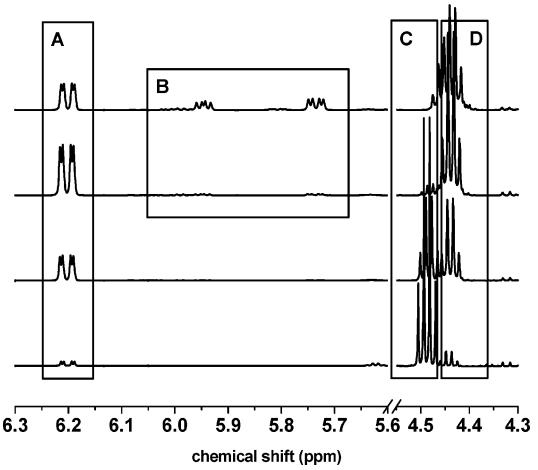

Figure 3. Four ^{1}H NMR spectra at different reaction times. From bottom to top: *t* (min) = 17, 137, 257, and 377. A, single monomer adduct; B, oligomer adducts; C, initial xanthate; D, single monomer adduct and oligomer adducts.

of xanthate X3 led to the simultaneous formation of oligomeric adducts ($n = 1$, 2, and 3). This was attributed to the monomer derived radicals having better leaving group ability than the *tert*-butyl R group. More than 1 mol equiv of monomer units was consumed before complete conversion of the initial CTA, indicating that propagation had already occurred to a significant extent. In such a so-called "hybrid" system,[6] higher molar mass material is obtained from the beginning of the reaction, and new xanthate end-capped chains are formed late in the polymerization, leading to broad molar mass distribution of the resulting polymer. It needs to be stressed that the possible causes

[†] Department of Chemistry and Polymer Science, University of Stellenbosch.
[‡] Central Analytical Facility, University of Stellenbosch.
[§] BASF Research.
[⊥] Eindhoven University of Technology.
* Corresponding author. E-mail: L.Klumperman@tue.nl.

10.1021/ma061843z CCC: $33.50
Published on Web 10/12/2006

Table 1. Relationship between Initialization and Molecular Weight Distribution

monomer	CTA	conv (%)	M_n[a] (g mol^{-1})	PDI[a]	selective initialization (time, min)[b]
VAc	X1	<1			yes (1320)
	X2	28	9 700	1.26	yes (25)
	X3	54	21 500	1.43	no
VP	X1	27	14 400	1.32	yes (270)
	X2	26	15 500	1.34	no[c]
	X3	48	31 900	1.74	no

[a] Experimental molar masses obtained by size exclusion chromatography (using RI detection) in THF with PS calibration for poly(vinyl acetate) (PVAc) and in HFIP with PMMA calibration for poly(*N*-vinylpyrrolidone) (PVP) prepared via RAFT polymerizations mediated by X1 or X2 or X3 in bulk at 60 °C for 3.5 h (PVAc) or 6 h (PVP); $[monomer]_0/[xanthate]_0 = 450$; $[xanthate]_0/[AIBN]_0 = 10$. [b] Initialization refers to selective formation of the single monomer adduct investigated by in-situ ^{1}H NMR spectroscopy polymerizations in C_6D_6 at 70 °C; $[monomer]_0/[xanthate]_0 = 5$. [c] See Supporting Information.

of hybrid behavior can be (1) choice of the Z group,[7] (2) ability of the R group to fragment from the intermediate radical (relative to the oligomer/polymer chain), and (3) ability of the R group radical to react with the monomer. The variation of R and Z groups of RAFT agents and their study via in-situ ^{1}H NMR spectroscopy will quickly pinpoint the origin of poor selectivity in initialization. The system VAc-X2 showed fast and selective initialization whereas NVP with X2 underwent a hybrid behavior regarding initialization as well as significant side reactions, which are still under investigation. It is likely that 2-carboxyethyl and NVP derived radicals have similar reactivities. Consequently, fragmentation occurs statistically on either side of CTA adduct radicals. The number of propagation steps prior to release of the R group will affect the polydispersity. This number remains low in the system VP-X2, and therefore PDI is probably not going to be much higher than in VP-X3 where initialization is completely selective.

Bulk polymerizations of NVP and VAc with low concentrations of CTA were performed in order to correlate the characteristics of initialization with the molar mass distribution of the polymers (Table 1). It was confirmed that selective initialization leads to more narrowly distributed molar masses, whereas the absence of initialization results in higher polydispersities, while still producing polymer chains end-capped with the xanthate mediating moiety.

In conclusion, in-situ ^{1}H NMR spectroscopy can quantitatively probe the mechanism of initialization involved in the transformation of a CTA into a dormant oligomeric chain. Conversely, kinetic studies combined with molar mass distribution characterization are not sufficient to pinpoint the origin of either inhibition or high polydispersities in RAFT/MADIX-mediated polymerization.[8] The results presented here show that NMR spectroscopy allows a defined distinction to be made between a "hybrid" RAFT mediated polymerization and an ideal RAFT-mediated polymerization for the first time. Moreover, it allows the investigation of the origin of the hybrid behavior. In this specific investigation the leaving and reinitiating abilities of the CTA R group were correlated to the occurrence of selective initialization, which in turn was correlated to well-defined molar mass distribution. This technique can thus be used to directly probe the efficiency of a CTA in controlling the polymerization of a given monomer.

Acknowledgment. The authors thank the Central Analytical Facility of the University of Stellenbosch for generous time on the NMR spectrometers, Mr. Wieb Kingma at the Eindhoven University of Technology for SEC analyses, and the BASF AG for research funds.

Supporting Information Available: ^{1}H NMR peak assignments, in-situ NMR spectroscopy polymerization conditions, and concentration profiles. This material is available free of charge via the Internet at http://pubs.acs.org.

References and Notes

(1) Chiefari, J.; Chong, Y. K. B.; Ercole, F.; Krstina, J.; Jeffery, J.; Le, T. P. T.; Mayadunne, R. T. A.; Meijs, G. F.; Moad, C. L.; Moad, G.; Rizzardo, E.; Thang, S. H. *Macromolecules* **1998**, *31*, 5559−5562.
(2) Charmot, D.; Corpart, P.; Adam, H.; Zard, S. Z.; Biadatti, B. G. *Macromol. Symp.* **2000**, *150*, 23−32.
(3) McLeary, J. B.; Calitz, F. M.; McKenzie, J. M.; Tonge, M. P.; Sanderson, R. D.; Klumperman, B. *Macromolecules* **2004**, *37*, 2383−2394.
(4) McLeary, J. B.; McKenzie, J. M.; Tonge, M. P.; Sanderson, R. D.; Klumperman, B. *Chem. Commun.* **2004**, 1950−1951.
(5) Fischer, H.; Radom, L. *Angew. Chem., Int. Ed.* **2001**, *40*, 1340−1371.
(6) Barner-Kowollik, C.; Quinn, J. F.; Nguyen, T. L. U.; Heuts, J. P. A.; Davis, T. P. *Macromolecules* **2001**, *34*, 7849−7857.
(7) Chiefari, J.; Mayadunne, R. T. A.; Moad, C. L.; Moad, G.; Rizzardo, E.; Postma, A.; Skidmore, M. A.; Thang, S. H. *Macromolecules* **2003**, *36*, 2273−2282.
(8) Barner-Kowollik, C.; Buback, M.; Charleux, B.; Coote, M. L.; Drache, M.; Fukuda, T.; Goto, A.; Klumperman, B.; Lowe, A. B.; McLeary, J. B.; Moad, G.; Monteiro, M. J.; Sanderson, R. D.; Tonge, M. P.; Vana, P. *J. Polym. Sci., Part A: Polym. Chem.* **2006**, *44*, 5809−5831.

MA061843Z

CHAPTER 8

In chapter 8, *in situ* ^{31}P NMR was used to monitor the living radical copolymerization between styrene and *n*-butyl acrylate. Just like ^{15}N NMR in the experiments of chapters 2 and 3, ^{31}P NMR can be used for determination of the terminal monomer unit in a dormant chain. A prerequisite is the use of the phosphorous-containing nitroxide DEPN (also known as SG1). The experimental data were very suitable for parameter estimation exercises that led to the construction of an accurate polymerization model in Predici.

Reprinted with permission from *Macromolecules* **2011**, *44*, 6683-6690.

Macromolecules

ARTICLE

pubs.acs.org/Macromolecules

In Situ NMR and Modeling Studies of Nitroxide Mediated Copolymerization of Styrene and *n*-Butyl Acrylate

Lebohang Hlalele[†] and Bert Klumperman[†,‡,*]

[†]Department of Chemistry and Polymer Science, University of Stellenbosch, Private Bag X1, Matieland 7602, South Africa

[‡]Laboratory of Polymer Chemistry, Eindhoven University of Technology, P.O. Box 513, 5600 MB Eindhoven, The Netherlands

Supporting Information

ABSTRACT: The combination of *in situ* ^{1}H NMR and *in situ* ^{31}P NMR was used to study the nitroxide mediated copolymerization of styrene and *n*-butyl acrylate. The alkoxyamine MAMA-DEPN was employed to initiate and mediate the copolymerization. The nature of the ultimate/terminal monomer units of dormant polymer chains were identifiedand quantified by *in situ* ^{31}P NMR. Simulations of the styrene and *n*-butyl acrylate copolymerization mediated by DEPN were investigated using the Predici software package. The rate coefficients of reversible deactivation of chains with *n*-butyl acrylate as the terminal unit were estimated via parameter estimation studies using Predici. Good correlations were obtained between experimental data and simulated data.

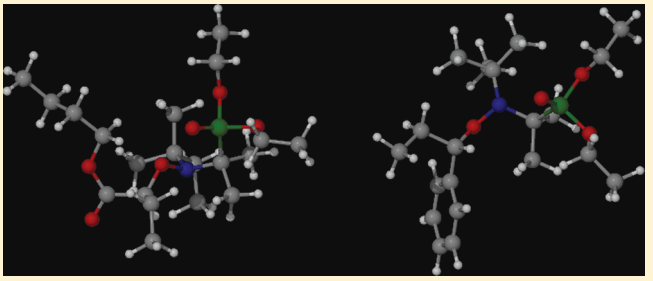

INTRODUCTION

In the past 2 decades, much attention has been focused on copolymerizations due to a wide variety of applications that can be served by copolymers.[1−4] In particular, styrene and *n*-butyl acrylate copolymers obtained via different techniques have been extensively studied and reported.[1,5,6] The use of *in situ* NMR in studies of living radical homo- and copolymerizations has proven to be very powerful.[7−10] Kinetic parameters such as reactivity ratios have been determined from *in situ* ^{1}H NMR data for different systems.[8,9] Information on copolymer composition has also been reported from *in situ* ^{1}H NMR data.[2,9]

In this contribution, we report the use of *in situ* ^{31}P NMR to monitor the copolymerization of styrene and *n*-butyl acrylate. The presence of phosphorus in the nitroxide *N*-*tert*-butyl-*N*-(1-diethoxyphosphoryl-2,2-dimethylpropyl)aminooxyl radical (DEPN, Scheme 1) used to mediate the polymerization allowed for the use of ^{31}P NMR to monitor dormant chains in the copolymerization system. Simulation of the copolymerization of styrene and *n*-butyl acrylate was also carried out using the Predici software package (Version 6.72.3). Validity of the use of k_c^B and k_d^B determined from homopolymerization data in the description of copolymerization kinetics is addressed.

EXPERIMENTAL SECTION

Chemicals. The alkoxyamine2-methyl-2-[*N*-*tert*-butyl-*N*-(1-diethoxyphosphoryl-2,2-dimethylpropyl)-aminooxy]propionic acid (MAMA-DEPN) was synthesized as described in the Supporting Information. Styrene and *n*-butyl acrylate (Plascon Research Centre, University of Stellenbosch) were washed with 10% aqueous solution of sodium hydroxide and then washed with distilled deionized water and dried with anhydrous magnesium sulfate. The respective monomers were then distilled under reduced pressure and stored at low temperatures. Deuterated dimethyl sulphoxide (DMSO-d_6, Cambridge Isotope Laboratories, 99%) and dimethylformamide (DMF, Aldrich) were used as received.

Scheme 1. Nitroxide DEPN and the Corresponding Alkoxyamine MAMA-DEPN Used in the Copolymerization of Styrene and *n*-Butyl Acrylate

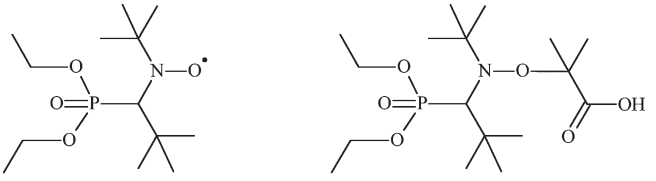

Procedure for the in Situ ^{1}H NMR Monitored Copolymerization. Styrene and *n*-butyl acrylate copolymerizations were followed via *in situ* ^{1}H NMR at 120 °C at different monomer feed compositions in DMSO-d_6. The ^{1}H NMR spectra were recorded on a 400 MHz Varian Unity Inova spectrometer. The ^{1}H NMR spectra were acquired with a 3 μs (40°) pulse width and a 4 s acquisition time. The NMR tube was first inserted into the magnet at 25 °C and the magnet fully shimmed on the sample and a spectrum collected to serve as reference at 25 °C. This was followed by removal of the sample from the magnet and the probe of the magnet was then heated to 120 °C and allowed to stabilize before

Received: May 21, 2011
Revised: July 27, 2011
Published: August 04, 2011

Scheme 2. Structures of Dormant Polymer Chains with *n*-Butyl Acrylate (A) and Styrene (B) as the Terminal Unit to Which the Nitroxide DEPN Moieties Are Attached

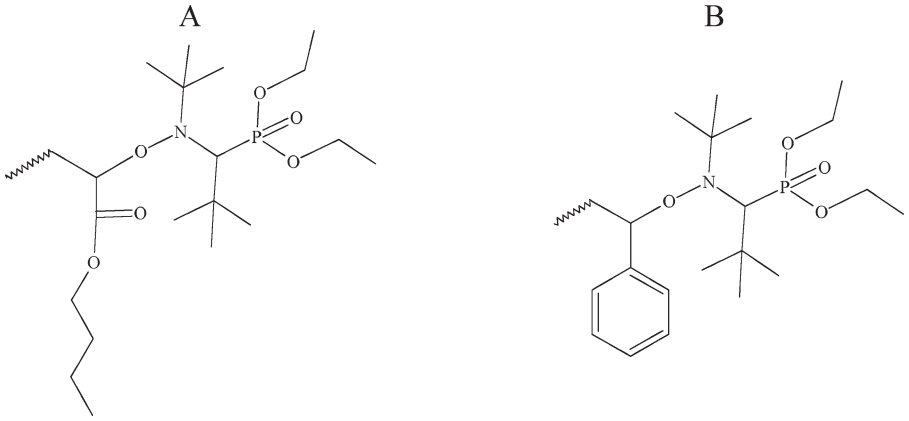

introducing the sample into the cavity of the magnet. After reinsertion of the sample, additional shimming was performed to acquire optimum conditions. The first spectrum was acquired 3−5 min after the reinsertion, followed by periodic spectra acquisition every 2 min for 90 min. Phase correction and baseline correction were performed automatically while integration of the spectra was carried out manually using ACD Laboratories 10.0 1D ^{1}H NMR processor. Concentration profiles were constructed relative to the reference (DMF).

In a typical copolymerization reaction, 30.1 mg of MAMA-DEPN (0.0789 mmol), 0.0722 g of styrene (0.693 mmol), 0.1314 g of *n*-butyl acrylate (1.025 mmol), 20 μL of DMF and 0.3113 g of DMSO-d_6 were thoroughly mixed and introduced into a J-Young type NMR tube. The DMF served as an internal reference material. The reaction mixture was degassed by three freeze−pump−thaw cycles and backfilled with nitrogen gas. The copolymerization was allowed to run for 90 min.

Procedure for the in Situ ^{31}P NMR Monitored Copolymerization. The ^{31}P NMR spectra were acquired with a 4.75 μs (45°) pulse width, a 1.6 s acquisition time, a relaxation delay of 1 s and an average of 23 scans per spectrum. Experimental procedures for the *in situ* ^{31}P NMR monitored copolymerization were identical to those of the *in situ* ^{1}H NMR monitored copolymerization experiments. The spectra were processed manually using ACD Laboratories 10.0 NMR processor.

In a typical copolymerization reaction, 30.3 mg MAMA-DEPN (0.0794 mmol), 0.1191 g styrene (1.1436 mmol), 0.1078 g *n*-butyl acrylate (0.8411 mmol) and 0.3094 g DMSO-d_6 were thoroughly mixed and introduced into a J-Young type NMR tube. The reaction mixture was degassed by three freeze−pump−thaw cycles and backfilled with nitrogen gas. The copolymerization was allowed to run for 90 min.

Modeling. The simulations of the copolymerization were carried out using the Predici software package (version 6.72.3).

RESULTS AND DISCUSSION

The presence of a phosphorus nucleus in the structure of the persistent nitroxide used in this study allowed for use of *in situ* ^{31}P NMR to probe the mechanistic features of styrene/*n*-butyl acrylate copolymerization. Preliminary homopolymerization reactions of styrene and *n*-butyl acrylate monitored via *in situ* ^{31}P NMR were carried out, following the chemical shift of the phosphorus of the nitroxide chain end moiety (Scheme 2). The ^{31}P NMR spectra of dormant species shown in Scheme 2 are shown in Figure 1. In the dormant state, the signal due to phosphorus in which styrene is the terminal unit differs from that

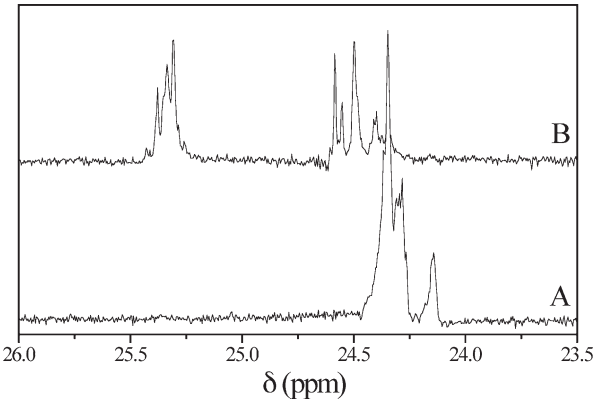

Figure 1. ^{31}P NMR spectra of dormant polymer chains with styrene (B) and *n*-butyl acrylate (A) as terminal units to which the nitroxide DEPN is attached in the respective homopolymerization reactions.

in which *n*-butyl acrylate is the terminal unit of the dormant chain. Thus, in copolymerization reactions the resulting phosphorus peaks can be used to distinguish dormant chains with either styrene or *n*-butyl acrylate as the terminal unit of a dormant polymer chain.

The ^{31}P NMR spectra for the homopolymerizations of styrene and *n*-butyl acrylate are shown in Figure 1. A complex multiplicity of signal peaks in both cases where styrene and *n*-butyl acrylate are terminal units is observed. The multiplicity can be explained by considering that the lone pair on the nitrogen of the nitroxide (in the dormant form) may align with the P═O making the nitrogen an active chiral center and the carbon α to the nitrogen is also a chiral center, such that there can exist the *rac*- or *meso*-forms of the structure. The two ethoxy groups attached to the phosphorus are also not magnetically equivalent. A typical ^{31}P NMR spectrum acquired during the copolymerization of styrene and *n*-butyl acrylate is illustrated by Figure 2, which shows two distinct regions of peaks. From the preliminary *in situ* ^{31}P NMR homopolymerization of both styrene and *n*-butyl acrylate (Figure 1), the regions of peaks in Figure 2 could be assigned. The region labeled "S" is a result of styrene being the terminal unit and the "S + B" region is an overlap of signal peaks

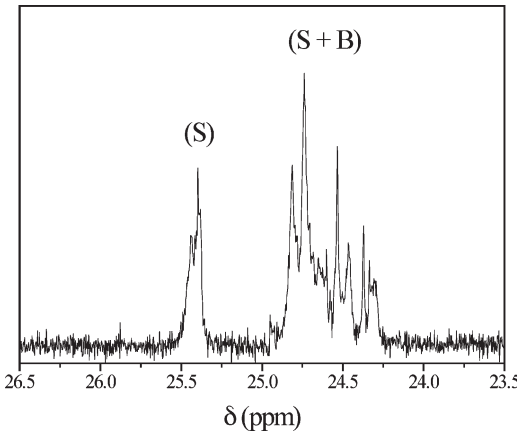

Figure 2. *In situ* ^{31}P NMR spectrum acquired 256 s into the copolymerization of styrene and *n*-butyl acrylate in DMSO-d_6 at 120 °C with the alkoxyamine MAMA-DEPN, at initial feed composition corresponding to $f_S^0 = 0.3$.

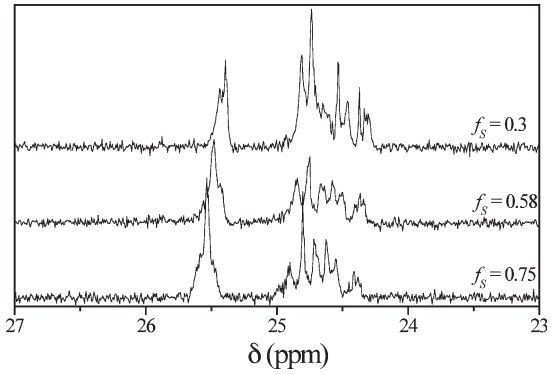

Figure 3. ^{31}P NMR spectra of the styrene/*n*-butyl acrylate copolymerization system at three initial feed compositions indicating signals due to dormant chains with styrene and *n*-butyl acrylate as terminal units.

resulting from styrene and *n*-butyl acrylate being terminal units to which the DEPN is attached.

For the *in situ* ^{31}P NMR homopolymerization of styrene, two regions of peaks were observed and their ratio remained constant throughout the entire polymerization time. With the knowledge of this ratio, the overlapping region (S + B) in Figure 2 could be resolved into two respective constituents, i.e. the contributions from dormant chains with styrene and *n*-butyl acrylate as the terminal units.

To assess the effect of the initial feed composition on the ^{31}P NMR spectrum, *in situ* ^{31}P NMR copolymerizations were conducted at different initial feed compositions. Kelemen et al. reported a significant variation in the ^{15}N NMR spectra as a function of initial feed composition.[11] In Figure 3, the ^{31}P NMR spectra are shown for three different initial feed compositions. The signal at 25.5 ppm due to styrene being the terminal unit, shifts upfield with the decreasing fraction of styrene in the initial feed composition. The change in chemical shift in the signal can be explained by considering the penultimate unit effects. At higher fractions of styrene in the feed, the contribution to the signal at 25.5 ppm is mainly due to the adduct PSS_i-DEPN. As the fraction of styrene in the feed is lowered, there is an increase in adduct of type PBS_i-DEPN, resulting in the shift of the signal.

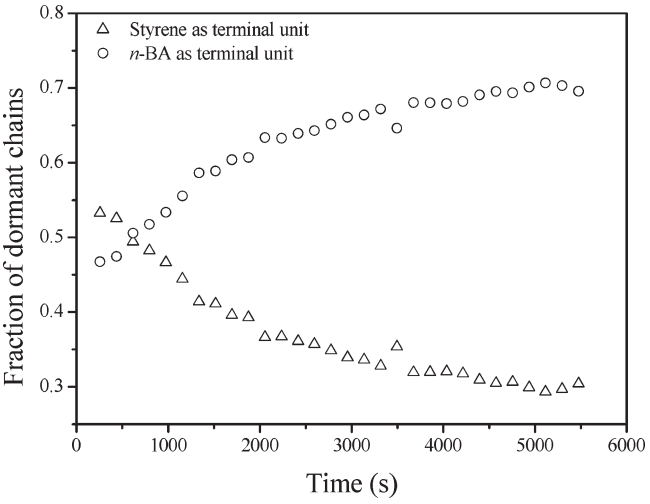

Figure 4. Evolution of the fractions of dormant chains with styrene and *n*-butyl acrylate as the terminal units for a copolymerization with $f_S^0 = 0.3$.

The possibility of the effect of the antepenultimate unit also exists, though it cannot be distinguished from that of the penultimate unit effect from this data. The respective signal intensities in Figure 3 vary with the initial feed composition as would be expected. However subtle, change in the shape of the ^{31}P NMR spectra is observed with varying initial feed composition. This latter observation can be related to the significant change reported in the ^{15}N NMR spectra of styrene/methyl acrylate system as a function of initial feed composition.[11]

Evolution of the fractions of dormant chains with styrene and *n*-butyl acrylate as terminal units for $f_S^0 = 0.3$, is illustrated in Figure 4. At early stages of the reaction, slightly more than 50% of the dormant chains have styrene as the terminal unit. At about 15% overall monomer conversion, the system has an approximately equal number of dormant chains with styrene and *n*-butyl acrylate as the terminal unit. Beyond the 15% conversion, the fraction of dormant chains with *n*-butyl acrylate as the terminal unit gradually increases to a total of about 70%.

At monomer feed compositions below the azeotrope (with respect to styrene), the relative rate of styrene consumption is faster than that of *n*-butyl acrylate. The result is composition drift, which leads to a decrease in the fraction of styrene and an increase in that of *n*-butyl acrylate. As a result, at monomer feed compositions below the azeotrope, the fraction of dormant chains with styrene terminal unit will show a gradual decrease with polymerization time or overall monomer conversion.

Two *in situ* NMR copolymerization experiments were conducted with both samples prepared as identical as possible. One was followed via *in situ* ^{1}H NMR and the other via *in situ* ^{31}P NMR. From the former technique, conversion data was obtained that could be correlated with the terminal unit data from the latter technique. The results are summarized in Figure 5. From Figure 5, the fraction of dormant chains with *n*-butyl acrylate as the terminal unit is illustrated as a function of overall monomer conversion and instantaneous feed composition with respect to *n*-butyl acrylate. With increasing overall monomer conversion, the instantaneous feed composition of *n*-butyl acrylate will increase gradually for copolymerizations conducted with an initial feed composition below the azeotropic feed composition for styrene.

Because of the overlap of peaks in the *in situ* ^{31}P NMR monitored copolymerizations, an alternative method was required to

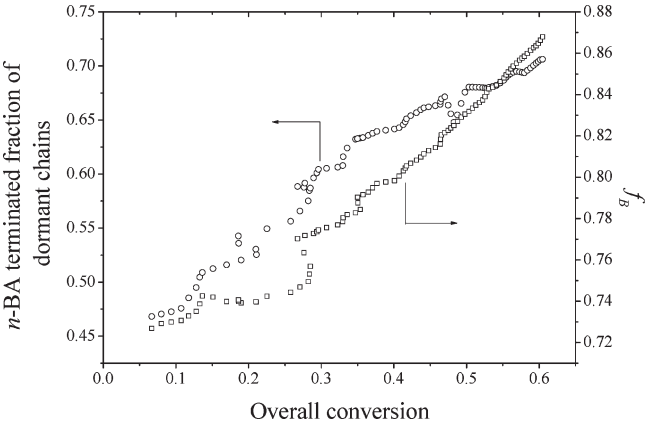

Figure 5. Evolution of the fraction of dormant chain with the *n*-butyl acrylate as the terminal unit and instantaneous feed composition as a function of overall monomer conversion for the copolymerization of styrene and *n*-butyl acrylate with $f_S^0 = 0.3$.

validate the data. Simulations of the styrene/*n*-butyl acrylate were carried out with the Predici software package for comparison with the experimental data. The implicit penultimate unit model (IPUM) was considered in the simulation of the copolymerization process. The terminal unit model (TUM) has been found inadequate in the description of average propagation rate coefficient, and for the purpose of the rate description of copolymerization processes, more comprehensive copolymerization models like the penultimate unit model (PUM) are employed. Before validation of the *in situ* ^{31}P NMR results on tracking the terminal unit of dormant chains, the copolymerization model was tested against experimental data in the feed composition range $0.2 \leq f_S^0 \leq 0.8$. The full copolymerization model description is illustrated by Scheme 3, with the applicable rate coefficients in Table 1.

Figures 6 and 7 illustrate simulated and experimental evolution of styrene and *n*-butyl acrylate concentrations with time. A discrepancy between the experimental and simulated data is observed. Two possible explanations for the observed discrepancy between the experimental and simulated data with regard to monomer concentration profiles are considered. The first explanation involves consideration of penultimate unit effects on activation/deactivation equilibria. The second possible explanation that will be discussed further in this paper involves assessing the validity of the use of k_c^B and k_d^B determined from *n*-butyl acrylate homopolymerizations in kinetic description of copolymerizations. In *n*-butyl acrylate homopolymerization, chain transfer is a well documented phenomenon resulting in coexistence of secondary propagating radicals (SPRs) and tertiary midchain radicals (MCRs).[19−21] In the presence of a free nitroxide, both the SPRs and MCRs can undergo reversible deactivation (Scheme 4).[22]

Because of the reversible deactivation of both the SPR and the MCR, the equilibrium can be described by eq 3, assuming steady state conditions. As a result, one can argue that the equilibrium constant determined from *n*-butyl acrylate homopolymerization is a composite value describing the two processes illustrated in Scheme 4.

$$k_d[\mathrm{P{-}X}] + k_d^t[\mathrm{Q{-}X}] = k_c[\mathrm{P^\bullet}][\mathrm{X}] + k_c^t[\mathrm{Q^\bullet}][\mathrm{X}] \qquad (3)$$

Scheme 3. Implicit Penultimate Unit Model (IPUM) for the Copolymerization of Styrene and *n*-Butyl Acrylate Implemented into the Predici Software Package

RY			⇌	R·	+ Y	k_{act} / k_{deact}
R·	+ S		→	PSS_1·		k_{add}^S
R·	+ B		→	PBB_1·		k_{add}^B
PSS_i·	+ S		→	PSS_{i+1}·		k_p^{SSS}
PSS_i·	+ B		→	PSB_{i+1}·		k_p^{SSB}
PBS_i·	+ S		→	PSS_{i+1}·		k_p^{BSS}
PBS_i·	+ B		→	PSB_{i+1}·		k_p^{BSB}
PBB_i·	+ B		→	PBB_{i+1}·		k_p^{BBB}
PBB_i·	+ S		→	PBS_{i+1}·		k_p^{BBS}
PSB_i·	+ B		→	PBB_{i+1}·		k_p^{SBB}
PSB_i·	+ S		→	PBS_{i+1}·		k_p^{SBS}
PSS_i·	+ Y		⇌	PSS_iY		k_c^S / k_d^S
PBS_i·	+ Y		⇌	PBS_iY		k_c^S / k_d^S
PSB_i·	+ Y		⇌	PSB_iY		k_c^B / k_d^B
PBB_i·	+ Y		⇌	PBB_iY		k_c^B / k_d^B
PSS_i·	+	PSS_i·	→	D		k_{tc}^{SS}
PBB_i·	+	PBB_i·	→	D		k_{tc}^{BB}
PSB_i·	+	PSB_i·	→	D		k_{tc}^{BB}
PBS_i·	+	PBS_i·	→	D		k_{tc}^{SS}
PSS_i·	+	PBB_i·	→	D		k_{tc}^{SB}
PSS_i·	+	PSB_i·	→	D		k_{tc}^{SS}
PSS_i·	+	PBS_i·	→	D		k_{tc}^{SS}
PBB_i·	+	PSB_i·	→	D		k_{tc}^{BB}
PBB_i·	+	PBS_i·	→	D		k_{tc}^{SS}
PSB_i·	+	PBS_i·	→	D		k_{tc}^{SS}

However, in the copolymerization case (Scheme 5), chain transfer to polymer can be regarded negligible if not nonexistent.[22] Thus, the equilibrium involving chains with *n*-butyl acrylate terminal units (reactions 4 and 5 in Scheme 5) are governed by the rate coefficients that govern reaction (1) in Scheme 4. The use of the equilibrium kinetic parameters determined from homopolymerization (with chain transfer to polymer present), can thus introduce an inaccurate description of the copolymerization process (Figures 6 and 7).

Parameter estimation (PE) studies with the Predici software package were then carried out to determine the optimum values of k_c^B and k_d^B for which the model would fit the experimental data in the feed composition range studied.

The results of the PE study are summarized in Table 2. These optimum values were then adapted into the model to replace the values indicated in Table 1 for further modeling studies of the copolymerization process. Figures 8−11 illustrate the evolution of both styrene and *n*-butyl acrylate concentrations with time, at two feed compositions. An improved correlation between experimental and simulated data was observed in the feed composition

Table 1. Rate Parameters Used in the Simulation of the Nitroxide-Mediated Copolymerization of Styrene and *n*-Butyl Acrylate As Depicted in Scheme 3

coefficient	A	E (kJ/mol)	Value (120 °C)	refs
k_{act}	2.4×10^{14} s^{-1}	112.3	0.289 s^{-1}	12
k_{deact}			5.0×10^{6} L mol^{-1} s^{-1}	13
k_{add}^{S}	6.7×10^{6} L mol^{-1} s^{-1}	16.5		13, 14
k_{add}^{B}	4.0×10^{6} L mol^{-1} s^{-1}	19.8		13, 14
k_{p}^{SS}	4.27×10^{7} L mol^{-1} s^{-1}	32.5		15
k_{p}^{BB}	2.31×10^{7} L mol^{-1} s^{-1}	18.1		16
r_S			0.74	this work[a]
r_B			0.23	this work[a]
s_S			0.48	17
s_B			0.06	17
k_{c}^{S}			2.6×10^{5} L mol^{-1} s^{-1}	13
k_{d}^{S}			7.5×10^{-3} L mol^{-1} s^{-1}	13
k_{c}^{B}			2.8×10^{7} L mol^{-1} s^{-1}	13, 18
k_{d}^{B}			1.55×10^{-3} L mol^{-1} s^{-1}	13
k_{tc}^{SS}			1.8×10^{8} L mol^{-1} s^{-1}	13
k_{tc}^{BB}			7.34×10^{7} L mol^{-1} s^{-1}	13
k_{tc}^{SB}			1.0×10^{8} L mol^{-1} s^{-1}	estimate

[a] The reactivity ratios of styrene and *n*-butyl acrylate were estimated from the high conversion in situ ^{1}H NMR data following the method described by Aguilar et al.[8]

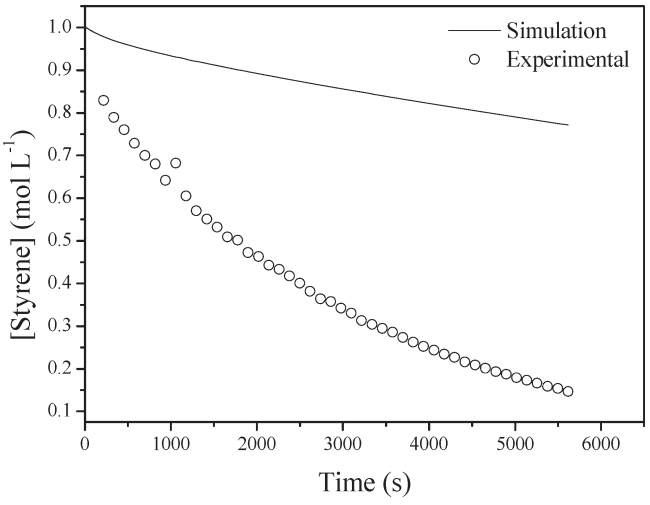

Figure 6. Simulated vs experimental evolution of styrene concentration with time for $f_S^0 = 0.3$. k_c^B and k_d^B values used in the simulation are in Table 1.

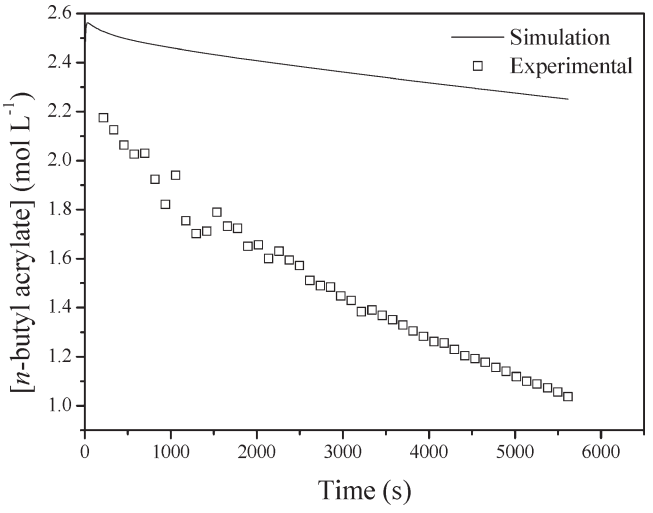

Figure 7. Simulated vs experimental evolution of *n*-butyl acrylate concentration with time for $f_S^0 = 0.3$. k_c^B and k_d^B values used in the simulation are in Table 1.

range studied when the values of k_c^B and k_d^B determined from the PE study were used. Figures 8 and 9 illustrate the agreement between the model and experiments below the azeotropic feed composition of the styrene/*n*-butyl acrylate system, while Figures 10 and 11 show the agreement above the azeotropic feed composition.

To further probe how representative the proposed model is of the real copolymerization system, simulations were carried out to predict the terminal unit of dormant chains. Figures 12 and 13 illustrate the evolution of fraction of dormant chains which possess *n*-butyl acrylate as the terminal unit at two different initial feed compositions. Even though the ^{31}P NMR were marked by overlap of peaks from dormant chains with styrene and *n*-butyl acrylate as terminal units, the method of analysis used to separate both signals resulted in data that is comparable with the simulation data from the proposed model.

A reasonable quantitative agreement is observed between model and experimental data. However, a fairly poor qualitative agreement between the model and experimental data is observed, with the greatest deviation at early reaction times. This deviation can be ascribed to the uncertainties in the approximated rate coefficients of first monomer addition (k_{add}^S and k_{add}^B). The actual values of the rate coefficients of addition of styrene and *n*-butyl acrylate to the 2-carboxyprop-2-yl radical are not known. But

Scheme 4. Two Equilibrium Reactions in the Nitroxide-Mediated *n*-Butyl Acrylate Homopolymerization Involving both the Secondary Propagating Radical (SPR, Represented by P) and the Tertiary Mid-Chain Radical (MCR, Represented by Q) with the Nitroxide Represented by Y

SPR NMP Equilibrium

$$P_i\cdot + Y \underset{k_d^B}{\overset{k_c^B}{\rightleftharpoons}} P_i\text{-}Y \qquad (1)$$

MCR NMP Equilibrium

$$Q_i\cdot + Y \underset{k_d^t}{\overset{k_c^t}{\rightleftharpoons}} Q_i\text{-}Y \qquad (2)$$

Scheme 5. NMP Equilibrium Reactions Involving the Chains with *n*-Butyl Acrylate Terminal Unit in Nitroxide-Mediated Copolymerization of *n*-Butyl Acrylate and Styrene Considering the Penultimate Unit Model

$$PSB_i\cdot + Y \underset{k_d^B}{\overset{k_c^B}{\rightleftharpoons}} PSB_i\text{-}Y \qquad (4)$$

$$PBB_i\cdot + Y \underset{k_d^B}{\overset{k_c^B}{\rightleftharpoons}} PBB_i\text{-}Y \qquad (5)$$

Table 2. Optimum Values of k_c^B and k_d^B Obtained from the Parameter Estimation Study

coefficient	optimum value	95% confidence interval
k_c^B	5×10^5	$\pm 1 \times 10^5$
k_d^B	7×10^{-4}	$\pm 1 \times 10^{-4}$

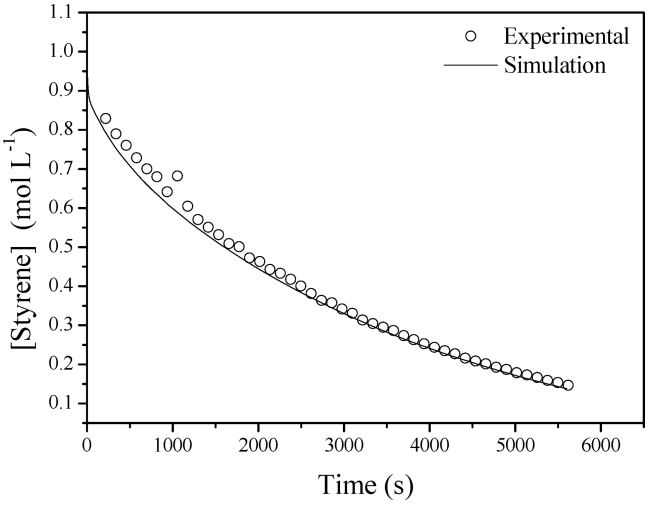

Figure 8. Simulated and experimental evolution of styrene concentration with time for $f_S^0 = 0.3$. k_c^B and k_d^B values used are 5×10^5 L mol^{-1} s^{-1} and 7×10^{-4} s^{-1}, respectively.

these rate coefficients are believed to be close to those of addition of similar monomers to 2-(alkoxy)carboxyprop-2-yl radical utilized in the model.[13] The selectivity of the primary radical for addition to styrene and *n*-butyl acrylate, governed by the rate coefficients of addition of the respective monomers, will determine the fraction of each respective dormant species, before the steady-state conditions are attained. This will occur until such a point that the radical ratio in the copolymerization system is governed by the reactivity ratios.

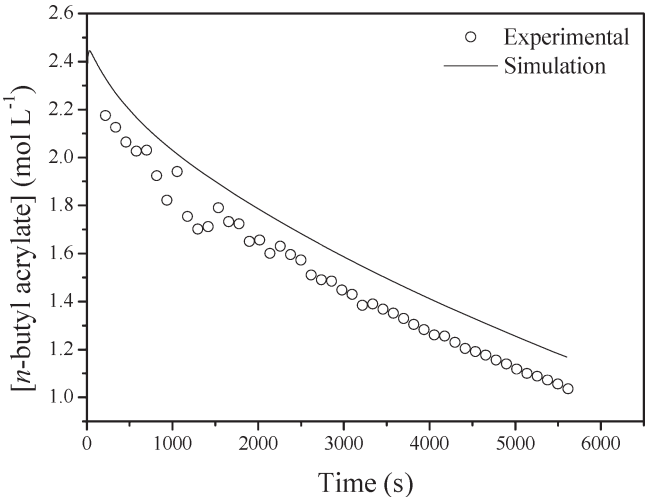

Figure 9. Simulated and experimental evolution of *n*-butyl acrylate concentration with time for $f_S^0 = 0.3$. k_c^B and k_d^B values used are 5×10^5 L mol^{-1} s^{-1} and 7×10^{-4} s^{-1}, respectively.

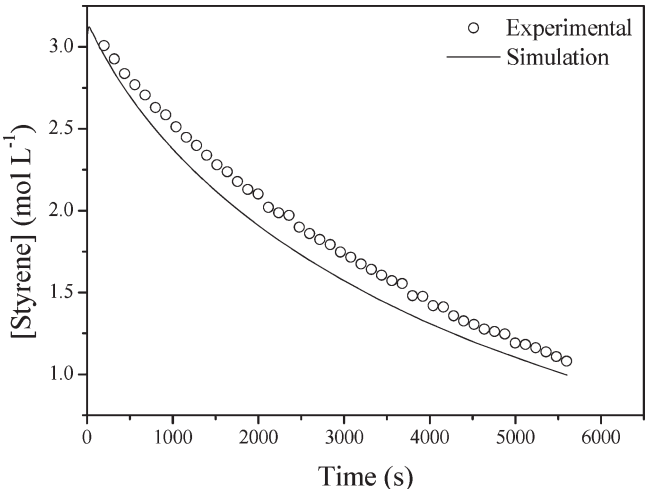

Figure 10. Simulated and experimental evolution of styrene concentration with time for $f_S^0 = 0.8$. k_c^B and k_d^B values used are 5×10^5 L mol^{-1} s^{-1} and 7×10^{-4} s^{-1}, respectively.

Further improvements of the model are however required, on both the qualitative and quantitative description of the copolymerization system with respect to the terminal unit of the dormant chains. In the Supporting Information further extensions to the parameter estimation studies are considered, with prime interest in improving the qualitative description of the fraction of dormant chains with either styrene or *n*-butyl acrylate as the terminal unit to which the nitroxide is attached. It turns out that the simultaneous parameter estimation of four rate parameters does not lead to a unique solution. Although the quality of the fit to the experimental data improves, it is difficult to judge what the physical relevance of the parameters is.

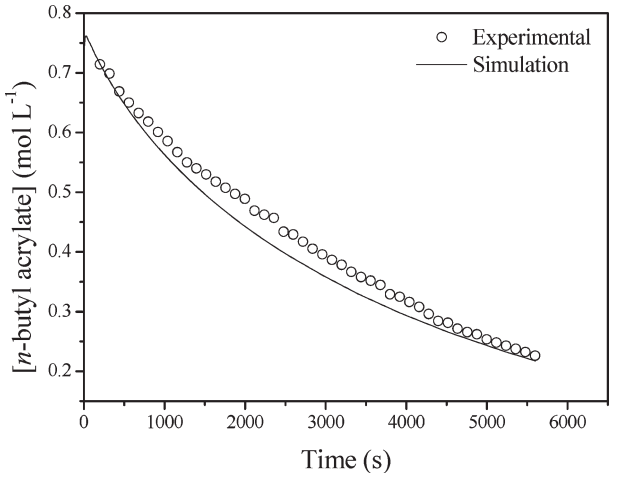

Figure 11. Simulated and experimental evolution of *n*-butyl acrylate concentration with time for $f_S^0 = 0.8$. k_c^B and k_d^B values used are 5×10^5 L mol^{-1} s^{-1} and 7×10^{-4} s^{-1}, respectively.

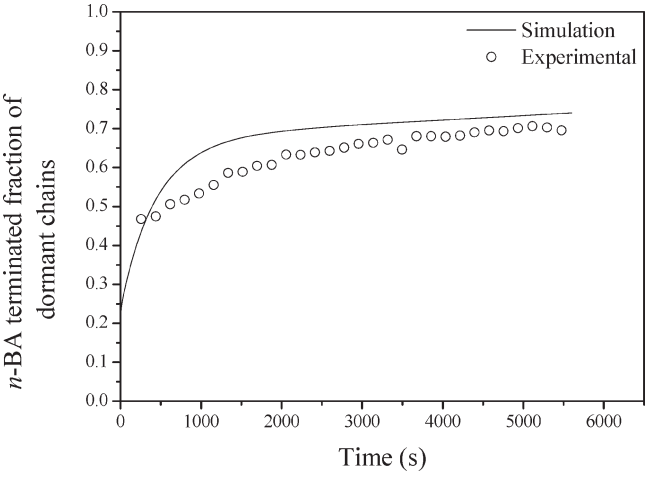

Figure 12. Experimental and simulated fractions (as a function of time) of dormant chains with *n*-butyl acrylate as the terminal unit in the copolymerization of styrene and *n*-butyl acrylate with $f_S^0 = 0.29$.

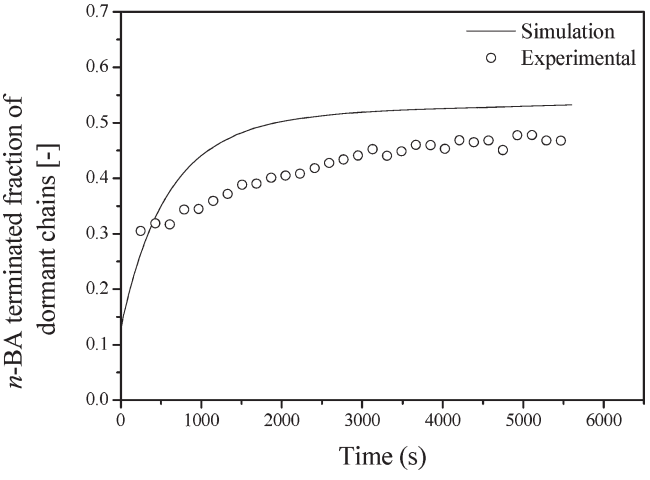

Figure 13. Experimental and simulated fractions (as a function of time) of dormant chains with *n*-butyl acrylate as the terminal unit in the copolymerization of styrene and *n*-butyl acrylate with $f_S^0 = 0.58$.

CONCLUSION

In situ ^{1}H and ^{31}P NMR monitored copolymerizations of styrene and *n*-butyl acrylate were successfully carried out. The copolymer composition curve was constructed from the *in situ* ^{1}H NMR data and was found to be in good agreement with a curve predicted from the reactivity ratios determined in this study. The terminal units of dormant polymer chains were profiled as a function of polymerization time via *in situ* ^{31}P NMR. The values of the rate coefficients describing the equilibrium involving the *n*-butyl acrylate terminal unit (k_c^B and k_d^B) were determined by fitting (via the parameter estimation tool of the Predici software package) the model to data extracted from *in situ* ^{1}H NMR experiments. The obtained values of k_c^B and k_d^B resulted in good agreement between the model and experimental data in the initial feed composition range studied. The resulting model also yielded good agreement between simulations and (dormant chain) terminal unit data extracted from *in situ* ^{31}P NMR experiments.

ASSOCIATED CONTENT

Supporting Information. Synthetic procedure for the synthesis of the alkoxyamine MAMA-DEPN including the ^{1}H NMR spectrum, analysis of the *in situ* ^{31}P NMR data, and simulation of styrene/BA copolymerization with PREDICI. This material is available free of charge via the Internet at http://pubs.acs.org

AUTHOR INFORMATION

Corresponding Author
*E-mail: bklump@sun.ac.za.

ACKNOWLEDGMENT

The authors thank Heidi Assumption and Elsa Malherbe for assistance with *in situ* NMR experiments. The authors would like to acknowledge Stellenbosch University and the South African Research Chairs Initiative (SARChI) from DST and NRF for financial support.

REFERENCES

(1) Arehart, S. V.; Matyjaszewski, K. *Macromolecules* **1999**, *32*, 2221–2231.
(2) Barner-Kowollik, C.; Heuts, J. P. A.; Davis, T. P. *J. Polym. Sci., Part A: Polym. Chem.* **2001**, *39*, 656–664.
(3) Börner, H. G.; Kühnle, H.; Hentschel, J. *J. Polym. Sci., Part A: Polym. Chem.* **2010**, *48*, 1–14.
(4) Hawker, C. J.; Elce, E.; Dao, J.; Volksen, W.; Russell, T. P.; Barclay, G. G. *Macromolecules* **1996**, *29* (7), 2686–2688.
(5) Benoit, D.; Grimaldi, S.; Robin, S.; Finet, J.-P.; Tordo, P.; Gnanou, Y. *J. Am. Chem. Soc.* **2000**, *122*, 5929–5939.
(6) Ziaee, F.; Nekoomanesh, M. *Polymer* **1998**, *39* (1), 203–207.
(7) Pound, G.; McLeary, J. B.; McKenzie, J. M.; Lange, R. F. M.; Klumperman, B. *Macromolecules* **2006**, *39*, 7796–7797.
(8) Aguilar, M. R.; Gallardo, A.; Fernández, M. d. M.; Román, J. S. *Macromolecules* **2002**, *35* (6), 2036–2041.
(9) Abdollahi, M.; Mehdipour-Ataei, S.; Ziaee, F. *J. Appl. Polym. Sci.* **2007**, *105*, 2588–2597.
(10) Barner, L.; Barner-Kowollik, C.; Davis, T. P. *J. Polym. Sci., Part A: Polym. Chem.* **2002**, *40*, 1064–1074.
(11) Kelemen, P.; Klumperman, B. *Macromolecules* **2004**, *37*, 9338–9344.
(12) Bertin, D.; Gigmes, D.; Marque, S. R. A.; Tordo, P. *Macromolecules* **2005**, *38*, 2638–2650.

(13) Chauvin, F.; Dufils, P.-E.; Gigmes, D.; Guillaneuf, Y.; Marque, S. R. A.; Tordo, P.; Bertin, D. *Macromolecules* **2006**, *39*, 5238–5250.
(14) Zytowski, T.; Knühl, B.; Fischer, H. *Helv. Chim. Acta* **2000**, *83*, 658–675.
(15) Beuermann, S.; Buback, M. *Prog. Polym. Sci.* **2002**, *27* (2), 191–254.
(16) Barner-Kowollik, C.; Günzler, F.; Junkers, T. *Macromolecules* **2008**, *41*, 8971–8973.
(17) Chambard, G. Ph.D. Thesis, Technische Universiteit Eindhoven, Eindhoven, The Netherlands, 2000.
(18) Chauvin, F.; Alb, A. M.; Bertin, D.; Tordo, P.; Reed, W. F. *Macromol. Chem. Phys.* **2002**, *203* (14), 2029–2041.
(19) Willemse, R. X. E.; Herk, A. M. v.; Panchenko, E.; Junkers, T.; Buback, M. *Macromolecules* **2005**, *38*, 5098–5103.
(20) Nikitin, A. N.; Hutchinson, R. A.; Buback, M.; Hesse, P. *Macromolecules* **2007**, *40*, 8631–8641.
(21) Junkers, T.; Koo, S. P. S.; Davis, T. P.; Stenzel, M. H.; Barner-Kowollik, C. *Macromolecules* **2007**, *40*, 8906–8912.
(22) Hlalele, L.; Klumperman, B. *Macromolecules* **2011**, *44*, 5554–5557.

CHAPTER 9

The experiments from chapters 3 and 8 have a lot in common, except that the former is governed by conventional radical polymerization kinetics and the latter is governed by living radical polymerization kinetics. It is generally accepted that the reaction kinetics of the propagating radical are identical for conventional radical polymerization and for living radical polymerization. This allows for a very interesting comparison between the ratios of terminal monomer units in active chains and those in dormant chains. Chapter 9 provides an interesting insight into this comparison for styrene – acrylate copolymerization.

Reprinted with permission from *ACS Symp. Ser.* **2012**, *1100*, 47-58.

Chapter 4

Terminal Monomer Units in Dormant and Active Copolymer Chains

Lebohang Hlalele[a] and Bert Klumperman[*,a,b]

[a]Department of Chemistry and Polymer Science, University of Stellenbosch, Private Bag X1 , Matieland 7602, South Africa
[b]Laboratory of Polymer Chemistry, Eindhoven University of Technology, P.O. Box 513, 5600 MB Eindhoven, The Netherlands
[*]E-mail: bklump@sun.ac.za

Experimental and simulation results comparing radical ratios and terminal monomer units for dormant species in the copolymerization of styrene with methyl acrylate and *n*-butyl acrylate are reported. The copolymerization of styrene and methyl acrylate was considered under conventional radical copolymerization conditions. Styrene and *n*-butyl acrylate copolymerization was conducted via controlled/living radical copolymerization (LRcP), using a nitroxide as a mediator. From the results it can be concluded that the fraction of styrene-terminal active chains is much larger than the fraction of styrene-terminal dormant chains. From the results it can be concluded that the fraction of styrene-terminal active chains decreases with time in the LRcP. Good agreement is obtained between the experimental data and simulated data.

In Progress in Controlled Radical Polymerization: Mechanisms and Techniques; Matyjaszewski, K., et al.; ACS Symposium Series; American Chemical Society: Washington, DC, 2012.

Introduction

Since the pioneering work on controlled/living radical polymerization, much work has been done to date on homo- and copolymerization reactions. A lot of attention has been directed towards understanding and comparing the kinetic and mechanistic features in both controlled/living radical copolymerization (LRcP) and conventional free radical copolymerization (FRcP) (*1–5*). However, very little experimental data has been published in the literature in which the radical ratios in a copolymerization system have been compared for an LRcP *vs*. a free radical copolymerization (FRcP) system. Kelemen *et al*. studied the radical ratios for the FRcP of styrene and methyl acrylate at different initial feed compositions (*6*). They employed the use of radical trapping agents to terminate polymer chains that grew under free radical conditions. In a copolymerization reaction, two distinct chain end radicals are possible. Recent work in our group on the study of terminal units in a nitroxide-mediated LRcP of styrene and *n*-butyl acrylate has indicated a significant difference between the terminal monomer unit in a dormant chain, compared to the terminal unit in a chain trapped during FRcP (*7*). Due to mediation of the copolymerization with a nitroxide species, the term LRcP will be used to refer to the class of controlled radical copolymerizations governed by the reversible deactivation mechanism.

In this contribution, we report on the determination of terminal monomer units in active chains (from FRcP) and dormant chains (from LRcP). A comparative simulation study of the copolymerization reactions is reported. Predici simulation of conventional free radical styrene/methyl acrylate copolymerization compared to the controlled styrene/*n*-butyl acrylate copolymerization simulation under the implicit penultimate unit model for both conventional and controlled radical polymerizations are discussed. It is assumed, within reasonable approximation that the two acrylate monomers should behave in relatively similar fashion.

Experimental

Materials

The alkoxyamine 2-methyl-2-[*N*-*tert*-butyl-*N*-(1-diethoxyphosphoryl-2,2-dimethylpropyl)-aminooxy]propionic acid (MAMA-DEPN) was synthesized as described elsewhere (*8–11*). Styrene and *n*-butyl acrylate (Plascon Research Centre, Stellenbosch University, South Africa) were washed with 10 % aqueous solution of sodium hydroxide and then washed with distilled deionised water and dried with anhydrous magnesium sulphate. The respective monomers were then distilled under reduced pressure and stored at low temperatures. Deuterated dimethyl sulphoxide (DMSO-d_6, Cambridge Isotope Laboratories, 99%) was used as received.

In Progress in Controlled Radical Polymerization: Mechanisms and Techniques; Matyjaszewski, K., et al.; ACS Symposium Series; American Chemical Society: Washington, DC, 2012.

Styrene/*n*-butyl acrylate copolymerization procedure. Styrene and *n*-butyl acrylate LRcPs were followed via *in situ* ^{31}P NMR at 120 °C at different monomer feed compositions in DMSO-d_6. The ^{31}P NMR spectra were acquired with a 4.75 μs (45°) pulse width, a 1.6 seconds acquisition time, a relaxation delay of 1 second and an average of 23 scans per spectrum. The NMR tube was first inserted into the magnet at 25 °C and the magnet fully shimmed on the sample and a spectrum collected to serve as reference at 25 °C. This was followed by removal of the sample from the magnet and the probe of the magnet was then heated to 120 °C and allowed to stabilize before introducing the sample into the cavity of the magnet. After re-insertion of the sample, additional shimming was performed to acquire optimum conditions. The first spectrum was acquired 3 – 5 minutes after the re-insertion, followed by periodic spectra acquisition every two minutes for 90 minutes. The spectra were processed manually using ACD Labs 10.0 NMR processor®.

In a typical copolymerization reaction, 30.3 mg MAMA-DEPN (0.0794 mmol), 0.1191 g styrene (1.1436 mmol), 0.1078 g *n*-butyl acrylate (0.8411 mmol) and 0.3094 g DMSO-d_6 were thoroughly mixed and introduced into a J-Young type NMR tube. The reaction mixture was degassed by three freeze-pump-thaw cycles and backfilled with nitrogen gas. The copolymerization was allowed to run for 90 minutes.

Simulations

The simulations of the copolymerization were carried out using the Predici software package (version 6.72.3). The implicit penultimate unit model was assumed for the simulations of both FRcP and LRcP processes. The implemented model and kinetic parameters employed are shown in Schemes 1 and Table 1, and Scheme 2 and Table 2, respectively.

Under the simulation conditions chosen for the FRcP, the chains initiated by radicals I• and R• propagate before they are irreversibly terminated by the nitroxide. At 70 °C, the nitroxide TEMPO can form a stable C – ON bond, in contrast to nitroxides such as DEPN. Due to relatively similar reactivity parameters of the two copolymerization systems, direct comparisons can be made, evaluating the fraction of the active radical species and that of the dormant species. Dormant species in LRcP undergo continuous reversible activation-deactivation cycles, whereas in FRcP, the chosen temperature is such that once trapping by the nitroxide occurs, there is no subsequent activation of such a species.

In Progress in Controlled Radical Polymerization: Mechanisms and Techniques; Matyjaszewski, K., et al.;
ACS Symposium Series; American Chemical Society: Washington, DC, 2012.

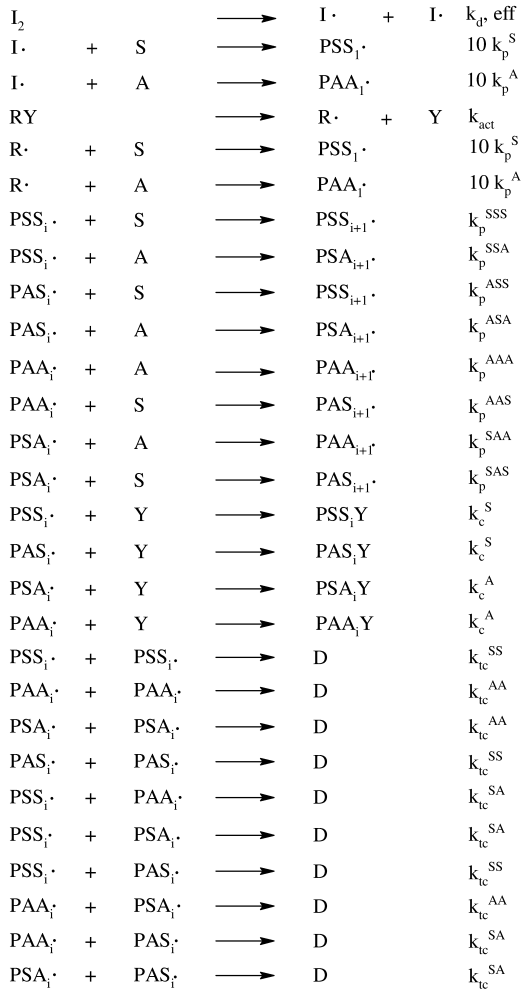

Scheme 1. The penultimate unit model for the copolymerization of n-butyl acrylate (B) and styrene (S) mediated by nitroxides (LRcP), implemented into the Predici software package.

In Progress in Controlled Radical Polymerization: Mechanisms and Techniques; Matyjaszewski, K., et al.; ACS Symposium Series; American Chemical Society: Washington, DC, 2012.

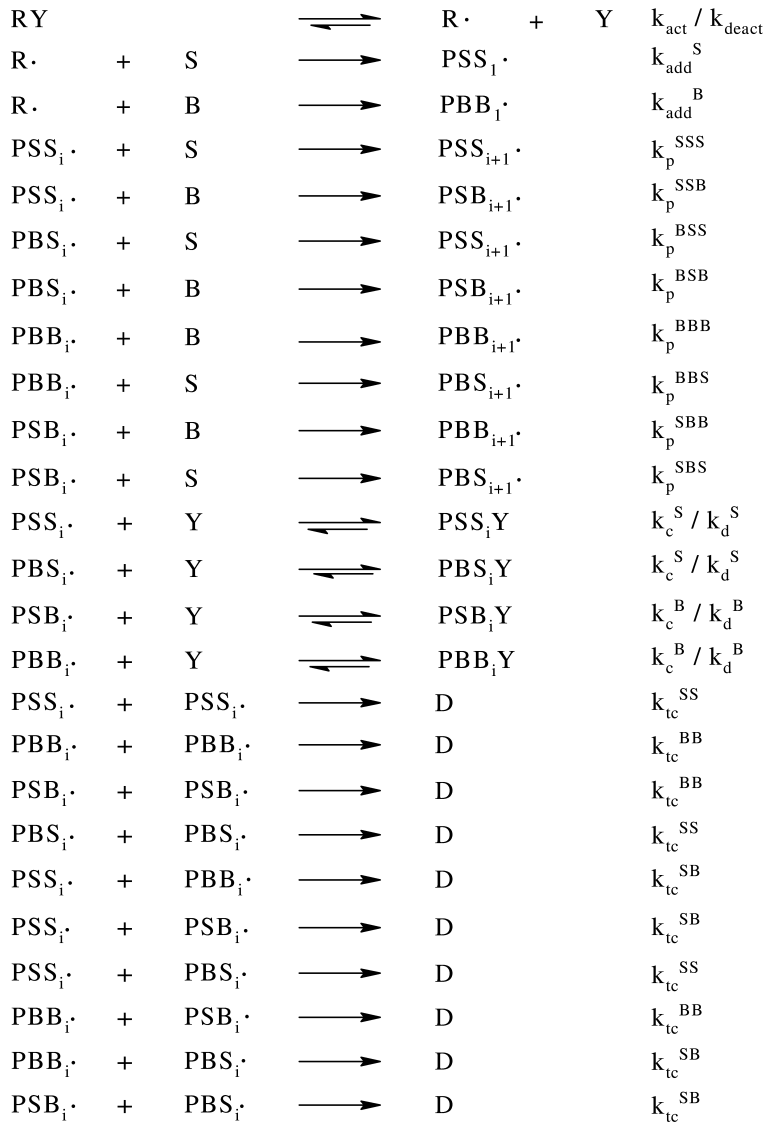

Scheme 2. The penultimate unit model for the conventional radical copolymerization (FRcP) of methyl acrylate (A) and styrene (S), implemented into the Predici software package.

In Progress in Controlled Radical Polymerization: Mechanisms and Techniques; Matyjaszewski, K., et al.; ACS Symposium Series; American Chemical Society: Washington, DC, 2012.

Table 1. Rate parameters used in the simulation of the nitroxide mediated copolymerization at 120 °C as depicted in Scheme 1

Coefficient	*A*	*E (kJ /mol)*	*Value (120 °C)*	*Refs*
k_{act}	2.4×10^{14} s^{-1}	112.3	0.289 s^{-1}	(*12*)
k_{deact}			5.0×10^{6} L mol^{-1} s^{-1}	(*13*)
k_p^{SS}	4.27×10^{7} L $mol^{-1}s^{-1}$	32.5		(*14*)
k_p^{BB}	2.31×10^{7} L $mol^{-1}s^{-1}$	18.1		(*15*)
r_S			0.74	(*7*)
r_B			0.23	(*7*)
s_S			0.48	(*16*)
s_B			0.06	(*16*)
k_c^S			2.6×10^{5} L $mol^{-1}s^{-1}$	(*13*)
k_d^S			7.5×10^{-3} L $mol^{-1}s^{-1}$	(*13*)
k_c^B			5×10^{5} L $mol^{-1}s^{-1}$	(*7*)
k_d^B			7×10^{-4} L $mol^{-1}s^{-1}$	(*7*)
k_{tc}^{SS}			1.8×10^{8} L $mol^{-1}s^{-1}$	(*13*)
k_{tc}^{BB}			7.34×10^{7} L $mol^{-1}s^{-1}$	(*13*)
k_{tc}^{SB}			1.0×10^{8} L $mol^{-1}s^{-1}$	Estimate

In Progress in Controlled Radical Polymerization: Mechanisms and Techniques; Matyjaszewski, K., et al.; ACS Symposium Series; American Chemical Society: Washington, DC, 2012.

Table 2. Rate parameters used in the simulation of the conventional radical copolymerization at 70 °C as depicted in Scheme 1

Coefficient	*A*	*E (kJ /mol)*	*Value (70 °C)*	*Refs*
k_d	1.58×10^{15} s^{-1}	128.74	3.996×10^{-5} s^{-1}	(*6*)
eff			0.6	
k_{act}			4.9×10^{-4}	(*6*)
k_p^{SS}	4.27×10^7 L $mol^{-1}s^{-1}$	32.5		(*14*)
k_p^{AA}	3.61×10^6 L $mol^{-1}s^{-1}$	13.9		(*17*)
r_S			0.73	(*6*)
r_A			0.19	(*6*)
s_S			0.41	(*6*)
s_A			0.41	(*6*)
k_c^S			1.0×10^8 L $mol^{-1}s^{-1}$	
k_c^A			5.0×10^8 L $mol^{-1}s^{-1}$	
k_{tc}^{SS}			1.0×10^8L $mol^{-1}s^{-1}$	
k_{tc}^{AA}			1.0×10^8 L $mol^{-1}s^{-1}$	
k_{tc}^{SA}			1.0×10^8 L $mol^{-1}s^{-1}$	

In Progress in Controlled Radical Polymerization: Mechanisms and Techniques; Matyjaszewski, K., et al.; ACS Symposium Series; American Chemical Society: Washington, DC, 2012.

Results and Discussion

For the LRcP experiments, the alkoxyamine employed was a DEPN-based alkoxyamine illustrated in Figure 1. The presence of phosphorus in the nitroxide structures allows for the copolymerization reactions to be followed via *in situ* ^{31}P NMR spectroscopy (*7*).

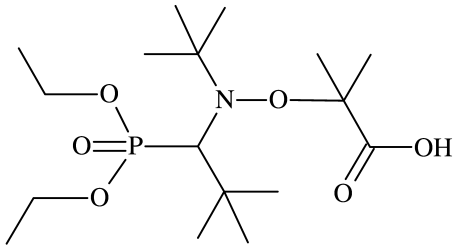

MAMA-DEPN

Figure 1. The structure of the DEPN-based alkoxyamine, MAMA-DEPN, used to initiate and mediate the copolymerization of styrene and n-butyl acrylate.

The evolution with time of the fraction of dormant chains with an acrylate as the terminal unit is illustrated in Figure 2. Detailed description of the simulation is described elsewhere (*7*). In contrast to the results illustrated in Figure 2, radical trapping experiments for an FRcP of styrene and methyl acrylate show behaviour completely opposite to that observed for the LRcP of styrene and *n*-butyl acrylate. The comparison between the fraction of dormant chains with an acrylate at the terminal unit for FRcP and LRcP processes is illustrated in Figure 3. For a FRcP, a direct correlation can be drawn between the ratio of the two radical species and the ratio of the trapped species. But such is not the case for the nitroxide mediated copolymerization.

From Figure 3, only at $f_A^0 \geq 0.9$ is a significant fraction of chains with an acrylate as the terminal monomer unit observed for conventional radical copolymerization. However, such is not the case for the nitroxide-mediated copolymerizations, where the fraction of dormant chains with acrylate as the terminal unit is observed to increase gradually with increasing initial fraction of the acrylate monomer in the monomer feed.

The evolution of the fraction of active chains with styrene as the terminal unit, for both FRcP and LRcP processes is illustrated in Figure 4. The difference in the two profiles illustrated in Figure 4 is attributed to the different radical reactivity ratios for the two systems. However, such a difference in the radical reactivity ratios does not disallow for the direct comparison of the two systems.

In Progress in Controlled Radical Polymerization: Mechanisms and Techniques; Matyjaszewski, K., et al.;
ACS Symposium Series; American Chemical Society: Washington, DC, 2012.

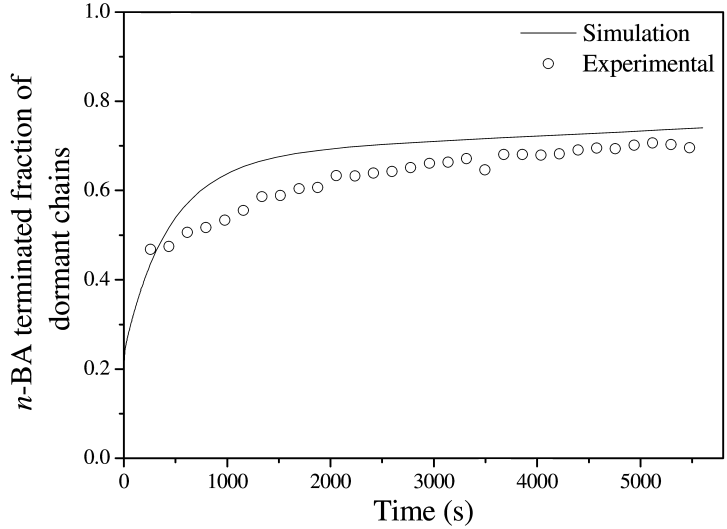

Figure 2. Experimental and simulated evolution of the fraction of dormant chains with n-butyl acrylate as the terminal monomer unit for the nitroxide mediated copolymerization of styrene and n-butyl acrylate for $f_A^0 = 0.71$.

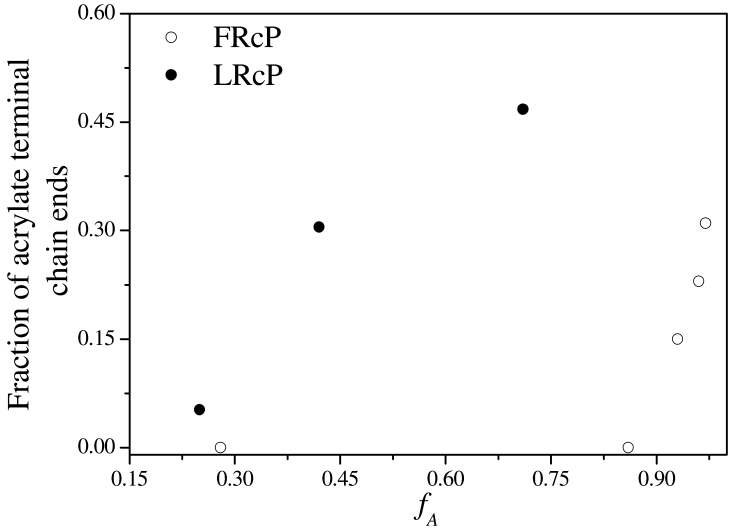

Figure 3. Evolution of nitroxide-terminated chains with an acrylate terminal monomer unit as a function of the fraction of the acrylate monomer in the feed taken at monomer conversion ca 5%.

In Progress in Controlled Radical Polymerization: Mechanisms and Techniques; Matyjaszewski, K., et al.; ACS Symposium Series; American Chemical Society: Washington, DC, 2012.

According to Figures 3 and 4, the fraction of dormant species with a specific monomer as the terminal monomer unit cannot be correlated to the fraction of the respective active radicals in the LRcP system. The fraction of the respective radicals is identical in both FRcP and LRcP, as would be expected from the virtually identical copolymer composition data of the respective techniques.

For FRcP of an acrylate with styrene, where $r_S > r_A$ and $k_p^S << k_p^A$, a greater fraction of active chains will have the styrene moiety as the terminal monomer unit. However, in nitroxide-mediated LRcP involving an acrylate and styrene, activation and deactivation coefficients control that dormant species with an acrylate at the terminal monomer position are far long-lived relative to those with styrene. The result is an accumulation with time of dormant species with an acrylate at the terminal monomer position (Figure 2). This observation made for nitroxide-mediated LRcP also holds true in all reversible deactivation copolymerizations, whereas the situation in reversible-addition fragmentation chain transfer (RAFT) mediated copolymerization is slightly different due to the degenerative chain transfer process.

The simulated fraction of dormant chain ends with an acrylate terminal monomer unit, in LRcP and chain ends resulting from trapping experiments in FRcP are illustrated in Figure 5. The increase in fraction of dormant chain ends with an acrylate in LRcP is well in agreement with the observations reported in Figure 2. In LRcP, the increase in the fraction of dormant chain ends with an acrylate monomer unit is comparable to values reported in Figure 3 for corresponding feed composition. In Figure 5, the fraction of trapped living chain ends with acrylate terminal monomer unit in FRcP remains low, in agreement with results illustrated in Figure 3 for the corresponding feed composition.

For both FRcP and LRcP, similar fraction of active chains with respective terminal monomer unit are observed. However, a contrasting behaviour is observed in the comparison of the nitroxide-capped chain ends in LRcP with the active chain ends in LRcP and FRcP. In FRcP, the nitroxide-capped chain ends result from trapping of chains that grow under conventional free radical conditions by irreversible combination with TEMPO. In FRcP, the fraction of nitroxide-capped chain ends with terminal acrylate monomer unit can directly be correlated to the fraction of active chains with an acrylate terminal monomer unit. However, in LRcP the fraction of nitroxide-capped chain ends with an acrylate monomer unit increases with time due to the relatively smaller equilibrium constant (K). The smaller equilibrium constant implies that dormant chain ends with acrylate as the terminal monomer unit are long-lived relative to their counterparts with styrene as the terminal monomer unit. As such, the accumulation with time of the dormant chain ends with acrylate as the terminal monomer unit is observed in both simulation and experimental data.

Based on the results reported in this contribution, a hypothesis can be put forward with regard to the synthesis of styrene and acrylate block copolymers. Since one of the pre-requisites for a narrow molecular weight distribution is fast initiation, it would seem ideal to synthesize the styrene block first, and the acrylate block second. The macro-alkoxyamine of styrene decomposes faster than that of the acrylate counterpart.

In Progress in Controlled Radical Polymerization: Mechanisms and Techniques; Matyjaszewski, K., et al.;
ACS Symposium Series; American Chemical Society: Washington, DC, 2012.

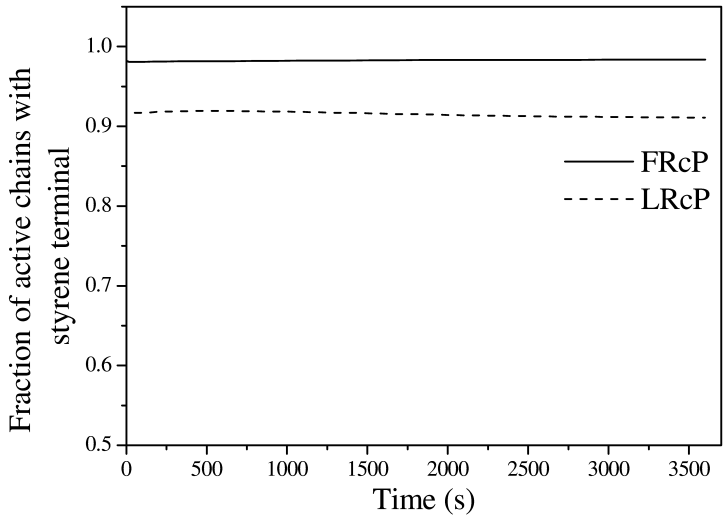

Figure 4. Simulated fraction of active chains with styrene as the terminal monomer unit as a function of time for $f_A^0 = 0.86$.

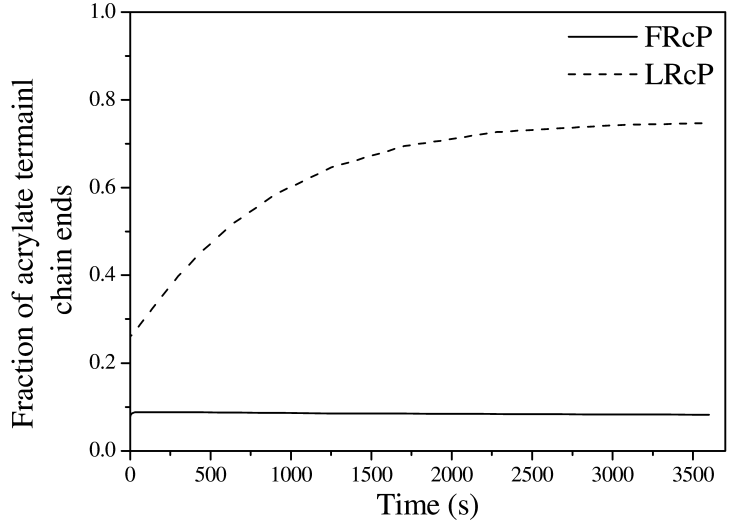

Figure 5. Simulated fraction of dormant and trapped chain ends with an acrylate terminal monomer unit as a function of time for $f_A^0 = 0.86$.

In Progress in Controlled Radical Polymerization: Mechanisms and Techniques; Matyjaszewski, K., et al.; ACS Symposium Series; American Chemical Society: Washington, DC, 2012.

Conclusions

A comparison between FRcP and LRcP with respect to chains terminated with the nitroxide has been reported. Simulations via the Predici software package were conducted for both LRcP and FRcP showing good agreement with experimental data. In FRcP, the evolution of fraction of living chain ends (from irreversible trapping with a nitroxide) with a styrene or an acrylate as the terminal monomer unit, can be directly correlated to the respective fraction of active chains. The simulation revealed that the fractions of active chains with either styrene or acrylate are similar in both FRcP and LRcP, as would be expected. In LRcP, the fraction of active chains with either styrene or acrylate as terminal monomer unit is different to the fractions observed for living chain ends.

References

1. Abdollahi, M.; Mehdipour-Ataei, S.; Ziaee, F. *J. Appl. Polym. Sci.* **2007**, *105*, 2588–2597.
2. Arehart, S. V.; Matyjaszewski, K. *Macromolecules* **1999**, *32*, 2221–2231.
3. Chambard, G.; Klumperman, B.; German, A. L. *Polymer* **1999**, *40*, 4459–4463.
4. Davis, T. P.; O'Driscoll, K. F. *Polym. Int.* **1991**, *24*, 65–70.
5. de la Fuente, J. L.; Fernández-García, M.; Fernández-Sanz, M.; Madruga, E. L. *Macromol. Rapid Commun.* **2001**, *22*, 1415–1421.
6. Kelemen, P.; Klumperman, B. *Macromolecules* **2004**, *37*, 9338–9344.
7. Hlalele, L.; Klumperman, B. *Macromolecules* **2011**, *44* (17), 6683–6690.
8. Couturier, J. L.; Guerret, O.; Bertin, D.; Gigmes, D.; Marque, S.; Tordo, P. U.S. Patent 20060142511, 2006, assigned to Arkema, France.
9. Guerret, O.; Couturier, J.-L.; Le Mercier, C. U.S. Patent 7126021, 2006, assigned to Arkema, France.
10. Smith, L. I.; Emerson, O. H. *Org. Synth.* **1949**, *29*, 18–21.
11. Talaty, E. R.; Boese, C. A.; Adewale, S. M.; Ismail, M. S.; Provenzano, F. A.; Utz, M. J. *J. Chem. Educ.* **2002**, *79* (2), 221–224.
12. Bertin, D.; Gigmes, D.; Marque, S. R. A.; Tordo, P. *Macromolecules* **2005**, *38*, 2638–2650.
13. Chauvin, F.; Dufils, P.-E.; Gigmes, D.; Guillaneuf, Y.; Marque, S. R. A.; Tordo, P.; Bertin, D. *Macromolecules* **2006**, *39*, 5238–5250.
14. Beuermann, S.; Buback, M. *Progr. Polym. Sci.* **2002**, *27* (2), 191–254.
15. Barner-Kowollik, C.; Günzler, F.; Junkers, T. *Macromolecules* **2008**, *41*, 8971–8973.
16. Chambard, G. Control of Monomer Sequence Distribution: Strategic Approach Based on Novel Insights in Atom Transfer Radical Polymerization. Ph.D Dissertation, Technische Universiteit Eindhoven, Eindhoven, 2000.
17. van Herk, A. M. *Macromol. Theory Simul.* **2000**, *9*, 433–441.

CHAPTER 10

This thesis spans a period of ten years in which research projects have been carried out to elucidate more of the mechanistic and kinetic details of radical (co)polymerization. In this chapter, we will reflect on the increase in knowledge that resulted from the work described in this thesis. The further applicability of *in situ* NMR techniques will be further discussed. Finally, an attempt will be made to list some of the challenges that remain for the next 10 years of research.

Epilogue

This thesis is a compilation of previously published work on the use of NMR spectroscopy in kinetic and mechanistic studies of radical polymerization processes. In this final chapter, the main achievements will be summarized and their impact on the understanding of radical polymerization will be assessed. In addition, remaining challenges will be addressed and translated into research opportunities for the next decade.

Achievements

Throughout the history of radical copolymerization it has been a challenge to perform model discrimination among the various copolymerization models. Most often, more than one model was able to adequately describe the experimental data. This is especially true when it comes to the elucidation of the penultimate unit effect on copolymer composition and propagation rate coefficients. At some point it became clear that a sensitive quantity to assess the penultimate unit effect is the ratio of the two propagating chain-end radicals.[1] However, the experimental determination of this ratio is not at all trivial. The typical concentration of radicals in a radical polymerization is around the detection limit of electron spin resonance (ESR) spectroscopy.

In this work we show that near-instantaneous trapping of growing radicals in a copolymerization and NMR spectroscopy of the resulting alkoxyamines is a powerful technique to determine the growing radical ratio. With that, we made the predicted method for model discrimination experimentally viable. The instantaneous trapping of the growing radicals is the Achilles heel of the technique. The rate of trapping will be dependent on the nature of the chain end radical and on the nature of the trapping agent. Hence, there are certainly examples where the nitroxides as used in this work will not be suitable. Further work is necessary to develop more universal trapping agents that meet all the criteria such as:

- Instantaneous trapping independent on the nature of the terminal monomer unit in a growing chain.
- Accurate quantification of the trapping products.

Since the first reports on Reversible Addition-Fragmentation chain Transfer (RAFT) mediated polymerization, inhibition and retardation phenomena were noticed for some combinations of monomers and RAFT agents. Although Moad and co-workers provided early qualitative explanations for the observations, detailed experimental data was lacking.

In this work we show the existence of very selective reactions that convert the original RAFT agent into its single-monomer adduct. In the case where addition of the leaving group of the RAFT agent to a first monomer is rate determining,

the first monomer consumption may lead to inhibition-like behavior. This process, for which we coined the name *initialization*, converts one monomer unit per RAFT agent molecule. Depending on the ratio of RAFT agent to monomer and on the relative rate constants, *initialization* may take quite some time and can easily be mistaken for inhibition if monomer conversion is determined via traditional means.

Work that is not included in this thesis has shown that *initialization* can also occur very rapidly, albeit still very selectively. In the case of the cumyl dihtiobenzoate-mediated copolymerization of styrene and maleic anhydride, *initialization* was completed within 3-5 minutes.[2] Alternatively, for *tert*-butyl-*O*-ethylxanthate-mediated polymerization of *N*-vinylpyrrolidone, the *initialization*, although still selective, may take up to several hours.[3] *In situ* NMR has shown to be a powerful tool to elucidate the details of the initialization process, and to assist in the selection of a suitable RAFT agent for a specific type of monomer.

A combined study into nitroxide-mediated copolymerization (NMcP) and conventional radical copolymerization (RcP) allowed us to shed more light on the nature of the propagating and dormant chain ends. For styrene – acrylate copolymerizations, it was shown that up to an acrylate fraction of f_A = 0.8 in the reaction mixture, there is virtually no measurable acrylate-terminal growing polymer radical. However, the fraction of acrylate-terminal dormant chains progressively increases to a fraction of around 0.5 for the same f_A = 0.8 monomer composition. This type of information can be quite essential if specific reactions aimed at one of the chain ends are targeted. An elegant example of such work was recently conducted by Heuts and co-workers who carried out cobalt-mediated catalytic chain transfer experiments on styrene – maleic anhydride – α-methylstyrene terpolymerizations.[4]

Remaining challenges

The eventual goal of increased understanding of polymerization processes is to maximize the degree of control over all aspects of the resulting polymer. This includes molar mass and molar distribution, but also includes monomer sequence and at some point maybe even tacticity. Further, there is an ever-continuing demand towards more complex polymer materials, *i.e.* variation in functionality, topology, ability to self-assemble, inclusion of stimuli-responsive behavior, etc.

Surely this means that techniques similar to the ones used in the current study need to be applied towards the elucidation of kinetic and mechanistic aspects of other polymerization processes. In principle all chain-growth polymerization processes would benefit from an approach such as presented in this thesis. Without an attempt to be comprehensive, processes that come to mind include:

- Olefin polymerizations (metallocene or Ziegler-Natta catalyzed)
- *N*-carboxyanhydride ring-opening polymerization
- Ni-catalyzed isocyanide polymerization

The presence of transition metal catalysts may pose several experimental challenges on some of these systems. However, it has already been shown by Haddleton and co-workers that *in situ* NMR spectroscopy is viable in Atom Transfer Radical Polymerization (ATRP) reactions, despite the paramagnetic character of Cu(II).[5]

As indicated above in the copolymerization studies, it can be essential to achieve instantaneous trapping of chain-end radicals. In our present studies we exclusively used nitroxides for this trapping process. Although nitroxides are efficient for several monomers, such as styrene, acrylates and dienes, there are several classes of monomers in which problems can be expected. In the case of methacrylates, disproportionation may occur, which will lead to an unsaturated chain end and a low molar mass hydroxylamine. Also in the cases of less activated monomers such as vinyl acetate and *N*-vinylpyrrolidone, nitroxides may not be the best choice. Which alternatives can we envisage to increase the scope of the mechanistic copolymerization studies? There are at least two avenues that can be explored in this respect. The first one is the use of microfluidics for the physical separation of initiation and trapping events. In other words, let the comonomer mixture with a photo-initiator flow through a microfluidic device in such a way that trapping can occur in a separate location after an accurately controlled propagation time in the order of 10 to 100 milliseconds. The trapping can then take place through a large excess of nitroxide, which will increase the trapping rate and bring it closer to "instantaneous". However, this does not solve the problem of side reactions as indicated for methacrylates (and other α-methyl monomers). The second approach is to switch to a different trapping agent, and preferably one that can be "tuned" in terms of its reactivity. An ideal candidate for that purpose would be the deactivator in ATRP, *i.e.* a Cu(II) complex. It has been shown that solubility and reactivity of Cu complexes can be tuned over a wide range. In combination with the abovementioned microfluidic device, trapping via a Cu(II) complex could be very efficient. The result would be a halide end-functional polymer chain. The detection of the ratio of the terminal monomer units in the trapped chains may be challenging via NMR spectroscopy. If the halide of choice in the trapping experiment is a bromide, this problem may be alleviated by replacing the bromide end group by a ^{15}N labeled azide. This efficient transformation of bromide into azide is nowadays often applied in the synthesis of precursors for the Huisgen 1,3-dipolar cycloaddition reaction.

A topic that is receiving increasing interest within the community of radical polymerization is that of monomer sequence control. Different approaches are being used to control the position of monomers along a polymer chain. The degree of control is nowhere near the precision seen in Nature, where for example proteins are synthesized with absolute fidelity. The approach of J.F. Lutz makes use of the high reactivity of substituted maleimides in a styrene copolymerization.[6] This allows the placement of a number of these units with different functionalities at different, fairly accurately controlled positions along the chain. Post-polymerization reactions then allow the synthesis of interesting chain topologies, such as cyclic polymers, 8-shaped polymers, etc. The approach of M. Sawamoto relies on polymerization of a methacrylate that happens concurrently with transesterification.[7] If this is carried out under the right

conditions, sequence-regulated polymers can be synthesized. In several cases, we have shown that *initialization* in RAFT-mediated polymerization can be extremely selective. A future challenge in radical polymerization is to find tools to control the selectivity in the initialization reaction. The CSIRO team was able to switch a RAFT agent between being suitable for a more activated monomer and for a less activated monomer by (de)protonation of the pyridine moiety that acts as the stabilizing (Z) group.[8] If this concept is better understood, and the kinetic implications thoroughly investigated, it will open further possibilities to tune the reactivity of RAFT agents and their associated ability to undergo selective initialization. This will then allow extension of selective initialization processes to larger chain length and hence move towards more precise sequence control.

Without having even touched upon control of tacticity, several complicated tasks remain to be completed in the field of radical polymerization. For each of these tasks, the use of sophisticated analytical techniques will be crucial. This is true for analysis of the polymer products as well as for *in situ* investigation of the polymerization process. Several examples of *in situ* NMR in this thesis have proven to contribute significantly to the understanding of polymerization processes. It is the author's strong belief that during the next decade, new examples will evolve at even higher levels of complexity.

References

1. Discussions with Prof A.M. van Herk, Dr. B.G. Manders and Dr. J.A.M. de Brouwer (Eindhoven University of Technology, the Netherlands).

2. van den Dungen, E.T.A.; Rinquest, J.; Pretorius, N.O.; McKenzie, J.M.; McLeary, J.B.; Sanderson, R.D.; Klumperman, B. *Aust. J. Chem.* **2006**, *59*, 742-748.

3. Pound, G.; McLeary, J.B.; McKenzie, J.; Sanderson, R.D.; Klumperman, B. *Macromolecules* **2006**, *39*, 7796-7797.

4. Sanders, G.C.; Duchateau, R.; Lin, C.Y.; Coote, M.L.; Heuts, J.P.A. *Macromolecules* DOI: 10.1021/ma301161u

5. Haddleton, D.M.; Perrier, S. ; Bon, S.A.F. *Macromolecules* **2000**, *33*, 8246–8251

6. Schmidt, B.V.K.J.; Fechler, N.; Falkenhagen, J.; Lutz, J.-F. *Nature Chem.* **2011**, *473*, 234-238.

7. Nakatani, K.; Ogura, Y.; Koda, Y.; Terashima, T.; Sawamoto, M. *J. Am. Chem. Soc.* **2012**, *134*, 4373-4383.

8. Benaglia, M.; Chiefari, J.; Chong, Y.K.; Moad, G.; Rizzardo, E.; Thang, S.H. *J. Am. Chem. Soc.* **2009**, *131*, 6914-6915.

Acknowledgements

At the end of this thesis, it rests me to thank all the people that contributed to the research described. The work started about a decade ago with the ^{15}N labeled compounds and the ^{15}N NMR spectroscopy studies. The main person in that research was Peter Kelemen, who worked as a post-doc in my group at Eindhoven University of Technology. The work was done in collaboration with Prof Johan Lugtenburg at Leiden University.

The rest of the work was conducted at Stellenbosch University, where several students had major contributions. In (more or less) chronological order they were James McLeary, Gwenaelle Pound-Lana and Eric van den Dungen for the work on *in situ* NMR and *initialization* studies and Lebohang Hlalele for the nitroxide-mediated polymerizations.

Apart from these students and post-docs, I would like to thank all present and past members of my research group for their efforts to contribute to the output of the group.

Further I would like to thank Prof Eugene Cloete, the present Deputy Vice-Chancellor of Research (former Dean of Science) of Stellenbosch University. He pointed out the possibility for me to pursue the DSc degree when we were discussing my application for permanent residence in South Africa.

Peter Mallon is gratefully acknowledged for his willingness to act as promotor for my DSc. His input and advice are highly appreciated.

Last but not least, I would like to thank my wife Linda and children (David, Luc, Tom, Maarten and Rosa) for their patience with me. It is not always easy to have a lab and an office that are almost 10,000 km away from home. I really appreciate the support that allows me to complete this thesis, but that also allows me to work in Stellenbosch.